Regulatory T cells limit antiviral CD8 T cell responses through IL-2 competition

Regulatorische T-Zellen limitieren antivirale CD8 T-Zellantworten durch IL-2 Konkurrenz

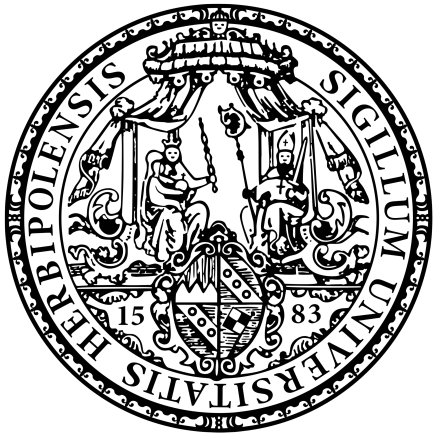

Doctoral thesis for a doctoral degree at the Graduate School of Life Sciences

Julius-Maximilians-Universität Würzburg

Section Infection and Immunity

submitted by

Lennart Rüttger

From Essen, Germany

Würzburg 2022

Submitted on: ……..……..

Office stamp

Members of the Thesis Committee

Chairperson: Prof. Dr. Jürgen Seibel

Primary Supervisor: Prof. Dr. Wolfgang Kastenmüller

Supervisor (Second): PD Dr. Knut Ohlsen

Supervisor (Third): Prof. Dr. Georg Gasteiger

Date of Public Defence: ……..……

Date of Receipt of Certificates: ……..

"Life is an echo.
What you send out, comes back.
What you sow, you reap. What you give, you get.
What you see in others, exists in you."

-Zig Ziglar

Abstract

Regulatory T cells (Treg) are critical immune cells to ensure immune homeostasis. Treg do so by establishing tolerance to self-antigens as well as food-derived antigens. Additionally, they fine-tune immune responses to limit the damage caused by inevitable inflammation during the resolution of an ongoing infection or anti-tumor response. Despite countless efforts to gain a detailed understanding of the mechanisms Treg utilize to regulate adaptive immune responses, *in vivo* evidence is rather limited. We were interested in the cell-cell interactions of Treg and their spatio-temporal dynamics during a viral infection. We sought to address Interleukin-2 (IL-2) competition as a viable mechanism to control anti-viral CD8 T cell responses.

We used intra-vital 2-photon imaging to analyze the interactions between Treg and activated T cells during viral infection. Additionally, we performed multiple loss- and gain-of-function experiments, addressing the IL-2 active signaling of CD8, CD4, and regulatory T cells to understand the competitive sensing of IL-2. Finally, we performed single-cell RNA sequencing to understand the cell-intrinsic differences in Treg caused by infection.

We found that IL-2 competition by Treg limits the CD8 T cell response and can alter the differentiation of CD8 T cells. Furthermore, we show that Treg do not arrest in proximity to CD8 T cells for prolonged periods and therefore are unlikely to regulate CD8 T cells *via* contact-dependent mechanisms previously proposed. Our data support an area control model in which Treg scavenge IL-2 while actively migrating through the LN, constantly limiting access to IL-2.
Establishing CD4 T cells as the major source of IL-2 during the later phases of infection, we provide direct evidence that Treg compete with CD8 T cells for CD4-derived IL-2.

Finally, we show that IL-2 limitation is in correlation with CD25 expression levels and has an impact on the differentiation of CD8 T cells. Altering the differentiation of CD8 T cells to increase effector or memory functions has huge implications in clinical treatments, e.g 'checkpoint immunotherapy'.
Especially in scenarios like checkpoint immunotherapy, where an efficient expansion of CD8 T cells is vital to the success of the treatment, it is invaluable to understand the spatio-temporal dynamics of Treg. Not only can the expansion phase be optimized, but

also side effects can be better controlled by ensuring the adequate timing of treatments and boosting the anti-inflammatory response after the initial establishment of CD8 T cells.

On top of this, the gained understanding of the regulatory mechanism of Treg can help to enhance the efficacy of autoimmune disorder treatments.

Overall, this study addressed highly relevant questions in the Treg field and answered aspects of Treg regulation, refining their mode of action and the spatio-temporal dynamics during viral infection, providing evidence for IL-2 competition as a major regulatory mechanism controlling antiviral CD8 T cell responses.

Zusammenfassung

Regulatorische T Zellen (Treg) sind wichtige Immunzellen die der Aufrechterhaltung der Homöostase dienen. Sie induzieren tolerogene Immunantworten gegenüber Antigenen des eigenen Körpers und erlauben uns die Aufnahme von harmlosen 'Fremdantigenen' aus unserer Nahrung, indem Sie unerwünschte Immunantworten unterdrücken. Zusätzlich ermöglichen Treg eine Feinabstimmung der adaptiven Immunantwort, indem sie die Entzündungsreaktion und die damit einhergehende Gewebeschädigung minimieren, zeitgleich aber die Expansion von Effektorzellen angepasst an das Infektionsgeschehen erlauben. So kann der Erreger schnellstmöglich bekämpft werden, ohne dass die Integrität des Gewebes beeinträchtigt wird und die Gewebefunktion aufrechterhalten werden kann.

Viele wissenschaftliche Studien haben sich bereits mit den Regulationsmechanismen von Treg beschäftigt. Es werden heutzutage unzählige Mechanismen beschrieben, die in den meisten Fällen jedoch auf Ergebnissen aus Zellkulturexperimenten beruhen und somit häufig unzureichend belegt sind. Aus diesem Grund wollten wir sowohl das zeitliche als auch räumliche Verhalten von regulatorischen T Zellen im Laufe einer viralen Infektion genauer untersuchen und dabei vor allem Zell-Zell Interaktionen analysieren. Besonderes Augenmerk lag dabei auf dem zuvor beschriebenen Mechanismus der Interleukin-2 (IL-2) Konkurrenz. Dieser zeichnet sich dadurch aus, dass regulatorische T Zellen IL-2, ein wichtiges Zytokin für das überleben von Effektorzellen, aufnehmen und somit die vorhandene Menge an IL-2 beeinflussen können. Dies geschieht in ständiger Konkurrenz zu Zellen der adaptiven Immunantwort.

Wir haben Zell-Zell Interaktionen von Treg mit ihren potenziellen Konkurrenten mithilfe von intravitaler Mikroskopie, im Laufe einer viralen Infektion untersucht. Außerdem haben wir verschiedene 'gain'-und 'loss-of-function' Experimente durchgeführt, um die IL-2 Konkurrenz zwischen CD8, CD4 und regulatorischen T Zellen besser verstehen zu können. Zusätzlich haben wir das Transkriptom von Treg in zwei verschiedenen Kontexten, Infektion und Homöostase, mittels einer Einzelzellanalyse miteinander verglichen.

Wir konnten zeigen, dass Treg dazu in der Lage sind antivirale T Zellantworten allein durch IL-2 Konkurrenz zu modulieren. Hierbei wird nicht nur die Anzahl, sondern auch die Differenzierung von zytotoxischen T Zellen beeinflusst. Dabei haben wir festgestellt,

dass Treg während der Immunantwort in Lymphknoten migratorisch aktiv bleiben und keine langen (> 15 min) Zell-Zell Interaktionen mit aktivierten CD8 T Zellen oder dendritischen Zellen eingehen. Dies deutet auf einen primär kontaktunabhängigen Regulationsmechanismus bei der Steuerung von antiviralen T Zellantworten hin.

Abschließend konnten wir zeigen, dass CD8 T Zellen während ihrer Expansionsphase stark auf von CD4 T Zellen produziertes IL-2 angewiesen sind. CD4 T Zellen stellen in dieser Phase der Infektion die Hauptquelle von IL-2 dar. So können Treg den Zugang von CD8 T Zellen zu der Hauptquelle von IL-2 räumlich soweit begrenzen, dass dies die Expansion und Differenzierung der CD8 T Zellpopulation nachhaltig beeinflusst.

Diese Studie beantwortet relevante Fragen zur Funktionsweise von regulatorischen T Zellen während einer viralen Infektion und zeigt vor allem die räumlichen und zeitlichen Komponenten der Regulation im Detail auf. Diese Studie zeigt, dass IL-2 Konkurrenz einen Hauptregulationsmechanismus von regulatorischen T Zellen darstellen und CD8 T Zellantworten unabhängig regulieren kann.

Dies ermöglicht die (Weiter-)Entwicklung und Präzisierung von klinischen Anwendungen und Therapieansätzen zur Bekämpfung von Krebs- und Autoimmunerkrankungen. Besonders für die Expansion von zytotoxischen T Zellen, welche bei der 'Checkpoint' Immuntherapie zur Behandlung von soliden Tumoren von besonderer Bedeutung ist, ist das Verständnis der Funktionsweise von regulatorischen T Zellen für den Erfolg der Behandlung entscheidend.

Contents

1 Introduction

1.1 Organization of the immune system

The immune system is a highly complex network of cells that protects us from disease. It maintains the healthy balance in our body, also described as homeostasis. The different functional units of the immune system are interlinked and communicate *via* signaling molecules (e.g. cytokines) to mount an appropriate defense against the encountered insult. Every immune response alters the delicate balance between inflammation and homeostasis and causes undesired effects concomitantly (Cohnheim, 1867; Medzhitov, 2010). Therefore, the immune system has evolved multiple mechanisms to tightly regulate each step of the immune response to minimize the damage caused by it (Cohnheim, 1867).

To fend off pathogens the body employs physical barriers such as the skin and mucosa. Features such as low pH, chemicals, and microbial colonization help to prevent pathogens from entering (Park and Lee, 2017). Once the first line of defense is breached, the immune system can rapidly mount protective measures to fight invading pathogens. Initially, the innate immune system responds first by recognizing highly conserved signals of invading pathogens. This mechanism is relatively broad as it detects a wide range of specific pathogen-associated molecular patterns (PAMPs) These patterns occur in basic building blocks of pathogens, like DNA or membrane structures and are recognized by specific pattern recognition receptors (PRRs) (Janeway, 1989). The innate immune system restricts the spread of pathogens and responds with diverse effector mechanisms (Medzhitov and Janeway, 2000). Some of the effector molecules released, activate the adaptive arm of the immune system.

In contrast to the innate immune system, the adaptive immune response is very specific towards unique short peptide sequences (antigens) and one cell only recognizes one specific sequence. This clonal selection theory however has been challenged, as cross-reactivity has been shown in multiple studies (Kersh and Allen, 1996; Mason, 1998; Wilson et al., 2004; Wucherpfennig et al., 2007). T and B cells have antigen-recognizing receptors that ensure pathogen-specific effector functions. The T cell receptor (TCR) assembly is a highly sophisticated process that ensures an extremely high diversity in the

T cell receptor repertoire (Germain, 2002). By recombination of multiple different gene segments, the TCR diversity is estimated to reach up to 10^8 unique TCR specificities (Arstila et al., 1999; Qi et al., 2014b). This enables the adaptive immune system to ensure broad coverage of nearly all peptide sequences possible. B cells have a markedly lower number of unique B cell receptor (BCR) specificities. Still, several mechanisms like somatic hypermutation and different isotype classes ensure increased diversification (Chaudhary and Wesemann, 2018). They produce antibodies against invading pathogens and enable the clearing of pathogens from the system. The antibodies produced by the B cells bind to the pathogen and this enables the removal of these 'opsonized' cells by phagocytes.

For T cells to act against a pathogen, they first need to be activated by encountering their cognate antigen. This is facilitated by antigen-presenting cells (APC), which present antigens on their surface and deliver additional activation signals to the naïve T cell. Often, conventional dendritic cells (cDC) act as the APC, despite macrophages (MΦ), B cells, follicular dendritic cells (FDC), and other cell types being able to present antigen, as well. cDC have higher capabilities to ensure fully fledged activation of T cells due to co-stimulatory signals they transmit, which are needed for the T cell. Should the T cell not receive these additional activation signals, they will be inducing anergy, a state of unresponsiveness (Harding et al., 1992).

The activation of naïve T cells mostly happens in secondary lymphoid organs (SLO) like the lymph nodes (LN), spleen, or mucosa-associated lymphoid tissues (MALT). These organs display a meeting point for adaptive immune cells and enhance the chances of encounter (Aoshi et al., 2008). Potentially, very few cDC carry antigen and need to encounter and activate a rare population of T cell precursors, specific for the antigen presented. For these two cell types to encounter each other, the location and timing must be orchestrated. Due to the migratory capacity of these cells, they can both efficiently home to SLO, facilitating their encounter. Secondary lymphoid organs provide a very suitable environment for antigen-specific cells to interact with multiple cDC and scan the tissue for their cognate antigen (Luckheeram et al., 2012; Stoll et al., 2002). The LN is a pivotal meeting point to induce adaptive immune responses and prevent the systemic distribution of pathogens. Additionally, the LN displays an early detection environment to manage infections in close proximity to the infected tissue. To fulfill the containment of pathogens and the induction of efficient immune responses the LN is structurally and functionally highly organized into functional niches.

1.2 Architecture of the lymph node

Structurally the LN is comprised of the capsule, subcapsular sinuses, B cell follicles, interfollicular areas, the paracortex, and the medulla. The LN harbors three main lineages of cells that are specialized to fulfill unique functional roles: stromal, myeloid, and lymphoid cells (Willard-Mack, 2006).

1.2.1 Stromal compartment

Stromal cells provide structure and secrete different soluble factors to create distinct niches for specific cell populations. Homeostatic cytokines like Interleukin-7 (IL-7) and chemokines like CCL19 (C-C motif ligand 19), CCL21, (C-X-C motif ligand 12) CXCL12 and CXCL13 are constantly produced in order to recruit the cells forming these specific compartments (Mueller and Germain, 2009; Onder et al., 2012). These chemokines provide locomotion cues to lymphocytes especially and form the basis for the segregation of B and T cell zones.

Fibroblastic reticular cells (FRC) and FDC produce CCL19/CCL21 and CXCL13 respectively, to form the T cell zone and B cell follicles. The paracortex is rich in CCL19 and CCL21 to support CCR7-mediated migration for naïve T cells, attracting them deeper into the LN cortex. In contrast, CXCR5 enables B cells to migrate along a CXCL13 gradient to the B cell follicles (Allen et al., 2004).

Lastly, lymphatic endothelial cells are the building blocks of lymphatic sinuses in the LN, which collect the lymph from afferent lymph vessels. Lymphatic endothelial cells express the atypical chemokine receptor ACKR4, which acts as a sink for CCL21 and thereby ensuring a constant chemokine gradient for cDC to be able to cross the epithelium and travel to deeper regions of the LN (Ulvmar et al., 2014).

Not only do stromal elements provide structural cues to cells, but they also fulfill a role in immune responses. They can modulate the sensitivity to immunomodulatory factors and induce tolerance. Beyond this, they supply the tissue with soluble mediators from the periphery *via* the conduit system. This is a network of interconnected stromal cells in the LN. The seemingly rigid structure is expandable during infection and makes the LN inhabitable for more cells, needed during the ongoing immune response (Chang and Turley, 2015; Rantakari et al., 2015; Sixt et al., 2005; Turley et al., 2010).

1.2.2 Myeloid compartment

The myeloid lineage can be divided into two major cell types in the LN: conventional dendritic cells (cDC) and macrophages (MΦ). This classification is very simplified and to be further refined by subdividing various subsets of resident and migratory cDCs on one hand and multiple highly specialized MΦ populations on the other hand.

In the LN, MΦ sample lymph for foreign pathogens. A specific subset of MΦ termed subcapsular sinus macrophages (SSM) is located at the subcapsular sinus arranged around the most peripheral regions of the LN. These $CD169^+$ MΦ are strategically positioned within the lymphatic sinus and enclose the B cell follicles. Pathogens draining into the LN *via* the lymphatics are first encountered by SSM (Honke et al., 2011).

MSM (medullary sinus macrophages) and PM (paracortical macrophages) are also located in the respective anatomical niches of the LN.

SSM are the first line of defense in the LN and prevent the dissemination of viral particles or other pathogens that drain from the tissue into the LN. In the case of a Vaccinia virus infection, they are acting as a scavenger of the infectious particles and ensure the first containment being very closely associated with the subcapsular sinus. Nevertheless, LN resident cDC also get infected, as they are strategically positioned within the same region even protruding their cell bodies into the sinus to capture antigen (Gerner et al., 2015). Once SSM get infected, they express anti-viral genes and display a crucial source of type-I interferon (IFN-I) (Iannacone et al., 2010).
In order to promote a sufficient humoral response, SSM initiate antigen handover to B cells at the T-cell B-cell border. This antigen handover is essential for the formation of germinal centers and the priming of B cells (Harwood and Batista, 2010; Qi et al., 2014a).

1.2.2.1 Conventional Dendritic cells

cDC play a key role in connecting the adaptive immune system to innate signals. They not only possess good antigen-presenting capabilities like most APC but also have the ability to deliver co-stimulatory signals to T cells to improve the quality of their response (Merad et al., 2013; Murphy et al., 2016). cDC are especially suited to stimulate naïve and memory T cells (Inaba and Steinman, 1984; Steinman and Witmer, 1978).

cDC utilize various mechanisms to present antigen. One of the most used routes of antigen-presentation is the direct presentation of cytosolic antigen *via* major histocompatibility complex (MHC) class I (Dudziak et al., 2007). This mode of presentation displays the "health status" of the cell. Antigen of the endogenous protein synthesis is presented constantly, as proteins are processed and loaded onto MHC class I molecules and brought to the surface of the cell. cDC are susceptible to infections by a selection of viruses. If a cDC becomes infected, it will present those viral particles on the surface in an MHC class I-dependent context. This allows CD8 T cells to sense the infection of the cDC. The CD8 T cell will be activated by the infected cDC and kill it eventually. In the context of viral infection, cDC play an essential role in the detection of infected cells leading to their elimination. Virus particles that are not synthesized within a cDC, need to be presented *via* a different pathway. This is not only relevant in the context of viruses but also in tumors. For cDC to activate CD8 T cells, they have to take up exogenous antigen from the sites of infection or tumor. It is believed that cDC can pick up exogenous antigen from dying infected cells (Albert et al., 1998). This exogenous antigen can be taken up and processed to be presented on MHC class I molecules. This process is called cross-presentation (Kurts et al., 1996).

In contrast to MHC class I-mediated presentation, there is also antigen being presented on MHC class II molecules. This enables the activation of antigen-specific CD4 T cells (Rudensky et al., 1991). Similar to cross-presentation, the antigen has to be exogenously taken up and processed. However, the antigen peptide fragments that are presented in the context of MHC class II are larger with 13-20 amino acids compared to 8-10 amino acids in the context of MHC class I presentation (Fremont et al., 1992; Guo et al., 1992; Rock et al., 2004).

Displaying the cognate antigen to a naïve T cell is essential for the activation of lymphocytes. Nevertheless, this is only one of the signals that cDC deliver to T cells to activate them. After activation *via* the TCR, the T cell needs further co-stimulatory signals. These signals are mediated by the cDC *via* co-stimulatory receptors like CD80/CD86 (signal 2). cDC upregulate these receptors as soon as they sense inflammation, tissue damage, or infection. This is achieved by PRR similar as in MΦ. Toll-like receptors (TLR), a class of PRRs that sense specific components or microbes, play a key role in this process. The TLR ligands can be components found on the surface of bacteria like flagellin, or more basic components of pathogens like DNA, RNA, or other proteins. Upon TLR signaling, which acts as a danger signal for cDC, maturation is induced (Akira

et al., 2006). The maturation induces changes in the expression of co-stimulatory receptors and leads to the upregulation of CCR7, which in turn promotes the migration towards a draining LN. This enables the cDC to interact with multiple lymphocytes, ensuring the accessibility of the specific antigen (Gatto et al., 2013; Probst et al., 2003; Sporri and e Sousa, 2005).

Furthermore, the activated cDC will release cytokines that will create a stimulating environment for the cells in the vicinity of the cDC. This helps the activation of naïve T cells and their guidance to the right environment for activation and supplies them with additional activation cues (signal 3).

In summary, T cells receive three major signals from cDC to get activated. First T cells get their antigen presented by an APC and this leads to TCR activation. Secondly, co-stimulatory signals are delivered by the activating cDC and enhance the potency of the T cell response. Lastly, the cDC secretes cytokines to enhance the quality of the T cell response. These are the commonly described three activation signals that T cells need in order to reach their full functional capacity (Curtsinger et al., 1999, 2005).

Subsets of cDC

Two major subsets of cDC have been described: cDC1 and cDC2 (Edwards et al., 2003). Both subsets can be further subdivided into migratory and resident cDC. Resident cDCs have been shown to not recirculate and reside in the tissue they have been initially homing to. In contrast, migratory cDC have the ability to migrate and transport antigen from tissue sites to the draining LN. They connect the tissue with the lymph system and enable early detection of foreign antigen. In mice, cDC are described as $CD11c^{hi}$ and $MHCII^{+}$ cells. While migratory cDC subsets express CD11b and other markers like CD103 (dermal DCs) and langerin, lymphoid tissue-resident cDC can express CD4, CD8$\alpha\alpha$ (a homodimer of the CD8 α-chain) or neither of these markers (Henri et al., 2001).
Activated migratory cDC transport antigen from the site of infection or damage to the LN. This migration is based on CCR7 and is achieved *via* the afferent lymphatic vessels that connect the tissue with the LN (Ohl et al., 2004; Teijeira et al., 2014; Worbs et al., 2017).
In contrast to LNs, which contain migratory and resident cDC, the spleen only harbors resident cDC.

It is still an ongoing debate to what degree migratory versus resident cDC contribute to the activation of CD8 T cells. Overall, this seems to be context-dependent. Recent evidence suggests that migratory cDC play a minor role in the activation of CD8 T cells, at least in the context of viral infection (Eickhoff et al., 2015). However, CD4 T cells have been shown to receive signals from migratory cDC cooperatively with resident cDC (Allenspach et al., 2008).

The cDC1 subset is characterized by the expression of XCR1, Irf8, Clec9a, and CD11c. cDC1 play an important role in cross-presentation and therefore are known to be strong activators of CD8 T cells in the context of infections. The XCR1 expression enables these cells to be recruited to sites of XCL1 release (Dorner et al., 2009). Typically, NK cells and CTL release XCL1. Our group has shown, that this receptor-ligand axis is essential during acute viral infection (Brewitz et al., 2017). Not only is the superior cross-presentation machinery unique to cDC1, but also their ability to produce cytokines like IL-12 enhances the quality of the CD8 T cell response. Further, it has been shown that IL-15 produced by cDC1 is essential for optimal priming of CD8 T cells in some contexts (Greyer et al., 2016).
While few resident cDC1 were found to be positioned close to the subcapsular sinus, most cDC1 can be found in the paracortex where they mainly interact with CD8 T cells (Kitano et al., 2016).

cDC2 on the other hand are less efficient in cross-presenting antigen to CD8 T cells and thus are not the main driver of CD8 T cell priming. cDC2 have a more prominent role in shaping CD4 T cell-mediated and innate immune responses. This is primarily achieved *via* MHC class II presentation. Also, cDC2 fulfill an important role in activating follicular helper T cells, leading to the formation of germinal centers and the production of high-affinity antibodies (Gerner et al., 2015; Gonzalez et al., 2010; Woodruff et al., 2014).
Therefore, cDC2 preferentially position in the peripheral regions of the LN close to lymphatic sinuses and the T cell B cell border. As potent inducers of T cell responses during inflammation, their positioning is functionally evolved to sample draining antigens and prime T cells as soon as former have been encountered.

1.3 T cell immunity

T cells are one of the key players in the adaptive immune system. The TCR-mediated recognition of their specific antigen makes them highly specific and effective. For the cognate antigen to be recognized efficiently, APC present antigen *via* two major classes of MHC molecules: MHC class I and MHC class II. T cells either express the CD4 or CD8$\alpha\beta$ co-receptor (heterodimer of CD8 alpha -and CD8 beta-chain). This receptor restricts the T cells to the specific antigen presented *via* either MHC class I or II molecules. CD4 T cells are MHC class II-restricted and CD8 T cells are MHC class I-restricted. These specializations enable CD8 T cells to recognize intracellular antigens as most cells in the body express MHC class I on their surface. If a cell has been infected by intracellular pathogens, in most cases the foreign protein will be processed and antigen from this protein will be loaded onto MHC class I molecules, which is then displayed on the surface of the infected cell.

1.3.1 CD8 T cells

CD8 T cells recognizing this antigen will become activated and release cytotoxic effector molecules to kill the infected cell. CD8 T cells that have recognized their cognate antigen and express cytolytic molecules are called cytotoxic T lymphocytes (CTL). There are several different cytotoxic effector mechanisms that induce apoptosis in the target cell (Bousso and Robey, 2003; Miller et al., 2002; Stoll et al., 2002; von Andrian and Mempel, 2003).

The release of cytotoxic molecules like granzyme and perforin is one major mechanism in CTL. Perforin induces the formation of pores in the membrane of the target cell and allows for the influx of granzyme and other extracellular components into the cell. Granzyme and extracellular signals then lead to the induction of apoptosis (Hassin et al., 2011; Hirst et al., 2003; Ratner and Clark, 1993). Release of tumor necrosis factor (TNF-α) will also induce apoptosis and additionally alert other cells of an ongoing infection. TNF-α is known as a pro-inflammatory cytokine that triggers several inflammatory processes in immune cells.

Another feature of CTL is the release of interferon-gamma (IFN-γ). This will induce activation of other effector cells and create a stimulatory environment to facilitate immune reactions against the infected cell.

CTL also can induce apoptosis *via* ligation of the Fas receptor (FasR) which induces a caspase-8/caspase-3-mediated apoptosis pathway. Similarly, this can be induced by TRAIL (TNF-related apoptosis-inducing ligand), a protein that functions as a ligand for specific death receptors that induce the same process of apoptosis *via* caspases (Brincks et al., 2008).

Activated T cells proliferate and have the potential to form memory populations that contribute to immunological memory. This feature is a hallmark of the adaptive immune system and protects the body from reoccurring infections. Memory cells can maintain their population by homeostatic proliferation at a constant slow rate. In the case of reinfection with the same pathogen, these cells have the capacity to respond extremely fast and help us to build long-lasting immunity against pathogens that have already been encountered. Memory cells have been shown to be very long-lived. Their maintenance depends on constitutive IL-7 and IL-15 signaling (Surh and Sprent, 2008).

1.3.1.1 Differentiation of CD8 T cells

During an immune response, the majority of effector CD8 T cells develop into short-lived effector cells (SLEC). These cells lose their capacity to proliferate upon re-encountering their cognate antigen. Therefore, these cells are also called terminal effector cells (TEC) (Parish and Kaech, 2009). Recent evidence additionally shows that TEC are not necessarily short-lived cells. The signals leading to differentiation into effector subsets are ill-defined.
However, it has been shown that increased inflammatory signals can lead to enhanced differentiation into TEC. Several studies have shown that multiple inflammatory cytokines, e.g. IL-2, type-I IFN, and IL-12, and also persisting antigen stimulation can lead to this skewed balance of differentiation (Curtsinger et al., 2003; Kalia et al., 2010; Kolumam et al., 2005; Pearce and Shen, 2007). After activation naïve CD8 T cells upregulate activation markers like CD69, CD44, and CXCR3. The latter is a chemokine receptor that responds to the interferon-induced chemokines CXCL9, CXCL10, and CXCL11 and thereby guides lymphocytes towards inflammatory regions of the LN. Due to more inflammatory stimuli, a higher abundance of antigen, and local production of cytokines, this environment favors the differentiation into TEC (Hu et al., 2011; Kurachi et al., 2011).
Chemokine gradients have been implicated to influence the differentiation of multiple

subsets of effector T cells. During the differentiation of CD8 T cells also cells with memory potential develop. These cells normally express the IL7R α-chain (CCR7 or CD127) and are termed memory precursor effector cells (MPEC).
Central memory cells, which have the greatest longevity and can maintain their population lifelong, express CD62L or L-selectin additionally to CCR7. These cells recirculate through the secondary lymphoid organs and are the ultimate keystone of immunological memory. The counterpart of this is tissue-resident effector memory T cells that remain in the tissue and have a less proficient long-term survival. Nevertheless, they respond faster and display the first line of defense in a recurring infection. In the tissue, they express CD103/CD69 and fend off pathogen entry at infection sites.

Another classification of memory potential is based on the expression of fractalkine receptor CX3CR1. During memory development three different populations of CX3CR1 expressing cells can be identified and the expression correlates with their capacity to proliferate and develop into central memory cells (Gerlach et al., 2016).
CX3CR1^{-}, CX3CR1^{int} and CX3CR1^{hi} cells can be distinguished. Whereas CX3CR1^{-} and CX3CR1^{hi} have been described before and give rise to classical central memory T cells and effector memory T cells, respectively, the intermediate CX3CR1 expression characterizes a stable subset of peripheral memory T cells that surveys non-lymphoid tissues (Gerlach et al., 2016). Peripheral memory T cells also give rise to central memory T cells and thereby maintain the memory T cell pool. The Effector memory population is mostly absent from peripheral tissues, indicating the unique migratory properties of these three distinct subsets and underlining their specific phenotypical adaptation to their niche.

While TEC differentiation has been shown to be facilitated by CXCR3 expression, the differentiation into memory subsets has been suggested to be enhanced by the expression of chemokine receptor CCR5 (Castellino et al., 2006; Prlic et al., 2006).

1.3.2 CD4 T cells

CD4 T cells are restricted to MHC class II antigen presentation. They support CTL differentiation by providing help to cDC. Also, CD4 T cells provide help to B cells, facilitating their differentiation into plasma cells or memory B cells, by providing signals such as co-stimulation, cytokines, or antigen. Their name originates from these findings hence they are also called CD4 T helper cells (Th). They release important cytokines

that serve to fight specific pathogens.
Each Th subset is distinct and expresses a unique combination of surface receptors, transcription factors, and secreted cytokines. Those subsets are all involved in host defense against specific microbial pathogens and therefore aid the immune system in creating a specific environment against the encountered pathogen. This contributes to the elimination of the pathogen and the subsequent activation of other immune cells.

Classically, CD4 Th responses are divided into two major subclasses of effector function: Th1 and Th2. The functionally distinct subclasses are defined by the cytokines they secrete. While Th1 cells release IFN-γ and TNF-α to support immune responses against intracellular pathogens, Th2 responses are mediated by IL-4, IL-5, IL-10, IL-13, and will defend the body against extracellular pathogens (Iwasaki and Medzhitov, 2004; Luckheeram et al., 2012).

By secreting cytokines and altering the environment the different Th subsets inhibit the development of opposing Th subsets: Th1 differentiation inhibits the development into Th2 cells and vice versa.

Th17 cells have been known to be important in the host defense against fungi and extracellular pathogens. They mainly release IL-17A and IL-17F, among other cytokines. It has been shown that pathogenic subsets of Th17 cells can also contribute to the pathogenesis of chronic inflammatory autoimmune diseases like inflammatory bowel disease (IBD).

Additional to the mentioned classes of T helper cells, T follicular helper cells (Tfh) contribute to the maintenance and proliferation of germinal center B cells and thus support the humoral response of the immune system (Breitfeld et al., 2000).

One very important Th subset is the subset of regulatory T cells. This subset functions in balancing the other Th subsets. The main cytokines released by Treg are IL-10, IL-35 and transforming growth factor beta (TGF-β)(Chen et al., 2003). These are anti-inflammatory cytokines that dampen the immune response and enhance immune homeostasis. Treg additionally exert control *via* self-tolerance mechanisms in order to restrict undesired immune responses against innocuous antigens. Here, we focus on the regulation of effector responses towards pathogens, albeit various additional functions Treg can fulfill.

More Th subsets have been described. Th9 cells seem to be important to fight parasitic helminth infections in humans and secrete mainly IL-9 (IL-10 in mice).

Th22 cells have been implicated in protecting against microbial skin infections. They mainly release IL-22.
However, it remains unclear whether these unique cytokine profiles in specific pathogen-induced environments represent an adaptation of previously discovered T helper cell subsets or represent a distinct lineage of helper cells (e.g. Th9 and Th22 subsets).

1.3.2.1 Regulatory T cells

The role of Treg in modulating an adaptive immune response towards pathogens and the mechanisms Treg utilize to do so are poorly understood. Various mechanisms of regulation have been proposed, mostly based on the proximity between Treg and the target cell.

Mechanisms of Treg suppression

Treg have been implicated in various regulatory processes. Many cell types can be regulated by broad functions of Treg and therefore numerous mechanisms to control target cells have been published. Here, we focus on the mechanisms regulating adaptive immune responses, which entails the regulation of either cDC or T cells. Regulatory mechanisms of Treg can be divided into targeting the T cell directly or the cDC and consequently the T cell indirectly (Vignali et al., 2008).

Indirect regulation of T cells

A potential point of regulation is the maturation of the cDC that activates the T cells. cDC provide co-stimulatory signals to CD8 T cells *via* co-stimulatory receptors such as CD80/CD86. These co-stimulatory signals enhance the quality of the response to the pathogen and allow full activation of T cells. Treg can interact with antigen-specific cDC and induce the downregulation of these co-stimulatory receptors. This leads to lower activation of CD8 T cells and an overall dampened response to the pathogen. The proposed receptor utilized by Treg to interact with the cDC is cytotoxic T-lymphocyte-associated protein 4 (CTLA-4) (Matheu et al., 2015). CTLA-4 exhibits immune checkpoint function and can act as an inhibitory receptor. Additionally, the affinity of CTLA-4 to bind to its ligands CD80 and CD86 is higher, compared to the affinity of the CD28 receptor on the CD8 T cell. Therefore, CTLA-4 acts as a competitive ligand for T cell stimulation leading to less activation in CD8 T cells.

It has been suggested that Treg can remove co-stimulatory molecules off the surface of the cDC *via* CTLA-4 – a process that has been described as transendocytosis (Ovcinnikovs et al., 2019). Treg remove the co-stimulatory molecules by "ripping out" parts of the membrane. This process happens in the immunological synapse that the Treg and the target cell form by interaction *via* CTLA-4 and CD80/CD86. Ovcinnikovs and colleagues have shown that transendocytosis mainly targets migratory cDC that carry antigen from the tissue to the draining LN. This limits the effect this process can have on viral infections that happen directly within the LN.

Another way of regulation that is supported by *in vitro* evidence is the removal of extracellular ATP, which acts as a signal for tissue damage and is highly inflammatory. Upon cell damage, ATP is released from cells and this can be sensed by purinergic P2 receptors. CD39 and CD73 are ectoenzymes expressed by B cells, cDC, and Treg to dephosphorylate the ATP. Activated Treg have high expression of CD39 and CD73 and this permits Treg to limit the pro-inflammatory environment by quenching the ATP-driven response. Deaglio and colleagues have shown that signaling *via* ADP sensing receptors of the A2A adenosine receptor family can further inhibit the function of cDC and activated T cells (Deaglio et al., 2007).

Direct regulation of T cells

Treg have been shown to secrete inhibitory cytokines, such as TGF-β, Interleukin-10 (IL-10), and Interleukin-35 (IL-35). These immunoregulatory cytokines lead to down-regulation of Th1 cytokines, MHC class II presentation, and co-stimulatory molecules, thereby dampening the strength of the Th1 response. This can either be acting indirectly on the cDC or directly on the T cell (Corthay, 2009; Sakaguchi et al., 2008, 2009; Vignali et al., 2008).

Treg express cytotoxic molecules (e.g. granzymes, perforins) that can give them the potential to directly kill effector cells like CD4 or CD8 T cells and thereby limit the population of expanding CD8 T cells. Whether this happens in the context of viral infections and is a viable mechanism to control immune responses remains elusive. So far, the evidence for *in vivo* killing of target cells by Treg is limited (Cao et al., 2007; Loebbermann et al., 2012).

One of the most evident mechanisms of Treg regulation is the IL-2 (Interleukin-2) deprivation of effector T cells. IL-2 is an important survival cytokine that Treg and activated

T cells compete for (Chinen et al., 2016; Kastenmuller et al., 2011; McNally et al., 2011; Morgan et al., 1976). By the ubiquitous expression of the IL-2 receptor α-chain, Treg have an advantage to scavenge IL-2. They have been shown to act as a sink for this important cytokine. The mechanism has been studied extensively *in vitro* but is not well understood *in vivo* (Busse et al., 2010). This is due to the fact that *in vivo* CD8 T cells are known to produce and sense their own IL-2 *in vivo* in an autocrine/paracrine manner. This would contradict the concept that Treg regulate CD8 T cells proximal to the site of priming, as the arrested CD8 T cells would have access to 'on-site' production of IL-2. IL-2 is bound by the IL-2 receptor. This receptor is a heterotrimeric protein expressed on the surface of immune cells, most prominently on lymphocytes. The receptor has three different compositions given by the combination of the IL2rα (CD25), IL2Rβ (CD122), and IL2rγ (CD132) chains. All three chains combine into the high-affinity receptor, which has a thousand-fold increased affinity to the IL-2 molecule (Stauber et al., 2006; Wang et al., 2005). Hence, IL2rα expression is considered most relevant for competitive IL-2 sensing by activated T cells.

Most Treg constitutively express CD25, CD122 and CD132, which enables them to sense IL-2 consistently with high-affinity. IL-2 controls Treg homeostasis and maintains their function (Amado et al., 2013; Barron et al., 2010; Chinen et al., 2016; Moriggl et al., 1999). Since the proliferation of Treg is IL-2 dependent, Treg population size is defined by IL-2 availability.
This has been supported by clinical studies showing higher Treg number in patients treated with recombinant IL-2 (Sim et al., 2014). In recent years, stabilization of *Foxp3* (forkhead box protein 3) expression has been identified as the underlying mechanism. *Foxp3* is the master transcription factor of the regulatory pathway in the development and function of Treg (Fontenot et al., 2005). The downstream signal transducer and activator of transcription 5 (STAT5) molecule is part of a highly conserved pathway activated by IL-2 binding in Treg. It is essential for Treg function and their proliferation (Charbonnier et al., 2019; Garg et al., 2019; Miyao et al., 2012; Rubtsov et al., 2010).

IL-2 signaling

IL-2 signaling is mediated by phosphorylation of tyrosine residues on the cytosolic domain of the IL-2 receptor. This is achieved by kinases that are activated by ligand binding and subsequent phosphorylation of the SH2 (src homology 2) domain. The tyrosine kinase adds a phosphate group to a specific residue of the receptor. STAT5 molecules can

bind to the phosphorylated Janus kinase (JAK) and the STAT5 c-terminal domain gets phosphorylated. The resulting phospho-STAT5 (pSTAT5) molecule dissociates from the receptor and forms either homodimers (pSTAT5-pSTAT5) or heterodimers with other stat molecules (e.g. pSTAT3). Translocation of the dimer into the nucleus is followed by binding to a response element, which then leads to transcriptional changes in specific genes, e.g. *Foxp3* (Chinen et al., 2016).

Phosphorylation of STAT5 molecules is very short-lived and the dimers formed are rapidly deactivated by proteins like protein inhibitor activated STAT (PIAS) or SH2 domain-containing protein tyrosine phosphatase-2 (SHP2). This makes the IL-2 signaling pathway highly dynamic and versatile. It has been shown recently that the constitutive or aberrant activity of this STAT5 signaling pathway is involved in human cancers, thus having a high medical relevance (Cumaraswamy and Gunning, 2012).

In a viral infection activated T cells need to upregulate the IL-2 receptor a-chain in order to compete efficiently for IL-2 as a potent survival cytokine needed for proliferation and effector differentiation (Boyman and Sprent, 2012; Malek et al., 2008). In this phase of infection, Treg have a competitive advantage over naïve or recently activated T cells as they constantly express CD25 on their surface (O'Gorman et al., 2009). Treg can already regulate the amount of IL-2 available to effector cells solely based on their CD25 expression. This early-infection time frame has been suggested to be highly relevant for the regulation of adaptive immune responses by Treg. Nevertheless, the *in vivo* evidence for this competition is lacking and it is unclear how Treg gain an advantage over cells, that are located in very close proximity to the source of IL-2. It is known that shortly after activation, CD8 T cells can produce IL-2, which they could use in an autocrine manner (D'Souza and Lefrancois, 2003). In this context, it is still unclear which cells provide IL-2 at a specific stage of the viral infection.

Role of the TCR in Treg

Previous studies suggest that the TCR plays an important role in the activation and maintenance of Treg. It is still unclear, whether Treg express TCRs recognizing self or foreign antigens. Even though without a functional TCR Treg cells do not lose their identity and remain able to consume IL-2, they fail to suppress immune responses. This was tied to the loss of activation of Treg which then led to the lack of suppressive capacity (Levine et al., 2014).

Subsets of Treg

One main distinction in Treg subsets depends on their origin. Thymic Treg (tTreg), just like conventional T cells, do originate from the thymus. They undergo selection and express the CD4 co-receptor, a TCR with relatively high auto-affinity. They also constitutively express the master regulator transcription factor Foxp3. Those Treg, also called natural Treg, mostly reside in the bloodstream and LN and restrict auto-reactive T cells.
Another less prominent subset of Treg named the peripheral or induced Treg (pTreg), are $CD4^+$ effector cells that express Foxp3 only after induction after they have already left the thymus. This may only happen under specific inducing conditions. IL-2 and TGF-β have been shown to facilitate this process (Zheng et al., 2007). It is a long-standing debate whether pTreg can be identified by the expression of *Nrp1* (Neuropilin 1) and *Ikzf2* (Ikaros family zinc finger 2, also known as Helios) (Singh et al., 2015; Weiss et al., 2012). The evidence suggests this might apply in some situations but does not seem to be universally applicable.

Still, there are multiple subsets of Treg depending on their differentiation, migration characteristics, and transcriptional profile. Similar to T helper cells, Treg can have a naïve, effector, and memory-like gene signature, describing the subsets commonly defined.

In lymphoid tissue two main populations can be found. Central Treg (cTreg) and effector Treg (eTreg). Among the eTreg, there is a small fraction of Treg that are tissue-adapted eTreg. These display expression of genes that are associated with tissue homing capacity and enable those cells to exert their function at specific locations (e.g., skin, gut, lung, etc.) (Delacher et al., 2020; Miragaia et al., 2019).
Central Treg are mostly naïve Treg that express markers associated with recirculation and key Treg signature. This signature consists of *Foxp3, Il2rα, Tcf7, Bcl2, Sell*, and *S1pr1* among others (Delacher et al., 2020).
In contrast to cTreg, eTreg express markers, known from other T cell populations as activation of effector markers, like *Klrg1, Tnfrsf9, Relb, Ikzf2* and *Pdcd1*. Further subpopulations of eTreg can express additional tissue-specific genes like *Rorα, Itgae, Fgl2*, and *Icos* in some instances (Delacher et al., 2020).

The role of Foxp3

Foxp3 is known to be a master regulator of the regulatory function of Treg (Fontenot et al., 2005). It is involved in the development and function of Treg. Positive feedback regulation of several Treg-specific genes leads to the stabilization of Treg lineage.
It was only recently discovered that the conserved non-coding sequence 2 (CNS2), a CpG-rich *Foxp3* intronic cis-element is protecting the stability of Foxp3 expression and thus is essential for Treg identity (Levine et al., 2014).
Nevertheless, it has been shown that under specific conditions Treg can lose their Foxp3 expression and become effector CD4 T cells, such as Th17 cells releasing IL-17 (Komatsu et al., 2014).

Defects in the *Foxp3* gene lead to dysfunction and have severe consequences for the host, for example autoimmune disorders and advert inflammation.
Additionally, Foxp3 controls several genes that are essential for the suppressive functions of Treg. Among these are *Il2, Cla4, Il2rα, Il10*, TNF receptor superfamily, member 18 (*Tnfrsf18*, also known as *Gitr*) and *Izumo1r* (Kim, 2009).

Impact on CD8 T cell differentiation

Treg have been shown to restrict auto-reactive T cells that escaped the regular control mechanisms of adaptive immune activation by co-clustering close to these cells (Liu et al., 2015). In a viral infection, this situation changes dramatically, as the immune response is desired and needs to be fine-tuned to ensure fast and efficient clearing of the pathogen while maintaining the integrity of the tissue.

Regulation *via* IL-2 competition describes an excellent way to ensure the fine-tuned regulation of CD8 T cell responses. Oyler-Yaniv and colleagues have shown elegantly *in vitro* that IL-2 regulation can be highly dynamic and allow for control of CD8 T cell expansion (Oyler-Yaniv et al., 2017).

Strong TCR stimulation will lead to IL-2 production by CD8 T cells and consequently upregulation of CD25, which allows them to access IL-2 locally. CTL need IL-2 to proliferate and exert their effector function. Treg constitutively express CD25 and can bind and consume IL-2 before CD8 T cells even get activated. This is needed for their activation and upregulation of effector molecules. Consequently, it limits the IL-2 availability. As soon as the activated CD8 T cells locally produce IL-2, the advantage gets lost and proximity between Treg and CD8 T cells is required. This has been observed in the

steady-state regulation of auto-reactive CD8 T cells(Liu et al., 2015).
In the regulation of viral responses, this system allows for fine-tuning to the amount of pathogen load. The more antigen from the pathogen gets presented the more CD8 T cells get activated and produce IL-2. The cytokine will be sensed by naïve Treg and activates them, driving competitive CD25 expression levels. This fine-tuning would only be relevant in the early stages of the infection as CD8 T cells start expressing high levels of CD25 and expand quickly, outnumbering Treg 3-4 days post-infection.

Balancing the amount of IL-2 available to the CD8 T cell population could be an elegant way to tune the effector versus memory ratio, as well. It has been proposed that effector CD8 T cells need prolonged exposure to IL-2 in order to differentiate into terminally differentiated effector T cells, which have the highest cytotoxic potential and are needed to fight the ongoing infection (Kalia et al., 2010). Also, it was shown that CD8 T cells lose their ability to produce IL-2 after differentiation into effector T cells (Aruga et al., 1997; Sallusto et al., 1999). Memory formation by memory precursor effector T cells seems to occur in precursors that have less exposure to IL-2 and reside in a less inflammatory niche of the LN (Kalia et al., 2010).
This is supported by studies showing that Treg depletion during primary viral infection does not alter the frequency of the resulting memory population. In contrast, the CD8 effector population was strongly increased potentially because of the increased availability of IL-2 (Kastenmuller et al., 2011).

In summary, Treg have the ability to alter the differentiation of the CD8 T cells during a viral infection. This can be controlled *via* IL-2 levels during the early phase of the adaptive immune response.

1.4 Migration of T cells

Lymphocytes enter the LN through specific entry sites termed high endothelial venules (HEV). Highly specialized endothelial cells express integrins and ligands ensuring that lymphocytes can adhere to the tissue and extravasate through the endothelial wall. This process can be described in three distinct phases. First T cells interact with addressin which is expressed on the endothelium, to slow down cell within the bloodstream. This interaction is mediated by peripheral node addressin (PNAd) binding its ligand L-selectin (also known as CD62L), which is expressed on all naïve T cells as well as memory T

cells. The process of interaction is referred to as tethering and rolling. T cells slow down and roll along the wall of the blood vessel, enabling further interaction of receptors in phase II. The T cell arrests by integrin leukocyte function-associated antigen 1 (LFA-1) binding to intercellular adhesion molecule 1 (ICAM-1) expressed on HEV. By activation of the integrin, arrest occurs and interaction of CCR7 with its ligands CCL21 and CCL19 takes place. Alternatively, the arrest can be mediated by the interaction of CXCL12 and CXCR4 in some cases (von Andrian and Mempel, 2003).

LN entry is a very tightly controlled process that ensures only memory and naïve CD8 T cells can enter. Even though other cell types express some of the ligands they are not able to home the LN, because all three specific signals are needed for efficient homing *via* HEV (Bajenoff et al., 2006). This becomes apparent in B cells as they express lower levels of L-selectin and thus home with lower efficiency to LNs compared to T cells.
Also, mature cDC for that reason cannot home the LNs, which renders antigen-pulsed cDC a very ineffective tool in clinical applications until now.

Within the LN, retention (CXCR4, CCR7) and exit signals (S1P) are in balance and regulate LN residency on different cells. Naïve CD8 T cells have been shown to reside in the LN for up to 21 hours. Naïve CD4 T cells remain in the LN for significantly less time, up to 12 hours.
CD8 T cells reside in the deeper areas of the paracortex within the LN. Here they interact mostly with cDC1.
T lymphocytes leave the LN *via* medullar sinuses, a process which is mediated by sphingosine-1-phosphate (S1P) upregulation on T cells (Cyster and Schwab, 2012).

1.5 Spatio-temporal dynamics of T cells activation

In a viral infection, virus particles of cytolytic viruses (e.g. Vaccinia virus) can drain to local lymph nodes through efferent lymphatics, where they induce a local infection in the LN. Here, infected cDC present viral antigens to naïve CD8 T cells, inducing their activation and subsequent production of inflammatory cytokines. CD8 T cells are activated in three distinct phases (Brewitz et al., 2017; Eickhoff et al., 2015; Mempel et al., 2004). First, naïve CD8 T cells circulate through the body in search of their antigen. They travel through multiple LNs and scan the tissue. Once they encounter their specific antigen presented by an APC (in this case a cDC), the naïve CD8 T cell

will have multiple short contacts with this cDC and progressively decrease its motility. This phase can take up to 8 hours during which the cell starts to upregulate activation markers (e.g. CD69, IL2rα), finally arresting at the cDC and staying in contact for a prolonged period. This marks the starting point of phase II, defined by this long-lasting stable interaction with the cDC. The activated CD8 T cell will integrate signals from the cDC and start producing inflammatory cytokines like IFN-γ and IL-2.
Additionally, the production of XCL1 by the CD8 T cell leads to the recruitment of cDC1 from the paracortex of the LN to the priming cluster in the interfollicular area. The antigen-specific recruitment of CD8 T cells leads to the formation of a cluster of CD8 T cells, arresting at the infected cDC for the initial priming. Additional cells are being recruited to the priming site, such as NK cells, plasmacytoid dendritic cells (pDC), and innate T cells. At the same time, CD4 T cells also get activated by different cDC in an antigen-specific manner. This again leads to clustering on a separate cDC in a slightly different compartment of the LN. The fact that two distinct clusters are formed could indicate that CD4 and CD8 T cells initially need different activation signals or different cues by the cDC and its environment.

After the initial activation of antigen-specific CD4 and CD8 T cells, these cells migrate to deeper areas of the LN, namely the paracortex where they interact with XCR1$^+$cDC. This interaction has previously been described as the second phase of T cell activation, described by Thorsten Mempel and others (Mempel et al., 2004). This prolonged interaction between effector cells and XCR1$^+$cDC lasts from 12-36 hours post-infection. The XCR1 receptor binds XCL1 and XCL2, which are produced by CD8 T cells and NK cells respectively, in the initial priming cluster. XCR1$^+$cDC are very potent in cross-presenting, a process defined by the uptake of antigen and presentation of the processed antigen *via* MHC class I molecules. This enables the cDC to integrate signals coming from MHC class I- and II-restricted cells, conveying CD4 T cell help to the activated CD8 T cell. The activated CD4 T helper cell is essential for cross-presentation of antigen by the XCR1$^+$cDC to CD8 T cells. It has been shown that CD4 T helper cells induce changes in XCR1$^+$cDC *via* CD40-CD40L interactions. This interaction triggers higher expression of the antigen-presentation machinery and enhances the co-stimulatory capacity of the cDC. This process seems especially important in contexts of MHC class I presentation, like anti-tumor responses. The antigen must first be taken up by the cDC and broken down into peptides which can then be loaded onto MHC class I molecules, to be accessible to cytotoxic T lymphocytes.

The CD4 T cell help enhances the cDC capacity to stimulate CD8 T cells, which in turn promotes a more potent CD8 T cell response. CTL can expand significantly better and have a higher capacity to produce IFN-γ. Additionally, the recall response in "helpless" CD8 T cell memory cells has been shown to be impaired (Eickhoff et al., 2015; Schoenberger et al., 1998; Shedlock and Shen, 2003; Sun and Bevan, 2003).

Based on transcriptional changes in mice many master transcription factors such as T-box expressed in T cells (T-bet), eomesodermin (EOMES), and inhibitor of DNA binding 3 (ID3) are altered in CD8 T cells by CD4 T cell help (D'Cruz et al., 2009; Joshi et al., 2007; Kaech and Cui, 2012). The secretion of IL-2 and IL-12 in the vicinity of the cDC by CD4 T cells and XCR1$^+$DC, respectively leads to upregulation of IL-2rα and IL-12 receptor on the CTL. This drives differentiation and metabolic changes, increasing the expression of effector molecules like TNF, Granzyme b, and IFN-γ.

Finally, lymphocytes upregulate certain chemokine receptors to position themselves perfectly in the microenvironment of the LN, where they first encounter their antigen. Expression of CXC-chemokine receptor 4 (CXCR4), CX3C-chemokine receptor 1 (CX3CR1) and matrix metalloproteinases (MMPs) increases the CTL migratory capacity and enables them to invade niches promoting their survival and differentiation.

Especially, CXCR3 has been implicated to alter the balance between memory and effector differentiation. As chemokine receptor gradients in the LN markedly influence their migration, it was suggested that CXCR3$^+$ cells are more prone to become effector cells (Hu et al., 2011; Kurachi et al., 2011). These studies argue that CXCR3$^+$ cells are more readily recruited to a more inflammatory environment by CXCL9 and CXCL10. This would also enable these cells to have access to recently activated CD4 T cells producing IL-2.

In summary, CD4 T cell help drives clonal expansion of CTL and their differentiation into effector and memory T cells. This is mediated by stimulation through the cross-presenting XCR1$^+$DC.

After activation of CD8 T cells in a viral infection, the cells undergo a proliferation phase called "expansion", a process well studied in the context of infection. During expansion mainly effector cells are generated to clear the pathogen. In an acute infection, three to four days after the infection the virus is cleared. The number of CD8 T cells reaches a maximum population size on day seven to eight post-infection.

This marks the start of the so-called contraction phase, cells that are no longer needed as short-lived effector cells will undergo apoptosis and the overall population size will contract. Still, not all of these cells undergo apoptosis. Few cells become memory cells and are destined to protect the body from reoccurring infections. These memory cells can respond rapidly to reinfection with the same pathogen and have a high potential for self-renewal.

Only recently it has been shown that the decision between memory and effector cell fate is imprinted earlier during the infection than initially proposed (Chen et al., 2019; Yao et al., 2019). Already on day three post-infection, cells seem to acquire typical signatures of memory cells. Treg might be able to regulate this fate decision early on during the viral infection. To which extent is this fate decision mediated by IL-2 consumption?
Not only is the proliferation of CD8 T cells and Treg influenced by IL-2, but also impacts critical metabolic and transcriptional pathways that define cell survival, effector differentiation, metabolic reprogramming, and memory formation. IL-2 can also induce activation-induced cell death (AICD) and thereby acts as an immunosuppressive.

1.6 Aim of the study

Infections skew the fine balance of homeostasis and cause inflammation and tissue damage. Treg are maintaining this balance by dampening the immune response thereby ensuring organ functionality and preventing tissue damage (Arpaia et al., 2015; Loebbermann et al., 2012, 2013). This dampening of the immune response needs to be tightly balanced to avoid deleterious effects slowing down the clearance of viral infections. By limiting the adaptive immune response Treg act to preserve essential organ functions of the host but enable the infection to be cleared. Multiple studies have shown that depletion of Treg during a viral infection leads to improved viral control (Kinter et al., 2004; Rushbrook et al., 2005) but concomitantly leads to enhanced collateral damage to the tissue (Loebbermann et al., 2012, 2013).

It is still unclear how Treg achieve this fine-tuned regulation and which mechanisms are utilized for the best possible clearance of the infection while maintaining tissue function.

The mechanism of T cell-mediated immune suppression has been studied in other contexts before. Loss of Treg function leads to severe autoimmune pathology even in steady-

state (Kim et al., 2007). Mechanistically, these studies show that Treg locate close to auto-reactive T cells and restrict their IL-2 access (Liu et al., 2015; Wong et al., 2021). This was supported by an *in vitro* study modeling IL-2 competition as a viable mechanism to control effector T cell responses (Oyler-Yaniv et al., 2017).

We wanted to address whether IL-2 competition is also relevant for Treg-mediated control in the context of viral infection. To understand the potential competition dynamics we aimed to additionally investigate the underlying Treg spatio-temporal localization and migration. Understanding the timing and spatial aspects of this regulation might allow for interventions tweaking the immune balance toward potentially beneficial clinical outcomes (e.g. immunotherapy).

This however requires a detailed understanding of the IL-2 competition. Another main aspect of this study was to reveal the competitive relationship between Treg, CD4, and CD8 T cells. We were interested in the *de facto* IL-2 consumption of each competitor in this environment and were determined to shed light on the impact of Treg regulation on the effector T cells.

In summary, this work is addressing two major points that have not been resolved so far in Treg biology. First, we established an understanding of the spatio-temporal dynamics of Treg during a viral infection. This further helped us to gain a detailed understanding of the IL-2 competition between Treg and effector cells, delineating the impact of Treg regulation through IL-2 competition on CD8 T cells and their effector function.

2 Material & Methods

2.1 Methods

2.1.1 Viruses

The viruses utilzed in this study were highly purified by using two consecutive sucrose gradient purification steps. VV-OVA and VV-G2 was previously described and generated by homologous recombination cloning techniques (Kastenmuller et al., 2013). The virus was stored at -80°C in cryo vials.

2.1.2 Mouse lines

Mice used were maintained under specific pathogen-free conditions, housed in individually ventilated cages (IVC). The mice were kept in an animal facility Zentrum für Experimentelle Molekulare Medizin (ZEMM) in Würzburg. C57BL/6J were purchased from Janvier, France. The animals were kept in accordance with the animal guidelines provided by the GV-SOLAS, the society for laboratory animal science. Transgenic and knockout mice were all on the same genetic background as control C57BL/6J mice. Animals used for experiments were age-matched and gender-matched, when necessary. Mice used were between 8-16 weeks old. Some mouse lines were set up by inter-crossing of the mouse lines mentioned in Table 2.1.

2.1.3 Treatment of mice

Infection

Virus infection was done locally by injecting virus diluted in PBS into the footpad (foothock, Kamala (2007)). In short, virus stock was diluted in 30 µL PBS to a final concentration of $1x10^6$-10^7 PFU VV-OVA and injected subcutaneously into the foot. Systemic infection with VV was performed by injection of $1x10^5$ PFU intraperitoneal in 100 ml of diluted virus in PBS.

Mouse strain	Reference	Description
B6	n.a.	C57BL/6JRj non-transgenic mice were purchased from Janvier Laboratories and used as wildtype controls (wt)
CD25ko x OT-1	Willerford et al., 1995	This mouse line is deficient in IL2rα expression and was inter-crossed with OT-1 resulting in CD8 T cells deficient in CD25
CXCR3ko x OT-1	Hancock et al., 2000	This mouse strain is CXCR3 deficient by targeted knock-out of the gene locus. This line has been inter-crossed with OT-1 resulting in OT-1 CXCR3 deficient CD8 T cells
FoxP3-DTR	Kim et al., 2007	This mouse strain contains an internal ribosome entry site (IRES), a human diphtheria toxin receptor (DTR) and an enhanced green fluorescent protein (EGFP) downstream of the internal stop codon of the x-linked FoxP3 gene. Treg are marked by EGFP and can be depleted by injection of diphtheria toxin (DTX)
FoxP3EGFP-cre-ERT2 x r26 LSL tdtomato	Rubtsov et al., 2010 Madisen et al., 2010	This mouse line carries a EGFP in the gene locus FoxP3 fused to an inducible Cre recombinase. Additionally, this intercrossed mouse line carries a tdtomato in the rosa 26 locus, which is not transcribed due to a stop codon in front of the gene, flanked by loxP sites. By tamoxifen application, the Cre translocates into the nucleus and the stop codon is cut out. Treg are labeled with fluorescent tdtomato and can be tracked
FoxP3-Luci-DTR	Suffner et al., 2010	This mouse strain co-expresses a luciferase, EGFP and a DTR. BAC transgenic targeting led to approx. 75 % depletion efficiency which prevents catastrophic autoimmunity
EGFP	Schaefer et al., 2001	The mouse strain expresses the fluorescent protein EGFP under the ubiquitin C promotor and was used as a reporter inter-crossed with other lines
IL2fl x CD8cre	Maekawa et al., 2008 Popmihajlov et al., 2012	This mouse strain expresses a CD8a-Cre, which leads to Cre activity in peripheral $CD8^+$ T cells, inter-crossed with a *IL2* gene knock-out construct that leads to excision of exon I and II of the *IL2* gene upon Cre activity These mice have peripheral CD8 T cells that are deficient in IL-2 production
OT-1	Hogquist et al., 1994	This mouse strain contains a transgenic insert in the TCRalpha-V2 and TCRbeta-V5 gene. The T cell receptor resulting from this recognizes ovalbumin (OVA) residues $OVA_{257-264}$ (SIINFEKL) in the MHC I context
P14	Pircher et al., 1989	This strain carries a re-arranged TCR which specifically recognizes the peptide P14 in the LCMV glycoprotein 2, GP61-80 epitope in an MHC class I restricted manner
SMARTA-1	Oxenius et al., 1998	This mouse strain is a TCR-transgenic mouse line. The $CD4^+$ T cells possess a TCR that recognizes the MHC class II restricted LCMV GP_{61-80} epitope
Tdtomato	Kastenmüller et al., 2013	This mouse stain expresses tdtomato downstream of a human ubiquitin C promotor. We used this strain inter-crossed with various mouse lines to congenically mark cells
Venus	Swanson et al., 2016	This mouse stain expresses venus downstream of a CAG promotor. We used this strain inter-crossed with various mouse lines to congenically mark cells

Table 2.1. List of mouse strains used in this study

Tamoxifen treatment

Tamoxifen treatment was done by oral gavage with a metal gavage needle. Tamoxifen was solubilized in corn oil (0.0192 g/3mL) and vortexed vigorously, then incubated 30 min at RT in a ultrasonic bath until solubilized. Mice were given 125 µL of suspension two weeks before the start of the experiment once per week *via* oral gavage.

The expression of the reporter was checked before and after treatment *via* blood analysis.

Depletions

Treg(DTX):

Treg were depleted by three consecutive intra-peritoneal injections of 100ul PBS with 500 ng of Diphteria toxin.

CD4 antibody depletion:

CD4 depletion was done by i.p. injection of 300ug of anti-CD4 Antibody (BioXell) or isotype control antibodies. CD4 Depletion was done 24-48 h before analysis.

CD8b antibody depletion:

CD8b depletion was performed on day -1 and 0 prior to starting the experiment by injection of 100ng intra-peritoneal

Adoptive T cell transfer and labelling

Isolation of naïve T cells was done from donor mice, in short spleens and peripheral Lymph nodes were harvested and homogenized through metal cell strainers. A red blood cell lysis was performed by resuspending the cell pellets in 5ml ACK-Buffer for 5 min. The lysis was stopped with PBS FCS and cells were spun for 8 min 1600 RPM at 4 °C. Cells were resuspended in Stemcell isolation buffer and cells isolated according to manufacturer protocol. To achieve purification of naïve T cells, biotinylated anti-CD44 antibody was added at a final concentration of 1:10000 to the antibody mix mentioned in the manufacturers protocol.

Non-fluorescent T cells were labeled either with 1uM Cell Tracker Green (CTG) or Cell trace Violet (CTV) by incubating the cells for 10 min in 37°C medium containing the labeling agent. This medium should not contain FCS. To stop the reaction cells are washed with a large volume of FACS buffer containing FCS. The cells were washed twice and counted in a Neubauer chamber, then adjusted to a concentration of $1x10^4$-$2x10^6$.

2.1.4 Flow cytometry

Cells in single-cell suspension were always kept in FACS buffer with 2 % FCS on ice. For surface staining cells were incubated shortly before staining with a blocking buffer

containing FC Block IgG serum (1:66) and normal mouse Serum (NMS) at a concentration of 1:100 in 50 µL total volume. A double concentrated antibody mix for surface receptors was added after 5-10 min in a volume of total 100 µL.

pSTAT5 staining protocoll

Harvested LNs were meshed in 1.5 ml centrifugation tubes with pestils and a meshing devive (VWR). The LN were harvested into 200ul of FACS Buffer, meshed and transferred to a 15ml centrifugation tube. Cell suspension was kept on ice at all times. The cells were fixed as soon as possible (not longer then 5 min after harvesting) with Lyse Fix buffer pre-warmed to 37°C for 10 min in a 37°C waterbath.

The following steps were done according to manufacturers protocol. In short, cells were washed 3x with PBS and permeabilized for 30 min with pre-chilled (-20°C) Perm Buffer III (BD) and washed three times after with FACS buffer.

Cells were then blocked for 15 min on ice (s.o.) and stained in 100 µL of surface antibody mix. Cells were washed three times in FACS buffer after staining and acquired on a Attune NxT Flow cytometry device.

For intracellular staining of transcription factors simultaneously with pSTAT5 the TFP Staining Kit was used and manufacturers instructions followed. In summary, cells were fixed in Lyse-Fix Buffer 1x on ice for 40-50 min, washed 3x in perm/wash buffer, permeabilized with pre-chilled Perm Buffer III 30 min on ice.

After multiple washing steps with perm/wash buffer, cells were stained as previously described. Intra-cellular antibodies were stained simultaneously with surface antibodies in a total volume of 100 µL.

Cell sorting (scRNA seq)

Foxp3$^+$ CD4$^+$ cells were sorted with a FACSAria cell sorter: Cells were kept strictly on ice to ensure the highest viability possible. Cells from each group were separately stained with a specific TotalSeq$_{\text{TM}}$ Antibody mix and cell surface antibodies mentioned above for 30 min on ice. Approximately 7500 Treg from each group were then sorted into the same tube and processed for sequencing.

Intravital two-photon imaging

Mice were anesthetized by breathing a isoflurane air mixture (2.5% for induction, 1-1.5% for maintenance, vaporized in an 80:20 mixture of O2 and air). When surgical tolerance was achieved popliteal LN was exposed and positioned to be imaged by intravital microscopy. The microscope is enclosed by a pre-warmed chamber which gives steady conditions for the exposed LN and mouse. The LN was always covered by pre-warmed NaCl solution to maintain physiological conditions.

To capture dynamic images a stack of up to 57 µm was imaged by step wise imaging of 3 µm layers at a time. One z-stack was acquired every 40 sec.

pSTAT5 transiency assay

Spleenocytes were incubated with hIL-2 for 20 min at 37 °C in RPMI and washed with a volume of 100x PBS FCS. A positive control was immediately fixed, giving a representation of the maximal signal per condition (10U/ml, 1U/ml, 0.01U/ml).

Every 10 min after washing of excess IL-2 one sample of the stimulated spleenocytes was fixed for 10 min at 37 °C and pSTAT5 protocol done as described in section paragraph 2.1.4.

For pSTAT5 transiency of CD8 T cells, IL-2 insufficient naïve CD8 T cells were isolated as described in paragraph 2.1.4.

T cells were then incubated with CD3/CD28 at a concentration of 1 µg/mL for 18 h at 37 °C in T-cell medium to bring up the surface expression of CD25 on the surface of T cells. CD25 was additionally stained to ensure proper activation and upregulation of the IL2 receptor chain α.

Cells were then mixed with purified CD4 T cells and incubated as described initially. Due to this Treg and CD8 T cells could be looked at in comparable incubation conditions. PSTAT5 signal was then assessed every 10 min after incubation in three different concentrations of hIL-2 for 20 min.

2.2 single-cell RNA sequencing

For sorting and staining of Treg see paragraph 2.1.4. Sorted single cells were encapsulated into droplets with the help of a ChromiumTM Controller and then processed following the anufacturer's protocoll. Individual cell transcripts were encapsulated with a bead, carrying a unique barcoded 16 base pair '10X Barcode' and a unique molecular identifier (UMI). The cDNA librariest were generated by a 'Chromium$_{\text{TM}}$ Single Cell 3' Library & Gel Bead Kit, also following the manufacturer's protocol. The Libraries were then quatified by QubitTM 3.0 Fluometer and quality was checked using a Bioanalyzer with the High Sensitivity DNA Kit. Libraries were then sequenced in a 50 bp paired end mode with the NovaSeq 6000 system. The demultiplexing of the sequencing reads was performed by the CellRanger software (version 2.0.1). The reads were aligned to a mouse mm10 reference genome using STAR aligner software. Quantification of the expression levels of mouse genes and the generation of gene-barcode matrices were extracted from the aligned reads. The following scRNA sequencing data analysis was performed by using the Seurat R package (version 3.2) (Stuart et al., 2019).

For identification of the hashtags for each cell, the HTODemux function in Seurat package was used with the standard parameters. Doublet exclusion was performed by excluding cells with more than one hashtag. Cells not identified with a hashtag were also excluded. All remaining cells were analysed in downstream analysis.

Quality control was performed as described by Stuart et al.. Viable cells were determined by excluding cells with more total transcripts than 10000. Also, cells with a higher percentage than 9% mitochondrial transcripts and a UMI count of above 2900 were excluded. The 2000 most variable genes were used for downstream analysis to calculate principal component plots after log-normalization and scaling. The principle component analysis (PCA) was utilized to create dimensional reduction and to visualize a uniform manifold approximation and projection(UMAP) plot, to identify unique clusters. Contaminating cells were excluded from the analysis by gene specific removal. B cells, monocytes, CD8 T cells, macrophages and NK cells were removed.

The pathway analysis was performed by using the Clusterprofiler package. GSEA MSigDB databases were used to check enrichment for IL-2 downstream genes (Mootha et al., 2003; Subramanian et al., 2005). Visualization of the cluster defining genes was done by the Viridis package.

2.3 Materials

2.3.1 Equipment

-Anesthetic apparatus: Tec3, Eickemeyer, Tuttlingen
-Balances: CP2201, Sartorius, Göttingen
-Centrifuge: Multifuge 3 S-R, Heraeus, Hanau; Sprout mini centrifuge, Biozym, Hessisch Oldendorf;
-Cryostat: CM 3050S, Leica, Hamburg
-Flow cytometer: FACSAria II, Becton-Dickinson, Heidelberg
Attune NxT 4 Laser, Thermo scientific fisher, Waltham Aurora Northern Lights 5-Laser Setup, Cytek Biosciences, Amsterdam Aurora Northern Lights 4-Laser Setup, Cytek Biosciences, Amsterdam
-Freezer: -20°C Liebherr, Biberach; -80°C VIP ECO ULT freezer, Panasonic, Avon Cedex
-Incubator: Binder, Tuttlingen
-Infrared lamp HP3616, Philips, Hamburg
-Lasers: Tunable Chameleon laser, Coherent, Santa Clara
-Stemcell technologies: purification magnet, Easy Eight and according CD4, CD8 T cell Isolation Kits, Vancouver, Canada
-Microscope: SP8, Leica, Hamburg
-Mouse cages: Tecniplast Smartflow, Hohenpeißenberg
-Neubauer Chamber: Assistent, Karl Hecht GmbH, Sondheim
-Pipette boy: Integra Biosciences, Biebertal -Pipette: Research plus (10, 20, 200, 1000), Eppendorf, Hamburg
-dissection tools: Bochem, Weilburg; Hammacher, Solingen; F.S.T., Heidelberg
-Refrigerator: 4°C Liebherr, Biberach
-Workbench (sterile): Envair ECO, ENVAIR GmbH, Emmendingen
-Vortex: neolab, Heidelberg
-Ice machine: Ziegra, Isernhagen, Germany

2.3.2 Consumables

-Canula: 100/50 Sterican, B. Braun, Melsungen
-FACS tubes: Sarstedt, Nümbrecht

-FALCON tubes: 15 ml, Greiner bio-one, Solingen 50 ml, Sarstedt, Nümbrecht
-Glas pipets: Greiner, Nürtingen
-Feather Nylon gauze Labomedic, Bonn
-Pipet tips: Ultratip 1000 µL, Greiner bio-one, Frickenhausen
TipOne 200 µL, STARlab, Hamburg
Pipette Tip 10 µL neutral, Sarstedt, Nümbrecht
-Nümbrecht Reaction tubes microtubes 0.5 ml, 1.5 ml, 2 ml, Sarstedt
-Nümbrecht Sterile filter AcroVac Filter Unit PES 0.2 µm Supor, Pall Life Sciences
-Dreieich Syringes 2 ml, 5 ml, BD Discardit II, Becton-Dickinson, Heidelberg
-Tissue culture plates TPP Tissue culture testplates 96, 24, 6 wells, Trasadingen

2.3.3 Chemicals and Reagents

-Ammonium chloride (NH4Cl) Merck, Darmstadt
-B8R 20 peptide Xaia custom peptides, Göteborg
-β-Mercaptoethanol (C2H6OS) Aldrich, St. Louis
-Brefeldin A Sigma Aldrich, München
-Bovine serum albumin (BSA) Roth, Karlsruhe
-Cell labelling dyes CFSE, CFDA SE cell tracer kit, Invitrogen, Eugene Cell tracker Orange (CMTMR), ThermoFisher Scientific, Eugene Cell Tracker Blue, Invitrogen, Eugene Cell Tracker Green, LifeTechnologies, Rockford
Dimethylsulfoxid (DMSO) AppliChem, Darmstadt
Diphtheria Toxin calbiochem, San Diego
-Disodium phosphate (Na2HPO4) AppliChem, Darmstadt
-Ethanol 70% (v/v) Otto Fischar, Saarbrücken
Ethylene diamine tetraacetic acid (EDTA) 0.5M pH 8.0, Applichem, Damstadt
-Embedding medium Tissue-Tek® O.C.T.™ Compund, Sakura, Alphen aan den Rijn
-Fetal bovine serum (FBS) Good Filtrated Bovine Serum, PAN Biotech
-Fluoromount-G® ebioscience, San Diego
-Gelatine from cold water fish skin (GCWFS) Sigma Aldrich, München
-Hydrochloric acid (HCl) Roth, Karlsruhe Hydrophobic Barrier
-(PAP) Pen ImmEdge™ Pen (H-4000), Vector Laboratories
-Burlingame Isofluran Forene® , AbbVie, Ludwigshafen
-Medium RPMI medium 1640 1x, life technologies, Rockford
-Monosodium phosphate (NaH2PO4) Merck, Darmstadt

-Normal Mouse Serum (NMS) LifeTechnologies, Rockford
-Normal Rat Serum (NRS) LifeTechnologies, Rockford
-Normal Rabbit Serum (NRaS) LifeTechnologies, Rockford
-Paraformaldehyd (PFA) AppliChem, Darmstadt
-Phosphate buffered Saline (PBS) Biochrom AG, Berlin
-Potassium bicarbonate (KHCO3) Merck, Darmstadt
-Penicillin/Streptomycin/Glutamine Thermo Fisher Scientific, Waltham
-Pluronic® F-127 LifeTechnologies, Eugene
-Sodium hydroxide (NaOH) Roth, Karlsruhe
-Sodium periodate (NaIO4) Sigma Aldrich, St. Louis Sucrose Sigma Aldrich, München
-Tris base AppliChem, Darmstadt
-Triton-X GERBU, Gaiberg
-Trypan Blue 0.4%,
-0.85% NaCl, BioWhittaker® , Lonza

2.3.4 Antibodies

-CD3ε F, 1:200 145-2C11 eBioscience, San Diego
-CD4 F, 1:200 RM4-5; IV, 500 µg GK1.5 BD Biosciences, Heidelberg; BioXcell, West Lebanon
-CD8α F, 1:200 5H10 ThermoFisher, Waltham
-CD8βIV, 53-5.8, BioXCell, BioXcell, West Lebanon, USA -CD25 F, 1:200 3C7, BD Biosciences, Heidelberg
-CD69 F, 1:200 H1.2F3 eBioscience, Sand Diego
-CD127 F, 1:200 A7R34 eBioscience, San Diego
-pSTAT5 F, 5 µL pY694, BD Biosciences, Heidelberg
-CD62L F, 1:200, MEL-14, Biolegend, San Diego
-Thy1.1 F, 1:400, OX-7, Biolegend, San Diego
-Thy1.2 F, 1:400, 30-H12, Biolegend, San Diego
-CD103 F, 1:300, 2E7, Biolegend, San Diego
-CD127 F, 1:50, A7R34, Biolegend, San Diego
-CCR2 F, 1:50, SA203G11, Biolegend, San Diego
-CD218a F, 1:50, P3TUNYA, ThermoFischer, Waltham
-CD278 F, 1:200, C398.4A, Biolegend, San Diego
-CD274 F, 1:200, 10F.9G2, Biolegend, San Diego

-Foxp3 F, 1:400, FJK-16S, ThermoFischer, Waltham
-GP33 tetramer F, 1:50 kindly provided by NIH
-GFP polyclonal, F 1:1000, ThermoFischer, Waltham
-Gzmb F, 1:200, GB11, BD Biosciences, Heidelberg
-Itgb7 F, 1:100 DIB27, Biolegend, San Diego
-Klrg1 F, 1:200, 2F1, Biolegend, San Diego
-Ly6c F, 1:400, HK1.4, Biolegend, San Diego
-TCR vα2 F, 1:200, B20.1, Biolegend, Sand Diego
-CD80 F 1:100, 16-10A1, Biolegend, San Diego
-CD152 F 1:100, UC10-439, Biolegend, San Diego
-CD44 F 1:100, IM7, Biolegend, San Diego
-TCRβF 1:200, H57-597, Biolegend, San Diego
-CXCR3 F 1:50, F CXCR3-174, Biolegend, San Diego

2.3.4.1 Kits

-CD4 T cell Isolation Kit, mouse, Stemcell technologies Inc, Vancouver, Canada
-CD8 T cell Isolation Kit, mouse, Stemcell technologies Inc, Vancouver, Canada
-Cytofix/Cytoperm BD Biosciences, Heidelberg
-Perm Buffer III, BD Biosciences, Heidelberg
-TFP Cytofix/Cytoperm Fixation Kit, BD Biosciences, Heidelberg
-5x Lyse/Fix, BD Biosciences, Heidelberg

2.3.4.2 Software

-Adobe Creative Suite CS6 Adobe; Illustrator, San José
-BD FACSDiva 8.0.1 BD Biosciences, Heidelberg
-FlowJo X 10.0.7 Tree Star, Inc., Ashland
-Imaris 8.2.1 Bitplane, Belfast
-Microsoft Office 2011 Microsoft, Unterschleißheim
-GraphPad Prism 9 GraphPad Software, La Jolla

2.3.4.3 Viruses

-Vaccinia Virus expressing OVA; provided by Jonathan Yewdell, National Institute of Allergy and Infectious Diseases, Bethesda
-Vaccinia Virus expressing G2, provided by Jonathan Yewdell, National Institute of Allergy and Infectious Diseases, Bethesda

2.3.4.4 Media and Solutions

All stock solutions and buffers are filtered sterile or are autoclaved. Afterwards the solutions, media and buffers are kept under sterile conditions.

-10x ACK buffer (Ammonium – Chloride – Potassium) 1.5 M NH4Cl, 100 mM KHCO3, 10 mM Na2EDTA in distilled water (pH value 7.2)
-Cell medium 8% heat-inactivated FBS, 50 µM β-Mercaptoethanol, 4 mM L-Glutamin, 100 U/ml Penicillin und 100 µg/ml Streptomycin in RPMI 1640 medium
-Easy sep buffer 0.5% (v/v) BSA, 2 mM EDTA in 1x PBS
-Immunhistology and flow cytometry Blocking buffer 1% (v/v) FBS, 1% (m/v) GCWFS, 0.3% (v/v) Triton-X in 0.1 M Tris, 1% NMS is added directly before use
-FACS buffer 2% (v/v) FBS, 0.02% (v/v) NaN3 in 1x PBS
-Fixation buffer (PLP) 2.12 mg NaIO4 in 3.75 ml
- P-buffer, 3.75 ml L-Lysine and 2.5 ml 4% PFA (pH value 7.4, adjusted with 10 M NaOH), preparation directly before use
-L-Lysin solution 0.2 M L-Lysine in P-buffer
-Na2HPO4 solution NaH2PO4 solution 0.2 M Na2HPO4 in distilled water 0.2 M NaH2PO4 in distilled water -P-buffer 40.5% (v/v) 0.1 M Na2HPO4, 9.5% (v/v) NaH2PO4 in distilled water (pH value 7.4)
-PFA solution 4% (w/v) PFA in PBS, gradually heated (pH value 7.4)
-Sucrose solution 30% (w/v) Sucrose in P-buffer Tris buffer 1 M Tris base in distilled water (pH value 7.5, adjusted with 10 M HCl)

3 Results

We were interested in the migrational behavior of Treg during an ongoing viral infection to better understand the underlying Treg mechanisms regulating adaptive immune responses *in vivo*. For this, we first looked at the interplay of all the above-mentioned cells, during the onset of Vaccinia virus infection in the popliteal LN (popLN).

3.1 Spatial dynamics of Treg during the priming of antigen-specific CD8 T cells

Proximity is one of the key aspects of Treg in most regulatory mechanisms. As we described previously, multiple different cell types (e.g. cDC, NK cells, and plasmacytoid DC) are recruited to the initial priming cluster of CD8 T cells (Brewitz et al., 2017). In particular, cDC and CD8 T cells engage in prolonged interactions and co-arrest during this phase (Mempel et al., 2004). We wanted to find out if and how Treg regulate CD8 T cells during priming. We sought to understand the Treg localization in relation to the arrested CD8 T cells and interrogate possible direct interactions between these two cell types.

To address these questions, we utilized intravital 2-photon imaging and analyzed the spatio-temporal dynamics of Treg. We used an inducible Foxp3-ERT2cre x R26 LSL tdTomato reporter system. This mouse strain expresses a fusion protein of a mutated human estrogen receptor and the Cre recombinase under the control of the *Foxp3* promoter (see Table 2.1). Upon tamoxifen treatment, the fusion protein undergoes a conformational change, which enables it to translocate to the nucleus and recombine the DNA sequence at loxP sites.

The mouse strain was intercrossed with the R26 LSL tdTomato reporter. This reporter carries a gene cassette with a constitutively active promoter inserted into the ROSA26 locus that also expresses a red fluorescent protein (tdTomato). The transcription of the mRNA is prevented by a stop codon expressed in front of the gene cassette. The stop codon, which is flanked by two loxP sites, can be removed via Cre recombination, allowing the transcription and subsequently the translation of the fluorescent tdTomato protein.

This mouse model eliminates two major limitations seen in previous Treg reporter systems (e.g. Foxp3-cre or Foxp3-EGFP).
First, the inducible Cre has a higher specificity than the constitutively active Cre. Indeed, the Foxp3-cre strain labeled all cells that previously expressed Foxp3. However, it has been shown that Treg can lose *Foxp3* expression and it is unknown if other cell types could have expressed the gene during their development (Rubtsov et al., 2010). The ERT2-cre only labels *bona fide* Treg that have active Foxp3 expression at the time of tamoxifen treatment. Even though only genuine Treg are labeled, the efficiency is slightly reduced and only approximately 85 % of Treg are labeled (Rubtsov et al., 2010). Secondly, the brightness of GFP and EGFP under the promoter of *Foxp3* is sufficient for histological analysis and even superficial intravital imaging approaches. However, we wanted to address the dynamics of Treg during the later phases of infection in which cells reside in the deeper areas of the LN. Therefore, we needed a reporter that enabled us to visualize signals from deeper areas of the lymph node. This was achieved with this brighter tdTomato reporter and a customized tunable laser that allowed optimal excitation of the tdTomato fluorescent protein.

We infected mice locally with Vaccinia-virus ovalbumin (VV-OVA) subcutaneously in the footpad. 12 h prior we transferred OT-1 T cells, that were TCR-specific for OVA and expressed a green fluorescent protein (GFP). To analyze the dynamics of Treg and their interaction with the antigen-specific T cells, we prepared the popLN for live imaging 7 h post-infection. Recordings of the cells were acquired for up to 60 min at a time.

We were expecting direct interactions or at least prolonged proximity between Treg and antigen-specific CD8 T cells or their interacting dendritic cells, as most proposed regulatory mechanisms rely on either a niche competition or a direct regulation of the target cell.

We discovered that Treg were indeed often in close proximity to the clustering CD8 T cells (OT-1)(Figure 3.1A). However, we could not find Treg stably interacting with CD8 T cells or spending prolonged time around antigen-presenting cDC, which is marked by the clustering CD8 T cells in green (Figure 3.1A). We also checked the distribution of Treg within the LN and did not see any accumulation of Treg around the antigen-specific T cell clusters (data not shown).
Additionally, we found that Treg do not arrest and seem to migrate without prolonged arrests during this phase of infection. This is supported by Treg showing higher migration speed, increased track length, and lower duration of migrational arrest compared to

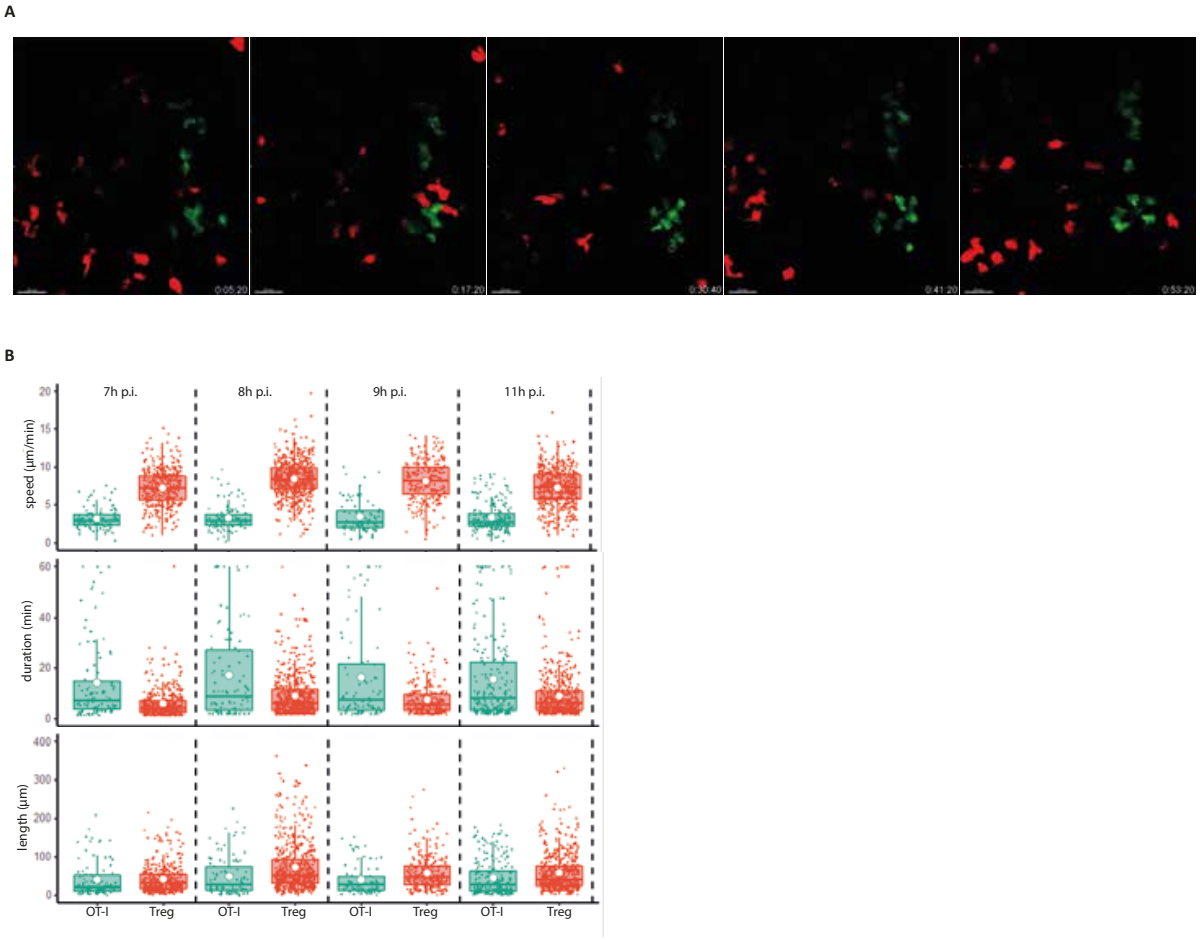

Figure 3.1. Intravital imaging of Treg dynamics during viral infection 8 h post-infection. We transferred 2-4x10^6 OT-1 T cells into Foxp3-ERT2cre-LSLtdTom mice that were previously treated with tamoxifen. One day later mice were infected with VV-OVA and prepared for intravital imaging 6-8h post-infection. (A) Treg dynamics during priming of antigen-specific CD8 T cells 8h p.i. Treg cells are shown in red and OT-1 T cells in green. The pictures are snapshots of intravital recordings for 60 min. The timestamps indicate the time frame of the recording. The scale bar indicates 20 µm. (B) Track analysis of Treg and OT-1 T cells comparing their migration speed, their duration spend arrested and track length. Each individual video from the same experiment has been analyzed (7-11h p.i.). This is a representative analysis of intravital imaging experiments with the same setup 8 h p.i. The data presented was acquired by Chloe Fenton.

antigen-specific CD8 T cells(Figure 3.1B). The majority of Treg displayed a migrational speed of 7 to 10 µm\min, whereas OT-1 T cells showed an average speed of 3 µm\min. The duration of OT-1 T cells spent arrested also drastically differs from Treg. Whereas the majority of Treg did not show migrational arrest for more than 15 min, OT-1 T cells arrested for varying time periods up to 60 min. The track lengths of Treg and OT-1 T cells did not reveal significant differences, despite Treg showing a trend towards higher track lengths compared to their counterpart.

Overall, we concluded that Treg do not show migrational arrest during the priming of CD8 T cells at the antigen-presenting cDC, but migrate in proximity. We can't rule out contact-dependent regulation by Treg, as we observed short contacts between Treg and OT-1 T cells.
However, we did not find any prolonged interaction, which indicates either that short interactions suffice to regulate the target cell or that Treg primarily regulate *via* contact-independent mechanisms.
CD4 helper T cells are not co-arresting at the same cDC during the priming of CD8 T cells but are primed in a distinct microniche (Eickhoff et al., 2015). During later phases of the infection activated CD4 helper T cells provide help to CD8 T cells around cDC1 in deeper areas of the LN.

3.2 Spatial dynamics of Treg during phase II of T cell activation

Next, we were interested in the migrational behavior of Treg during this phase, looking at potential interactions with CD8 T cells. Do Treg show proximity to antigen-specific T cells and further do they interact stably with them in order to regulate?
We analyzed Treg behavior during this later period of infection, when CD8 T cells are already primed by their cognate antigen.

To address this question, we chose the experimental setup described in section 3.1 but analyzed at later time points 20-24 h post-infection. We transferred OT-1 GFP^+ T cell prior to infecting tdTomato Treg reporter mice with VV-OVA and performed intravital imaging 20 h p.i. Clusters of OT-1 T cells gave us indication of ongoing interaction with $XCR1^+$cDC. We analyzed the behavior of Treg in proximity to the CD8 T cell cluster at the cDC1. Movement of Treg and OT-1 T cells was tracked in recordings of 60 min.

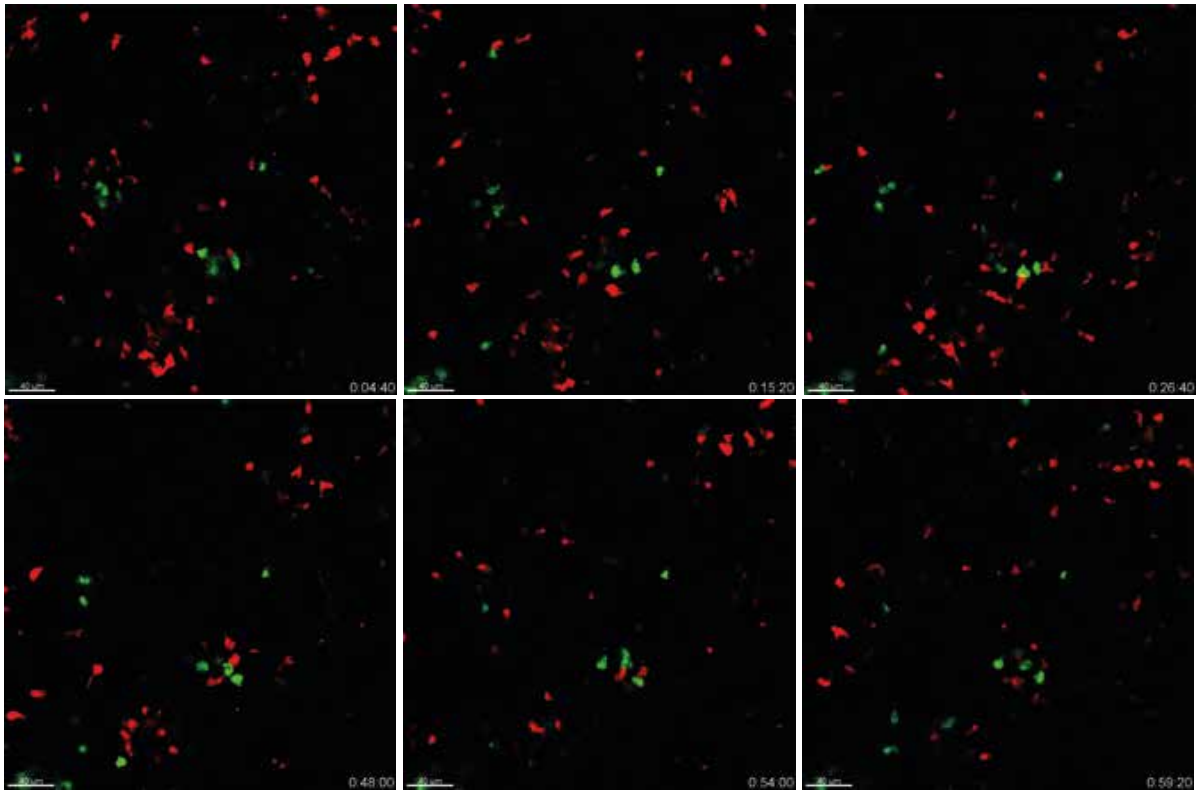

Figure 3.2. Intravital imaging of Treg dynamics during viral infection 20h post-infection. We transferred 2-4x10^6 OT-1 T cells into Foxp3-ERT2cre-LSLtdTom mice that were previously treated with tamoxifen. One day later mice were infected with VV-OVA and prepared for intravital imaging 18-20h post-infection. Shown are snapshots of an intravital imaging experiment conducted 20 h p.i. with Vaccinia virus. The picture show snapshots of clustered OT-1 T cells in green and Treg in red. The time during the 60 min recording is indicated by the timestamps. The error bar is 20 µm. The snapshots shown are representative of the imaging experiments 20-24 h p.i. The data presented was acquired by Chloe Fenton.

We did not find Treg showing migrational arrest. Despite transient proximity between Treg and CD8 T cells for short periods of time (<15 min), we did not find any Treg stably engaging in long-lasting interactions with CD8 T cells or the cDC they interacted with (Figure 3.2). Short contacts can be appreciated as seen in the third panel of the upper row in Figure 3.2. Despite short contacts the next panel shows the Treg already in a different position arguing against their arrest. Also, CD8 T cell clusters are less dense and Treg still migrate in proximity to the clusters. Some small loose accumulations of Treg can be seen (Figure 3.2, first panel), however, these accumulations do not show any association with OT-1 T cells.

This led us to the conclusion that Treg do not engage in prolonged interactions despite showing proximity to the OT-1 T cells even at later time points during the infection. A contact-dependent mechanism of regulation seems unlikely or multiple short interactions suffice to exert Treg function.
Nevertheless, there could still be the possibility that we overlooked stable interactions or did not check the right timing of the regulation process. A small fraction of cells might exert effector function and we can't exclude it with this approach. However, it has been shown before that Treg control of the effector pool size is strongest during the first 48 h of infection (Kastenmuller et al., 2011). We refined the results shown in the study and could show that strong regulation was exerted during the first 24 h (data not shown). This indicates that we addressed an adequate time period.
To exclude the possibility that we are missing the regulatory process within the live imaging experiments or overlooking a specific subset of actively regulating Treg or Treg that regulate *via* contact-independent mechanisms we performed an unbiased analysis of Treg functionality with single-cell RNA sequencing.

3.3 Transcriptional profiling of Treg during infection

Not only did we try to understand Treg heterogeneity to address specific subsets, but further were interested in transcriptional data that would support distinct localization of Treg in certain areas of the LN (e.g. chemokine receptors). The approach additionally offers insight into possible contact-independent regulation, e.g. Treg showing IL-10 production or enhanced expression of granzymes and perforins.

We wanted to compare Treg from an environment of steady-state and infection, to

assess the changes that Treg undergo within an inflammatory environment, where active regulation takes place.

To address the aforementioned, we sorted Treg from LN of uninfected and infected Foxp3-GFP-DTR mice and analyzed them *via* single-cell RNA sequencing. Here, we utilized the knock-in Foxp3-GFP-DTR reporter strain, because it was crucial to analyze all Treg. The knock-in construct of this strain allows for highly specific labeling of the cells (GFP within the gene cassette), despite the expression of GFP being very dim, which is not optimal in other experimental setups.
LNs from uninfected mice and Vaccinia infected mice (28 h p.i.; local infection, s.c.) were pooled from at least three mice per group and the separate groups stained with a distinct CD45/MHC-I antibody that carried a unique identifier barcode for each cell. This enabled us to determine from which experimental group each specific cell originated. Therefore, we were able to compare cells from two distinct conditions within the same single-cell analysis, while minimizing technical variances and mitigating batch effects. Cells were then counted, mixed at a 1:1 ratio, and sorted as GFP^+ $CD4^+$ $CD3^+$ single cells. This allowed us the best resolution in the scRNA sequencing data on both populations due to equal contribution from both groups.

The analysis of the data set resulted in unbiased clustering of 7 clusters in all Treg (Figure 3.3A). The infected and steady-state Treg form distinct clusters that can be distinguished by the hashtags used during the preparation (Figure 3.3B, C). The clusters can be divided into naïve-like Treg (*Ly6c1, Ccr7, Sell*), effector Treg (*Itgae*), and further subclusters (*Nr4a1*). The clustering of the steady-state Treg and the infected Treg shows high similarity and the cluster-defining markers are analogous within naïve-like Treg of infected and steady-state, e.g. cluster '0' and cluster '1' (Figure 3.3C). The uniform manifold approximation and projection (UMAP) shows 3 clusters for the uninfected group, as well as for the infected group(Figure 3.3A). Cluster '6' contained cells from both groups.
Heterogeneity seems to increase among naïve-like Treg in the infected group, showing two distinct clusters, whereas the heterogeneity was lost within the effector-like Treg showing one cluster less compared to the steady-state Treg.
Interestingly, some cells from the infected group showed high similarity with steady-state Treg, arguing that these cells were not impacted by the infection yet, or only recently homed to the LN (red dots within blue clusters Figure 3.3B). In comparison, within clusters from the infected group, only a negligible number of cells showed similarity to

steady-state Treg.

This indicated that the transcriptional profile of most Treg from the infected group was altered. These changes were likely induced by infection causing an inflammatory environment (Figure 3.3B). Despite the changes in transcriptional profile, the subset distribution that was found in steady-state Treg was maintained. To understand this better, we performed a 'geneset enrichment pathway' analysis to gain insight into the changes that Treg in infected mice undergo. The inflammatory environment and subsequent effects, like tissue damage, cell death, and output of immunomodulatory cytokines likely contribute to an altered gene signature in Treg from infected mice, therefore, clustering separately from steady-state Treg. Besides genes attributed to IFN-induced pathways, we also found genes from the 'IL-2 STAT5 signaling pathway' being enriched (Figure 3.3D, marked with red box). The increased IFN signature stems from viral infection, known to have pleiotropic effects in modulating the innate and adaptive response to pathogens, especially viruses (McNab et al., 2015).
Interestingly, genes within the 'IL-2 - STAT5 pathway' were markedly enriched and we tried to understand the basis of this.

First, we validated the results from the single-cell analysis on protein level and looked for additional markers that could facilitate the distinction between naïve-like and effector-like Treg.

The expression of the cluster-defining genes was validated in a flow-cytometry experiment, replicating a very similar experimental setup as in the single-cell analysis, to ensure the highest possible comparability of the data. In order to compare protein expression levels of surface and intracellular molecules, careful considerations in staining routine have to be made. Comparison of expression levels of proteins (gMFI) is more robust if the staining is done within the same cell suspension, so the concentration of antibody is equal for every cell. We achieved this by using Fopx3.LUCI-DTR thy1.1 mice for the infected group and thy1.1/thy1.2 heterozygous mice for the steady-state analysis. This enabled us to discriminate the cells from infected and non-infected animals via flow cytometry, similar to the hashtags in the single-cell sequencing analysis. Lymphocytes from steady-state LN and infected LN (VV-OVA, 28 h p.i. s.c.) from at least three mice per group were pooled and mixed at a 1:1 ratio (steady-state/infection) to be stained in the same medium and antibody concentration. We validated clusters defined by CD103 expression (effector-like Treg) and CD62L expression (naïve-like Treg) in both infected and steady-state LN (Figure 3.4A, B). This was in line with the single-cell sequencing

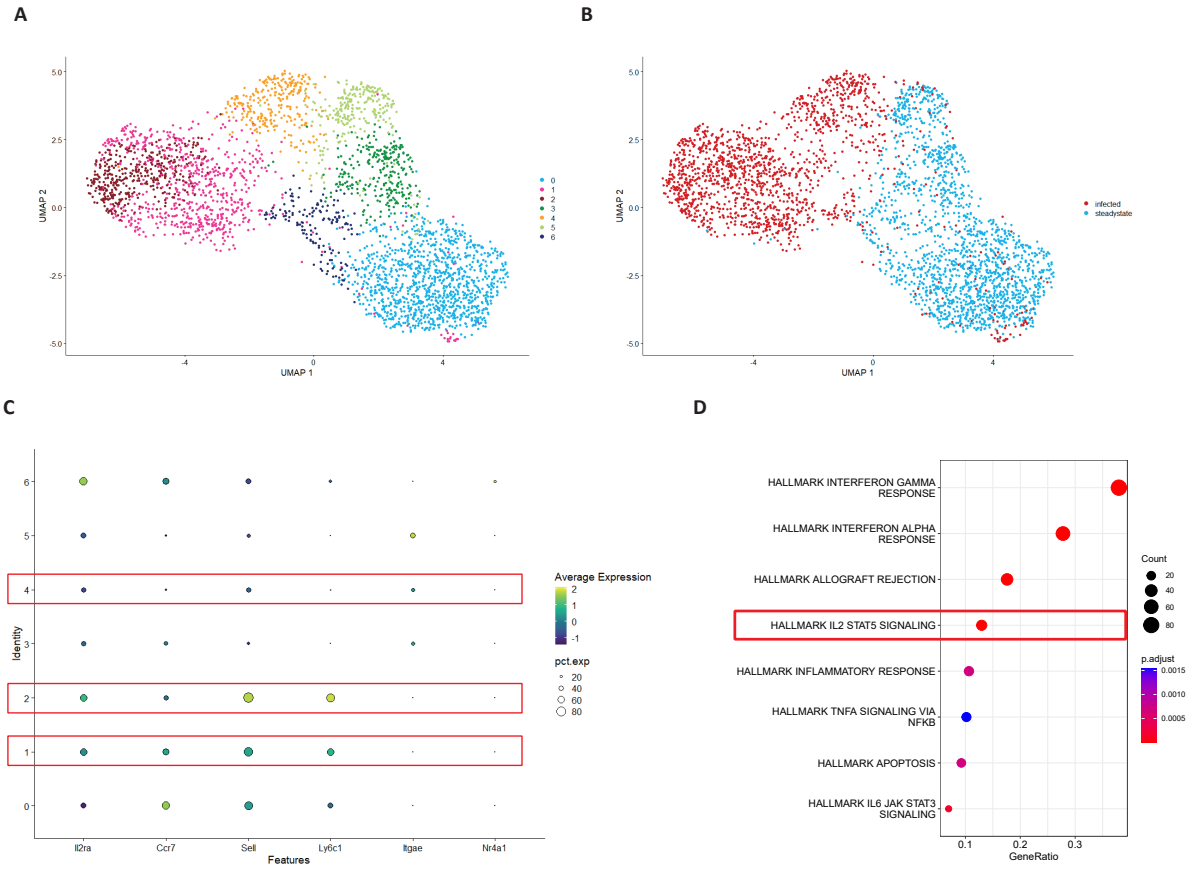

Figure 3.3. Single cell RNA sequencing analysis of Treg from infected and steady-state mice. Treg were isolated from VV (1x10^7 PFU) infected popLN 28 h p.i. and peripheral skin draining LNs from steady-state mice at the same time. Pooled LN from at least 3 mice were stained with antibodies and hash-tagged, separately within their group. Cell suspensions were mixed at a 1:1 ratio, sorted as single CD3$^+$ CD4$^+$ GFP$^+$ Treg and processed for single-cell RNA sequencing. (A) UMAP projection of 3187 single cells, clustering by their identity indicated by the color code. (B) UMAP of previously hash-tagged cells that stemmed from infected or steady-state hosts. (C) Dot plot of selected genes associated with identified clusters. Color represents mean expression values depicted for each cluster. The dot size refers to the fraction of cells in the cluster expressing the respective gene. The red boxes mark clusters that refer to the infected group. (D) Hallmark pathway analysis of differentially expressed genes (DEG) in the infected group of Treg compared to steady-state group Treg. As indicated by the red box, the hallmark IL-2 STAT5 signaling gene set was enriched among others. The dot size indicates the number of DEG allocated to the specific pathway and the color code indicates the adjusted p-value. Data represents one experiment with n=9 mice (4 infected, 5 control).

data shown in Figure 3.3C.

We compared the expression of multiple markers including the cluster-defining markers shown before (Figure 3.3C). We found a higher frequency of cells expressing Gzmb, CD62L and Ly6c. At the same time the frequency of cells expressing Icos, Il18r, and CD127 was higher in steady-state Treg. This seems to be based on enhanced retention of naïve-like Treg during infections getting activated, indicated by the higher proportion of Ly6c cells in Figure 3.4B. The expression level of Ly6c however remained unchanged as can be seen by comparable mean fluorescence intensity (MFI) between Treg from infected and steady-state environments (Figure 3.5C). This could indicate that more Treg are recruited into the LN overtime during the ongoing infection, which overlaps with our observation that infected mice generally had bigger LN and contained more Treg (data not shown). However, the subsets present in infected mice are very similar compared to steady-state mice.

In order to shed light on the IL-2 pSTAT5 pathway being over-represented in our differentially expressed genes (DEG) in Treg from infected mice (Figure 3.3D), we analyzed the expression of IL-2 downstream genes in all cells. We implemented an IL-2 score for each cell by an algorithm used in cell cycle analysis. It calculates a score based on the expression of DEG within the STAT5 pathway (Mootha et al., 2003; Subramanian et al., 2005). We wanted to understand if specific subsets showed an increased IL-2 signature or if all Treg were impacted equally.

To our surprise, all Treg expressed genes associated with the IL-2 STAT5 pathway. This was unexpected, as published data suggests that a specific subset of Treg suppresses auto-reactive CD4 T cells in steady-state mice (Wong et al., 2021). The IL-2 downstream analysis pointed towards a population-wide signature that might indicate that all Treg get activated. Most interestingly, the biggest change in the IL-2 score could be seen in naïve-like Treg in infected mice (Figure 3.5). We compared analogous clusters of naïve-like Treg within steady-state and infected Treg (in this case cluster '0' and '1'). Analogous clusters are arranged next to each other in Figure 3.5.
Due to their enhanced IL-2 signature we argue that especially naïve-like Treg receive more IL-2 during infection and get activated. This leads to an enhanced gene signature downstream of IL-2. Effector-like Treg seem to have seen IL-2 before and do not change dramatically in their signature. In conclusion, integrated over time all Treg seem to have access to IL-2 and therefore are able to be active in regulation.
After having shown that the downstream signaling of IL-2 in naïve-like Treg had in-

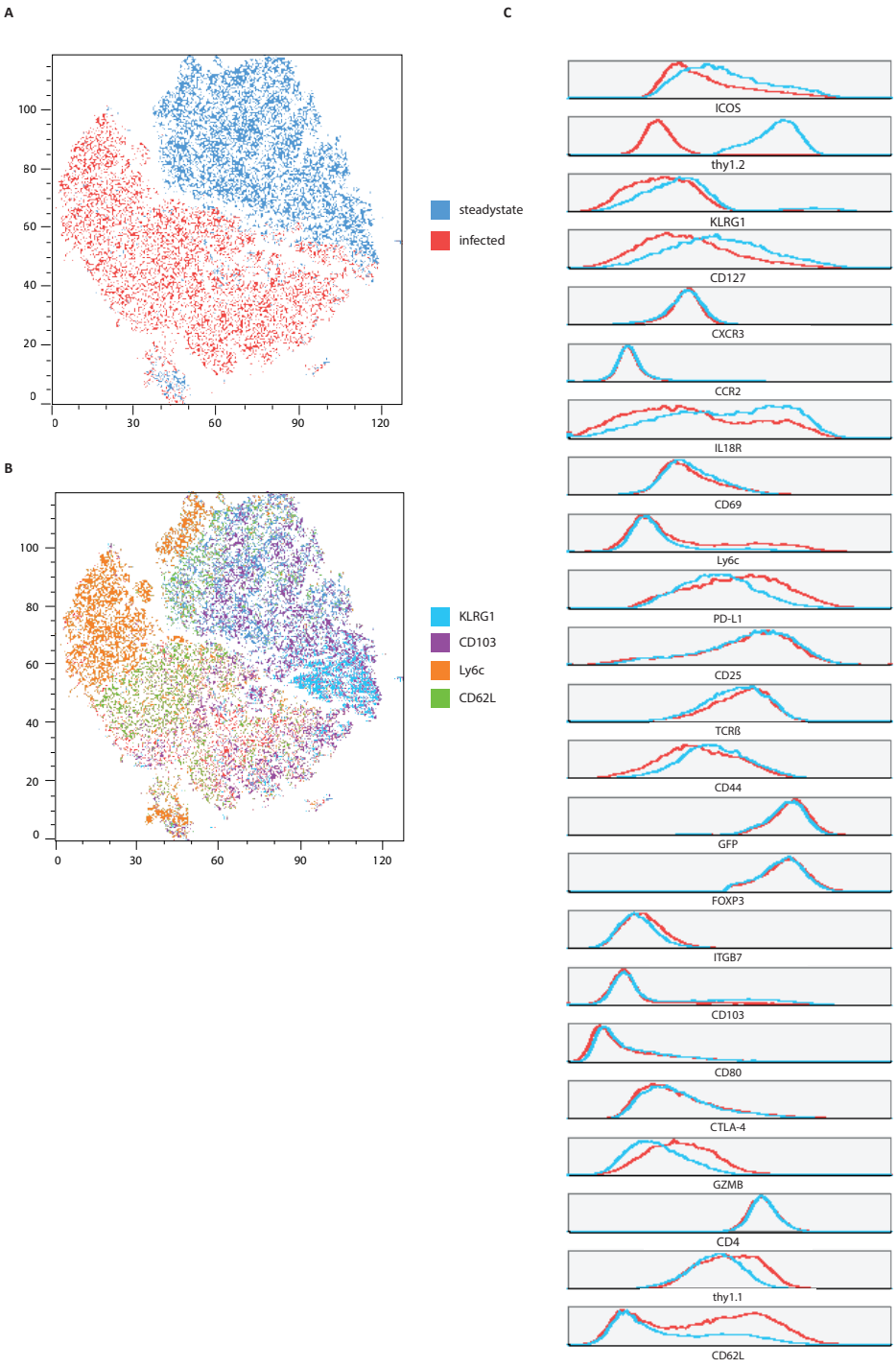
A
B
C
steadystate
infected
KLRG1
CD103
Ly6c
CD62L
ICOS
thy1.2
KLRG1
CD127
CXCR3
CCR2
IL18R
CD69
Ly6c
PD-L1
CD25
TCRß
CD44
GFP
FOXP3
ITGB7
CD103
CD80
CTLA-4
GZMB
CD4
thy1.1
CD62L

Figure 3.4. Flow cytometric validation of scRNA sequencing data. Congenically marked mice were either infected with Vaccinia virus for 28h (thy1.1) or remained uninfected (thy1.2). Replicating the single-cell sequencing approach, lymphocytes were isolated from peripheral skin-draining LNs and popLNs and mixed at an approximate 1:1 ratio. Lymphocytes were analyzed for their expression of various markers, identifying the subsets in the single-cell analysis. (A) tSNE plot of high-dimensional flow cytometry data from a mixed sample of infected group Treg and uninfected group Treg. tSNE is pre-gated on single-cell Treg identified by GFP expression and the group of each Treg can be re-identified by the congenic marker, which is indicated by the red and blue populations. (B) tSNE plot of subsets found in the flow cytometry analysis. RNA single-cell subsets could be identified in flow cytometry data and key molecules are indicated by color (light blue = Klrg1, violet = CD103, orange = Ly6c, green = CD62L). (C) Histogram overview of all markers comparing the groups infected versus uninfected. Data shown is representative of two independent experiments with (n $\geq$ 3 mice per experiment & per group).

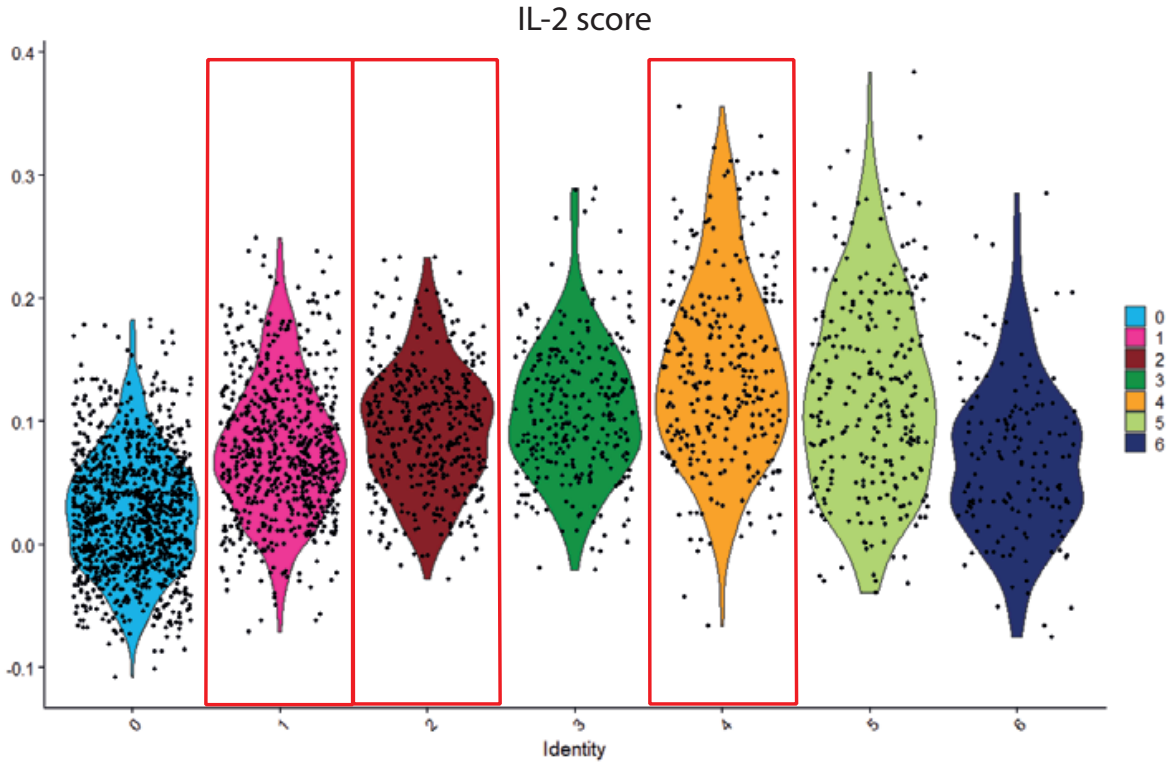

Figure 3.5. Downstream analysis of IL-2 signature genes. The IL-2 score is derived from the absolute number of genes expressed from the HALLMARK IL2 STAT5 SIGNALING geneset (199 genes) per cluster. The score was derived from the scRNA sequencing analysis by exchanging the gene list of the cellcycle scoring algorithm with the IL-2 gene list. The score compares analogous clusters in steady-state and infected groups of Treg populations. Red boxes indicate Treg stemming from the infected group. The numbers on the x-axis refer to the clusters found in the single-cell analysis.

creased, we were curious to explore the availability of IL-2 and the frequency of Treg having access to it.

3.4 IL-2 signaling in Treg and antigen-specific T cells

It has been shown before that Treg can compete for IL-2 with effector CD8 T cells *in vitro* (Oyler-Yaniv et al., 2017) and to understand the dynamics of this mechanism better, we looked at the phosphorylation of STAT5, one of the downstream targets of the IL-2 receptor in Treg. This molecule serves as a direct read-out of IL-2 signaling and allows us to understand, which cells have access to IL-2 at which time point during the infection.
We infected mice locally with VV and checked the frequency of pSTAT5$^+$Treg at different time points during the infection. In order to minimize technical variances of staining intensities and handling of samples, we infected the mice on different days to analyze multiple samples of different time points on the same day. We utilized local infection in the footpad, which drains to the nearest LN. As this infection does not cause systemic infection, we treated individual popLN as individual samples, despite being from the same mouse.
To identify Treg we used a Foxp3-GFP-DTR knock-in mouse model and utilized the gating strategy shown in Figure 3.6A. We were able to successfully stain CD8, CD4, and TCR-transgenic cells as well as their CD25 and pSTAT5 expression with high resolution, which needed careful optimization due to the harsh fixation protocol required to conserve the pSTAT5 signal. Despite the dim GFP expression of this reporter system, we were able to identify all Treg sufficiently by amplifying the GFP signal with an anti-GFP antibody. Also, the reporter system allowed for faithful identification of *bona fide* Treg, as this mouse model uses a gene insert within the actual *Foxp3* gene segment. Overall, this approach enabled us to gain detailed information about the fraction of Treg having access to IL-2. This enables us to make interpretations about the overall availability of IL-2 during the infection.

The steady-state frequency of pSTAT5$^+$Treg was approximately 20%, which is consistent with previously published data (Liu et al., 2015). Following infection, we observed an increased abundance of Treg in the popLN, as well as a higher fraction of pSTAT5$^+$Treg (Figure 3.6B, C). Within the first 12 h p.i., we did not observe a change in pSTAT5 frequency. The most prominent increase in pSTAT5 frequency among Treg was observed

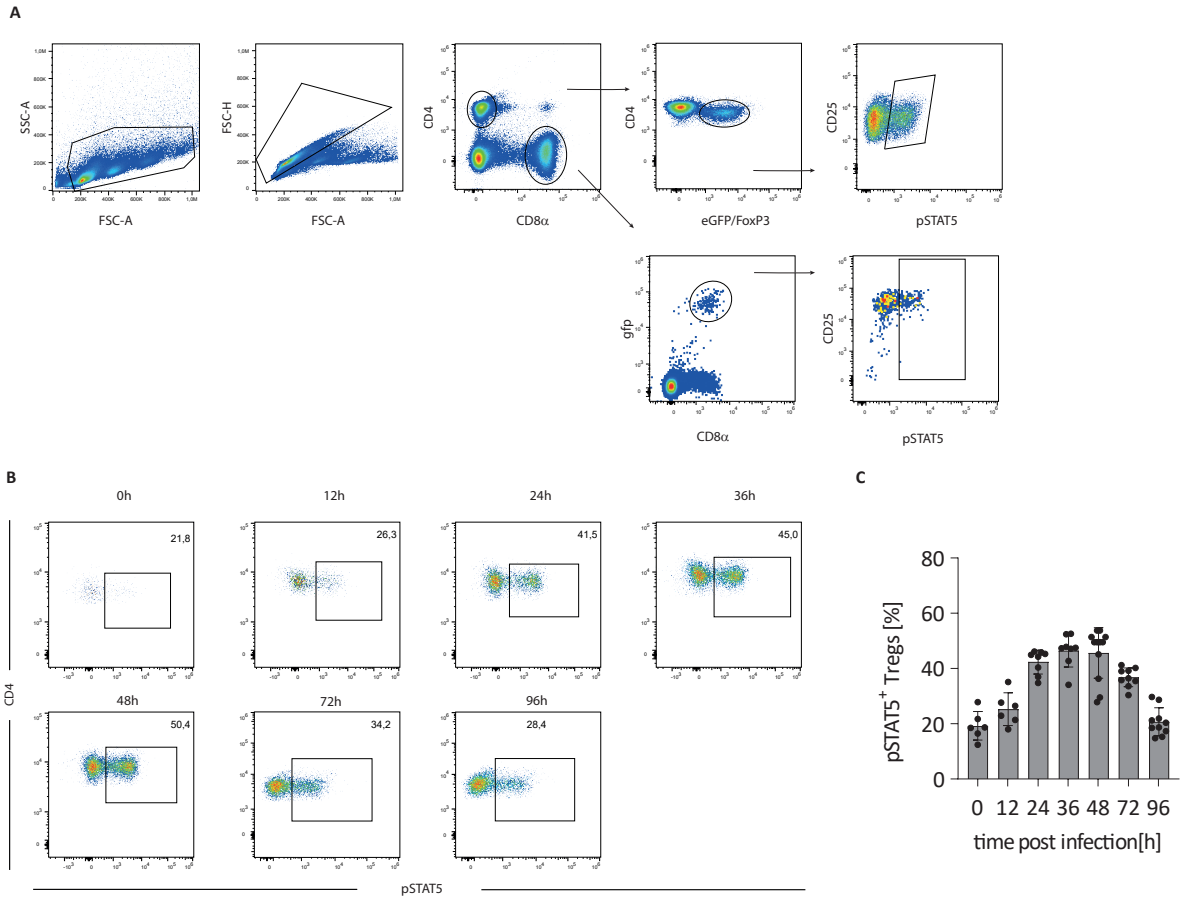

Figure 3.6. Flow cytometry analysis of T cells during a viral infection and pSTAT5 expression. Foxp3-DTR mice were infected with VV (1x10^7 PFU) and individual popLN isolated, meshed, and fixed immediately after dissection (A) Gating strategy of mouse T cells including Treg, CD4, CD8α, and antigen-specific T cells. The gating is done from lymphocytes to single cells, CD4 or CD8α T cell staining, GFP$^+$ Treg, and or GFP$^+$ OT-1 or smarta cells. The last plot in the upper panel shows the CD25 expression versus the pSTAT5 signal. (B) Time course of the pSTAT5 signal during a viral infection shown on Treg up to 96 h p.i. in representative flow cytometry plots from different experiments at indicated time points. (C) Frequency of pSTAT5$^+$Treg over the course of infection. Data is representative of at least two independent experiments (n $\geq$ 3 mice). Error bars indicate SD, data points represent individual popLN. In some experiments, single significant outliers were removed from data set.

between 12 h and 24 h going up from 25% pSTAT5$^+$Treg p.i. to approximately 40%, respectively. After, the frequency of pSTAT5$^+$Treg increased slightly from 24 h to 36 h and reached its maximum at 48 h post-infection with approximately 50% pSTAT5$^+$Treg. On days 3 and 4 post-infection, the availability of IL-2 for Treg seemed to decline again, shown by a lower frequency of pSTAT5$^+$Treg with 40% and approximately 20%, respectively.

Seeing increased frequencies of Treg being positive for pSTAT5 showed that Treg could indeed act as an IL-2 consumer, potentially competing for IL-2 in order to regulate CD8 T cells during a viral response. The increased pSTAT5 levels suggest an increased IL-2 production (Figure 3.6A), likely by activated CD4 and CD8 T cells, as previously published in LCMV infection (Humblet-Baron et al., 2016). Considering that Treg express CD25 early on and activated T cells being able to rapidly produce IL-2, not seeing a significantly increased frequency of pSTAT5$^+$Treg within the first 12 h was surprising. It indicates that Treg don't have access to the IL-2 produced early on or that secretion of IL-2 prior to 12 h is rather limited.

To address whether IL-2 competition by Treg could be a viable mechanism to control the expansion and differentiation of CD8 T cells *in vivo*, we tried to understand the relationship between consumption and production of IL-2. We wanted to find out if CD4 or CD8 T cells display the main source of IL-2 and in which way they consume IL-2.

For this, we first addressed the question of whether the absence of CD8 T cells alters the abundance of IL-2 that is seen by Treg.
As shown in Figure 3.6, Treg see more IL-2 during the course of infection, suggesting that more IL-2 is being produced over time. We addressed this question *via* a simple loss of function approach, depleting the endogenous CD8 T cell compartment by treatment with a very effective anti-CD8β depleting antibody that does not affect e.g. CD8α$^+$ cDC.

We did not observe major changes in the pSTAT5 frequency of Treg during the first five days of infection (Figure 3.7) comparing the control group against the CD8-depleted group. Treg had the same frequency of pSTAT5 at 12 h, 24 h, 48 h, 72 h, and 96 h within both groups. This either points to CD8 T cells not producing IL-2 or the Treg not having access to the IL-2 produced. CD8 T cells may produce IL-2 locally and consume it in an autocrine manner so that Treg do not have access to the released IL-2.
At 36 h a significant reduction in the frequency of pSTAT5$^+$Treg could be observed in

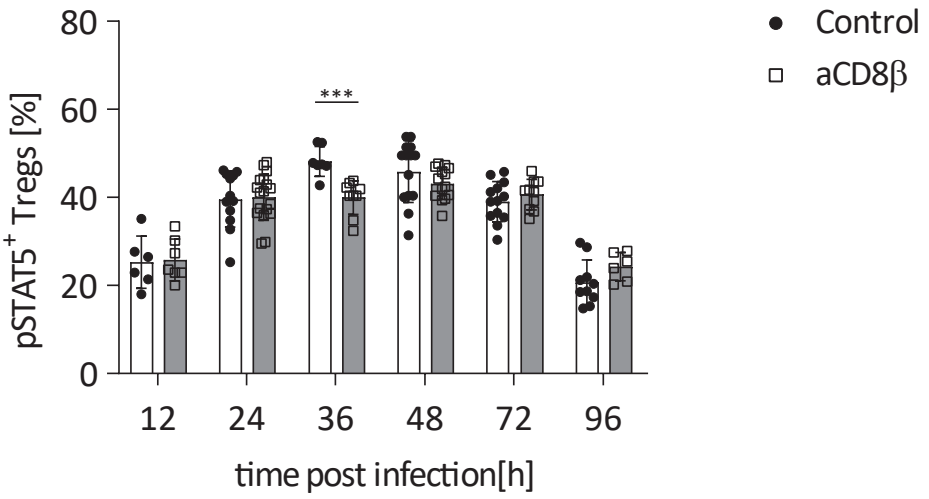

Figure 3.7. Impact of CD8 depletion on IL-2 availability for Treg. CD8 T cells were depleted by antibody depletion at day -1 and day 0 *via* injection of 300ug anti-CD8β. Plot shows the frequency of Treg expressing pSTAT5 12 h-96 h p.i. Data is representative of at least two independent experiments ($n \geq 3$ mice). Error bars indicate SD, data points represent individual popLN and statistical analysis was done with multiple t-test. ***p-value < 0.001.

CD8 T cell-depleted animals (Figure 3.7). The frequency was slightly decreased from 50% in the control group to 40% in the CD8-depleted group.

This indicated that the absence of CD8 T cells led to decreased pSTAT5 frequency in Treg, likely due to CD8 T cells minorly contributing to the IL-2 consumption of Treg at 36 h in the control group. Possibly, CD8 T cells positively impacted the IL-2 availability at 36 h p.i. reaching a significant difference in pSTAT5 frequency of Treg. However, this does not allow interpretations about the amount of IL-2 produced by CD8 T cells during the infection. It is known that CD8 T cells can consume IL-2 and therefore we can only make interpretations of whether CD8 T cells have a positive or negative impact on the IL-2 availability within the LN, by consuming more IL-2 than they produce or vice versa.

Another possible explanation for the decreased frequency in pSTAT5$^+$Treg at 36 h p.i. could be that only very few T cell precursors (100-200) exist initially and are activated over time to proliferate and fight the infection. This would suggest that the IL-2 production increases over time and only contributed significantly at 36 h p.i. when sufficient numbers of T cells had been activated and started to proliferate. This is supported by personal observations from *in vivo* proliferation assays showing that the first antigen-

specific CD8 T cells start proliferating at 36 h p.i. (data not shown). Overall, CD8 T cells may produce IL-2 and Treg might consume it. However, we only found a significant difference at 36 h p.i. which suggests that our assay might not be sensitive enough, as it seems unlikely that only a 12 h time period is impacted.
Irrespective, we can conclude that CD8-derived IL-2 does not seem to be the major source of IL-2 for Treg.
To further address whether CD8 T cells can be an IL-2 source for Treg we increased the precursor numbers by transferring OVA-specific TCR transgenic T cells (OT-1) and infected with VV-OVA. We analyzed the pSTAT5 signal in Treg with additional producers and or consumers of IL-2 in the system.
In this experimental setup, between $10x10^4$ and $2x10^6$ were transferred to the mouse and activated by subsequent VV-OVA infection.

Treg did not show any difference in the frequency of pSTAT5 signal during any time points later than 12 h p.i. compared to an untreated group (Figure 3.6). However, at 12 h p.i. we found that in animals that received an OT-1 T cell transfer the pSTAT5 frequency of Treg was significantly increased to 40%-45% pSTAT5$^+$Treg, compared to approximately 25% in animals that did not receive a transfer. The frequency of pSTAT5$^+$Treg at 36 h and 48 h was very similar ranging from slightly below 45% up to 50% without transfer and 35% up to 45% in the transfer group. In both groups the frequency of pSTAT5$^+$Treg started decreasing at 72 h post-infection.
This mostly unchanged kinetics of STAT5 phosphorylation in Treg argues that CD8 T cells are not a major source of IL-2 for other cells in the LN during the course of infection. It seems that CD8 T cells do produce IL-2 early on, as indicated by the higher frequency of pSTAT5$^+$Treg at 12 h p.i. At later time points, Treg do not seem to have access to CD8-derived IL-2. They might contribute a minor amount of IL-2 in the first 24 h, which is consistent with a previous *in vitro* study and the result of the depletion of the endogenous CD8 T cells (Villarino et al., 2007). Some of the produced IL-2 by CD8 will be consumed in an autocrine manner by the activated CD8 T cells that have sufficient levels of IL2rα.

It is key to understand the source of IL-2 during VV infection to address competition as a regulatory mechanism. Therefore, we proceeded to look into CD4 T cells as a possible source of IL-2. Currently, experimental models available do not allow for the specific depletion of CD4 helper T cells, while protecting CD4$^+$ Treg cells. Therefore, we increased the precursor frequency of antigen-specific CD4 T cells as above with CD8

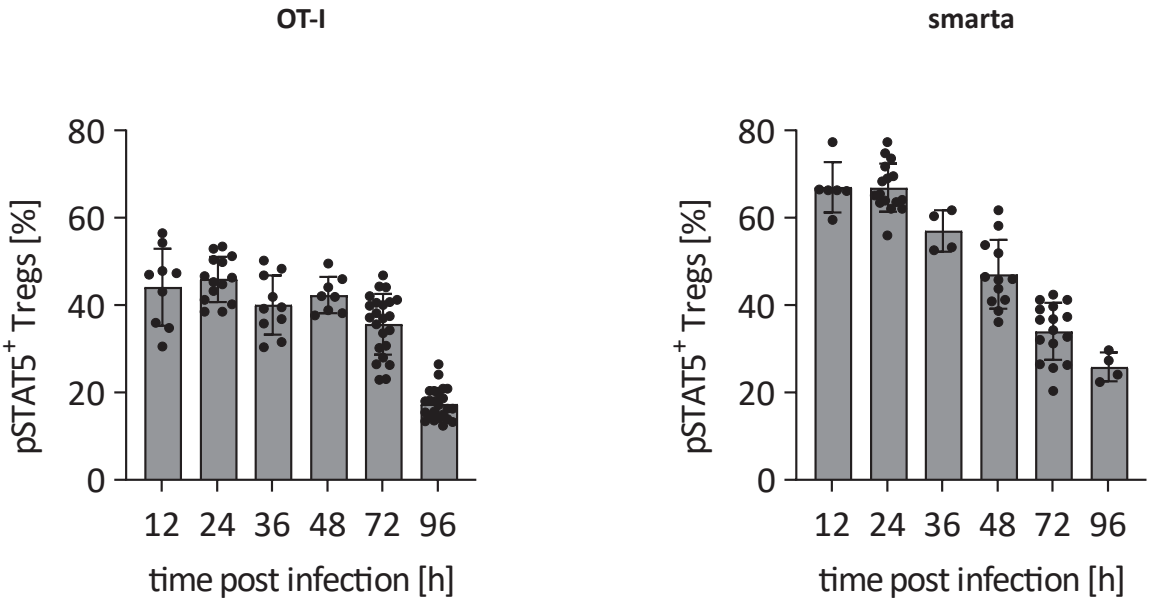

Figure 3.8. Impact of TCR-transgenic transfers on IL-2 availability of Treg. $1x10^4$-$2x10^6$ OT-1 CD8 T cells or $2x10^4$-$2x10^6$ smarta CD4 T cells were transferred at day -1. Foxp3-DTR mice were infected subcutaneously with VV-OVA/VV-G2 ($1x10^7$ PFU) and popLN analyzed at the indicated time points. All mice were sacrificed on the same day and all samples were treated equally. The first panel shows the transfer of OT-1 T cells and the impact of IL-2 sufficient producers/consumers on pSTAT5 frequency of Treg. The data shown is from at least two independent experiments with $n \geq 3$ mice. The second panel shows the same experimental setup with the transfer of smarta cells. The data shown is from at least two independent experiments ($n \geq 3$, n=2 (36 h, 96 h)). Error bars indicate SD, data points represent individual popLN.

T cells. Added antigen-specific CD4 T cells should give us insight into the net impact of CD4 T cells on the IL-2 levels seen by Treg.

Hence, we conducted a gain-of-function experiment, where similar to antigen-specific CD8 T cells, we added TCR-transgenic CD4 T cells (hereinafter called smarta cells) that recognize an LCMV peptide expressed within glycoprotein 2 (G2), $GP_{61\text{-}80}$. We transferred between $2x10^4$ and $2x10^6$ smarta cells and analyzed the frequency of pSTAT5$^+$Treg at 12, 24, 36, 48, 72, and 96 h p.i. with VV-G2 ($1x10^7$ PFU s.c).

We observed a largely increased pSTAT5 frequency among Treg and an earlier onset of the pSTAT5 signal compared to the endogenous kinetic (Figure 3.8, smarta panel). Whereas 20-25% of Treg showed pSTAT5 signal in experiments without T cell transfer at 12 h p.i., the frequency of pSTAT5$^+$Treg reached almost 70% with smarta cells present. The largely increased frequency of pSTAT5$^+$Treg reached its maximum at 24 h post-infection with 75% slowly decreasing over time. This was in stark contrast to the observations made in experiments without smarta transfer, where the frequency of pSTAT5$^+$Treg went from 25% at 12 h p.i. to a maximum of approximately 55% reached at 48 h, subsiding to almost steady-state levels at 96 h.
This data suggests a major contribution of antigen-specific CD4 T cells to the IL-2 consumed by Treg in the popLN. Not only does it indicate that CD4 T cells have a rapid and high output of IL-2 compared to CD8 T cells, but also Treg cells have access to the IL-2 and consume it. Whether CD4 T cells and Treg can both see the IL-2 produced is unclear.

To explore these possibilities, we wanted to address the IL2rα expression of smarta and OT-1 T cells. This allowed us insights into the capabilities of these cells to sense IL-2 with high-affinity and possibly compete with Treg. If smarta cells express the high-affinity IL-2 receptor, it is unlikely that they would not consume IL-2.

3.5 Expression level of CD25 on effector cells

Now, that we have established that CD4 T cells increase the net IL-2 availability within the popLN during the infection, we were curious about the CD25 levels of all T cells to better understand their capacity to compete for IL-2. The affinity of the IL-2 receptor is increased by a thousand-fold if all three sub-units of the receptor combine. The IL2rβ-chain and IL2rγ-chain are expressed rapidly by activated T cells (Shevach, 2012).

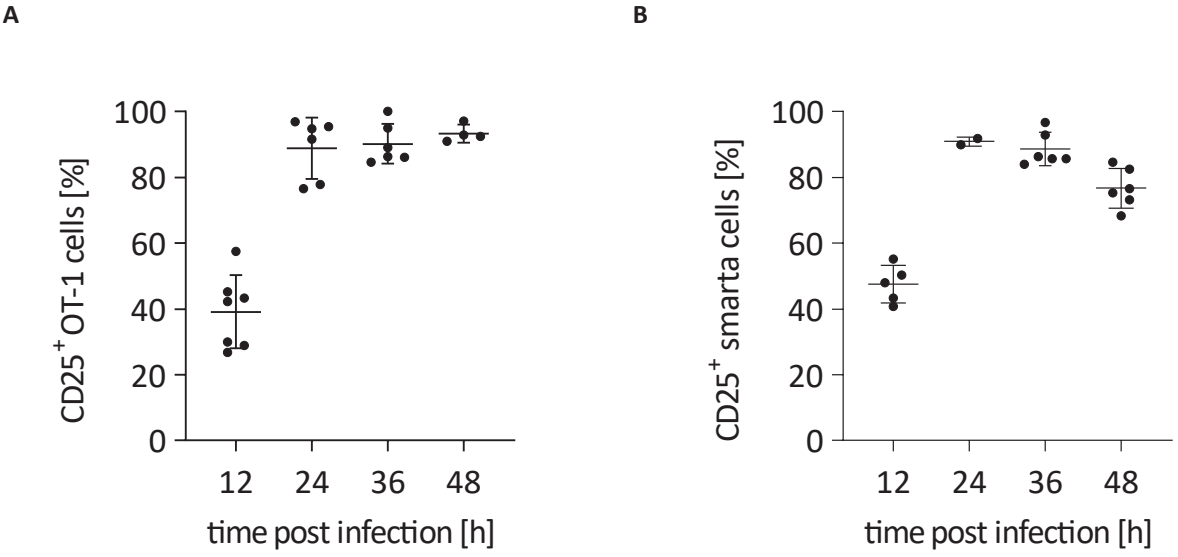

Figure 3.9. Frequency of CD25 expression on activated TCR-transgenic T cells. (A) $2x10^6$ OT-1 T cells were transferred to wt mice and infected with VV-OVA ($1x10^7$ PFU) s.c. PopLN were isolated and lymphocytes analyzed for their CD25 expression. ($n \geq 3$ mice per experiment). (B) $2x10^6$ smarta cells were transferred and wt mice infected with VV-G2 ($1x10^7$ PFU) s.c. and their CD25 expression shown by frequency of $CD25^+$ smarta cells. The data shown is from at least two independent experiments ($n \geq 3$, (48 h OT-1 n=2, 24 h smarta n=1)). Error bars indicate SD, data points represent individual popLN. Single significant outliers removed, e.g. 12 h (OT-1).

Consequently, the IL2rα-chain (CD25) is crucial for high-affinity sensing of IL-2.
We analyzed the expression of CD25 on CD4, CD8, and regulatory T cells. We again utilized TCR transgenic transfers and checked the expression of CD25 on those cells within the same animal. This made global CD25 expression comparable between Treg and its potential competitors, antigen-specific CD4 and CD8 T cells, independent of technical variances. Therefore, we compared the frequency of activated T cells expressing CD25 and also the density of receptors expressed on the surface (Figure 3.9, Figure 3.10).

At 12 h p.i. approximately 40% of activated CD8 T cells expressed CD25 and are therefore able to consume IL-2. At 24 h up to 95% of CD8 T cells express CD25. Also, at 36 h and 48 h p.i. the majority of CD8 T cells expressed CD25 with more than 90% being $CD25^+$ (Figure 3.9A).
CD4 T cells expressed CD25 within the same time frame(Figure 3.9B). At 12 h p.i. 50% of all transferred smarta cells expressed CD25 and at 24 h this frequency increase to 90%. Interestingly, the frequency decreased slightly over time, with 85-90% at 36 h and approximately 80% at 48 h. Nonetheless, the majority of activated T cells showed rapid induction of CD25 expression, indicating the capability to consume IL-2 and having high-affinity towards the cytokine.

Further, we compared the geometric MFI (gMFI) of CD25 expression between activated T cells and Treg in a ratio. By dividing the absolute gMFI of activated T cell by the absolute gMFI of Treg, we get a direct comparison, of which cell is more competitive in terms of affinity. On top of this, we accounted for the slight increase in CD25 levels within the Treg population over time due to known feed-forward feedback loops inducing higher expression of CD25 by IL-2 signaling (de la Rosa et al., 2004).
Conclusively, the ratio is a measure of the competitive CD25 receptor density at a population level.
As can be seen in Figure 3.10, smarta and OT-1 T cells express much lower levels of CD25 at 12 h p.i. For this comparison, only CD25 positive cells were considered. At 24 h p.i. OT-1 T cells already express higher CD25 levels on their surface, compared to Treg. In contrast to this, smarta cells only reach competitive CD25 gMFI levels in the late phase of infection (72 h, 96 h).
Of note, the OT-1 T cells already start decreasing CD25 expression levels at 96 h. This indicated a limitation of IL-2, as an auto-feedback loop ensures stable expression of CD25, which rapidly decreases as soon as pSTAT5 is not stably expressed. This is in line with decreasing pSTAT5 levels on Treg at 96 h, almost showing steady-state levels. In contrast, smarta cells reach the highest gMFI at this stage. This argues in favor of our previous data, showing that CD4 T cells are capable to increase the IL-2 consumption by Treg drastically during this phase and thus being 'on-site' of production allows them access to IL-2 and renders them able to sense IL-2 efficiently.

These findings established that T cells activated by their cognate antigen during Vaccinia infection can see IL-2 with high-affinity post 24 h. Also, the fraction of pSTAT5^{+}Treg increased at 24 h post-infection, indicating an increased IL-2 availability, likely coinciding with IL-2 production by activated T cells.
We were interested to see the competitive nature of IL-2 consumption as all T cells showed the ability to sense IL-2 at the peak of IL-2 availability.

3.6 pSTAT5 levels on antigen-specific effector cells

Despite the fact that Treg see IL-2 and the effector cells show rapid expression of CD25 being competitive in terms of affinity towards IL-2, this does not necessarily result in equal consumption of IL-2 *per se*. Differences in localization, migration, and temporal dynamics of the infection can lead to differences in IL-2 consumption of the effector

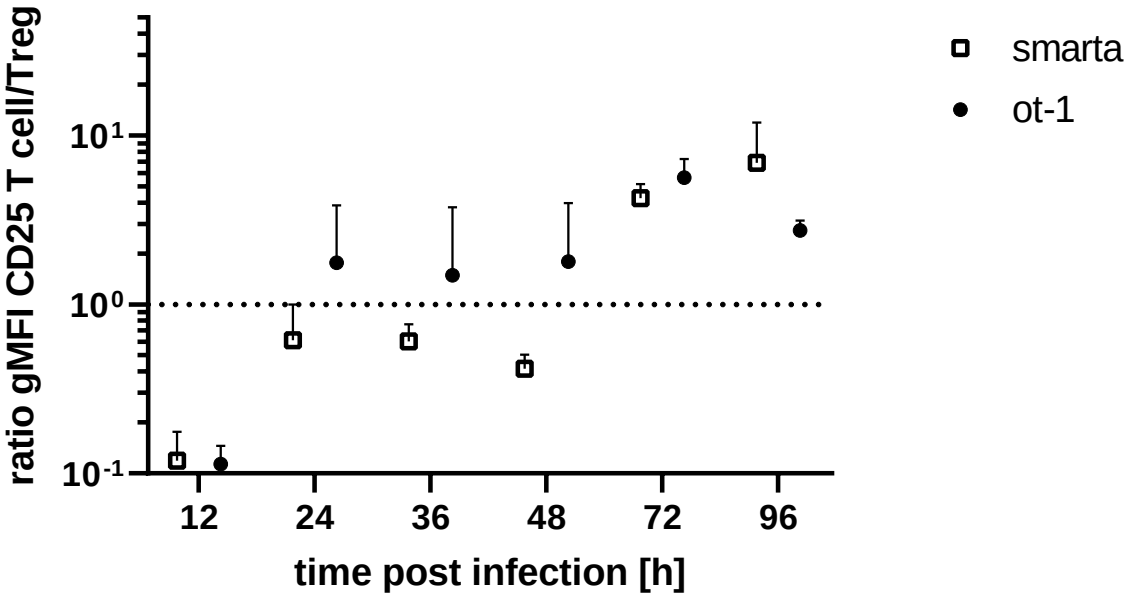

Figure 3.10. CD25 expression level comparison between Treg and TCR-transgenic T cells. 1x10^4-2x10^6 OT-1 T cells or 2x10^4-2x10^6 smarta cells were transferred to Foxp3-DTR mice and CD25 expression analyzed at the indicated time points post-infection (VV-OVA or VV-G2, 1x10^{7}PFU, s.c.) per individual popLN. The expression levels of the gMFI were normalized to the expression of Treg to compare within the same animal. Data is derived from at least two independent experiments (n $\geq$ 3 mice, n=2 (smarta 72, 96 h)). Error bars indicate SD, SD only displayed above data points.

cells. To address how relevant these factors are for IL-2 competition we analyzed the IL-2 downstream pSTAT5 signal of competing effector cells. We analyzed the frequency of CD4 and CD8 T cells that showed *de facto* signaling of IL-2 by pSTAT5 expression.

For this we utilized the same transfer model as in Figure 3.8, transferring TCR-transgenic OVA/LCMV reactive CD8/CD4 T cells, respectively. We analyzed their expression of pSTAT5 at different time points of the infection.

Treg in all instances showed higher or equal pSTAT5 frequency compared to activated CD8 T cells (Figure 3.11A & Figure 3.8). Despite 40% of all transferred CD8 T cells being pSTAT5$^+$at 24 h p.i., they did not quite reach the level of pSTAT5 compared to Treg that showed a frequency of 40-50% pSTAT5 at 24 h (Figure 3.11A). This argues that Treg are either positioned advantageous or have better access to IL-2 niches. Alternatively, they might have higher chances to encounter IL-2 due to distinct migrational activity scanning the LN constantly for IL-2, while CD8 T cells remain arrested for a substantial amount of time during the first 24 h of the infection.
CD4 T cells see even less IL-2, shown by their lower frequency of pSTAT5$^+$CD4 T cells at 24 h. 20% of CD4 T cells that have seen their antigen are pSTAT5$^+$. Whereas, CD8 T cells have a frequency of 30-40% pSTAT5$^+$cells between 24 h and 72 h, CD4 T cells have very low pSTAT5$^+$frequencies at 12 h from then on slowly increasing towards 96 h(Figure 3.11B). 96 h p.i. 40% of all transferred CD4 T cells express pSTAT5 and likely have consumed IL-2 recently. In comparison, 30% of all Treg show pSTAT5 expression at 96 h. Interestingly, this was the only time point, at which the frequency of pSTAT5 on activated T cells exceeded the pSTAT5 frequency among all Treg.
This supports that CD4 T cells represent a major source of IL-2 throughout the infection. Intuitively, the cells that produce IL-2 have the highest chance to encounter it. Also, their mean CD25 expression increased drastically at 72 h and 96 h post-infection, whereas CD8 T cells already show lower expression of CD25 again, indicating a lack of constant IL-2 consumption.

In summary, the data supports a model, where CD8 T cells might produce some IL-2 in the early phase of infection, up to 36 h. Also, CD4 T cells seem to produce IL-2 during this time but arguably have a higher output. As shown by the decreasing number of pSTAT5$^+$CD8 T cells, CD8 T cells seem to produce insufficient amounts of IL-2 to sustain a constant level of pSTAT5 frequency. Therefore, it has to be assumed that CD8 T cells depend on IL-2 from CD4 T cells in the late phase of infection. Treg see the highest amount of IL-2 during all phases of infection compared to the antigen-specific

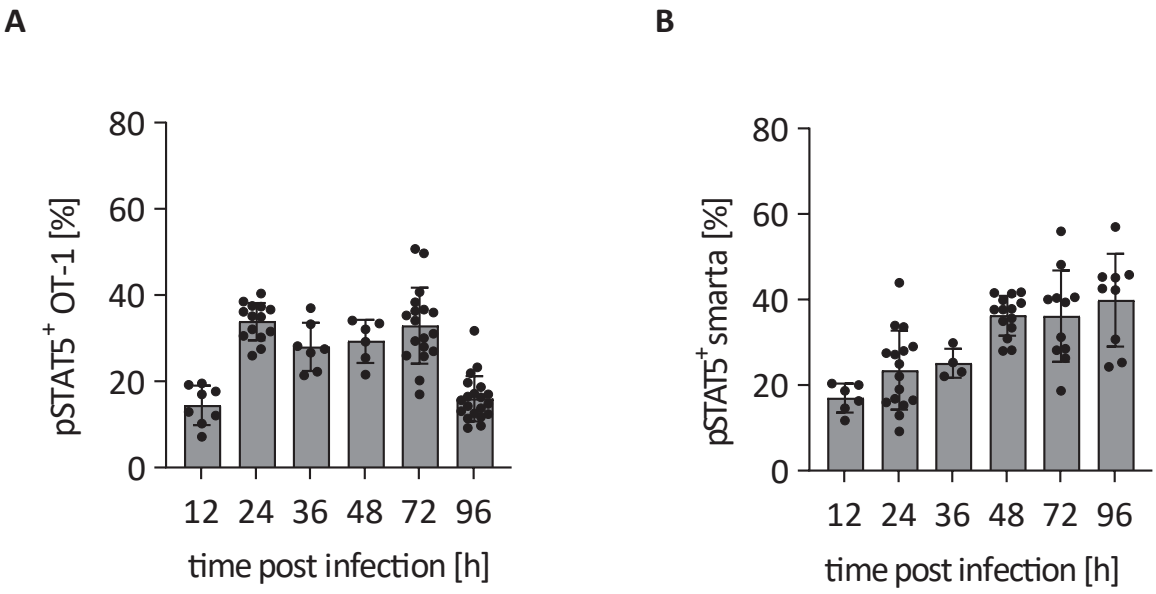

Figure 3.11. CD8 T cells show different temporal IL-2 signaling compared to CD4 T cells. $1x10^4$-$2x10^6$ OT-1 CD8 T cells or $2x10^4$-$2x10^6$ smarta CD4 T cells were transferred at day -1. Mice were infected subcutaneously with VV-OVA/VV-G2 ($1x10^7$ PFU) and popLN analyzed at the indicated time points. All mice were sacrificed on the same day and all samples were treated equally. (A) Transfer of OT-1 T cells and the IL-2 downstream signals shown by activated TCR-transgenic cells. The data shown is from at least two independent experiments with $n \geq 3$ mice. (B) Transfer of smarta cells and their IL-2 downstream signaling shown by frequency of pSTAT5$^+$smarta cells. The data shown is from at least two independent experiments with $n \geq 3$ mice, n=2 (36 h). Error bars indicate SD, data points represent individual popLN. Single significant outliers may have been removed.

cells. This argues for their competitive action. We wanted to find out how much the availability of IL-2 changes for antigen-specific T cells in the absence of Treg. This gives us an indication of the proportion of IL-2 that Treg consume and directly compete for. Does the IL-2 consumption of Treg actually limit the IL-2 availability for effector T cells?

3.7 Treg alter IL-2 availability of effector T cells

To test whether the absence of Treg increases the IL-2 availability for other cells during infection in the popLN, we depleted Treg during different stages of the infection and analyzed the frequency of pSTAT5$^+$smarta or OT-1 T cells transferred before infection. Depletion was performed by injection of one daily DTX dose at 24 and 48 h before the analysis, so the depletion did not interfere with the priming and cross-presentation of the antigen-specific T cells.
Indeed, Treg depletion led to a significantly increased frequency of pSTAT5$^+$OT-1 T cells at 72 h and 96 h p.i. (Figure 3.12). The fraction of pSTAT5$^+$OT-1 T cells increase from approximately 30-35% in the control group to 50% in the depleted group at 72 h p.i. At 96 h p.i. the frequency of pSTAT5$^+$OT-1 T cells changed from approximately 20% (control) to 30%.
These results show that the absence of Treg led to increased pSTAT5 signaling in OT-1 T cells, arguing for increased availability of IL-2. In the control group, Treg compete for this IL-2 and the CD8 T cells have less available. This competition does not seem to occur with CD4 T cells. We found no significant changes comparing the pSTAT5 frequency among smarta cells within the control and Treg-depleted group(Figure 3.13). The pSTAT5 frequency showed an increasing trend as seen in CD8 T cells from approximately 40% pSTAT5$^+$smarta cells (control) to 50% (Treg depletion) at 72 h p.i. This trend was even reversed at 96 h p.i. with smarta cells showing a lowered frequency of pSTAT5 from 30% in the control group to 25% pSTAT5$^+$smarta cells in the Treg-depleted group. In order to consolidate these results, a repetition of this experiment is needed to increase statistical robustness.

The findings indicate that CD4 T cells see the IL-2 produced and Treg are not in direct competition with them. In contrast, Treg compete with CD8 T cells for IL-2 consumption, as the absence of Treg resulted in a higher frequency of pSTAT5$^+$OT-1 T cells.

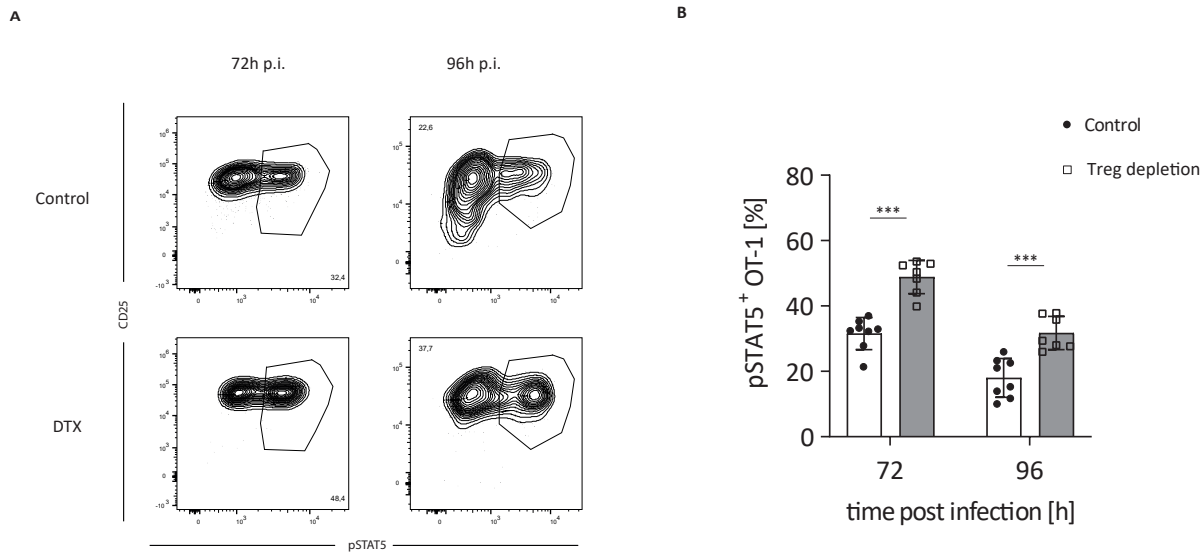

Figure 3.12. Treg compete for IL-2 with CD8 T cells during the expansion phase. Treg were depleted on two consecutive days 48 h before analysis. $1x10^4$-$1x10^5$ OT-1 T cells were transferred for 96 h and 72 h, respectively. (A) Representative flow cytometry plots of OT-1 cells CD25 expression and pSTAT5 signal. The number next to the gate indicates the frequency among all OT-1 T cells. DTX indicates depletion of Treg. (B) Plot of Treg sufficient versus Treg-deficient hosts and the frequency of $pSTAT5^+$OT-1 T cells in the aforementioned groups. The data shown is from at least two independent experiments($n \geq 3$ mice). Error bars indicate SD, data points represent individual popLN and statistical analysis was done with two-way ANOVA. ***p-value < 0.001

Despite previous evidence that IL-2 is mainly produced by CD4 T cells in the late phase of infection, we wanted to ensure our hypothesis was correct and performed an additional experiment using a different approach. We thought that depletion of all CD4 T cells could help us understand the contribution of CD4 helper T cells to the IL-2 pool. Of note, the depletion of all CD4 T cells leads to the removal of suppression, while also removing the potential source of IL-2 in CD4 helper T cells. By measuring the decrease in the pSTAT5 signal seen by CD8 T cells, we can get an indication of how much CD4-derived IL-2 is sensed by the CD8 T cells in the control group.
We depleted all CD4 T cells 48 h before the analysis of CD8 T cell (OT-1) pSTAT5 levels in the late phase of infection. This was done by treatment with an anti-CD4 depleting antibody *in vivo*.

Indeed, depletion of CD4 T cells nearly completely abolished pSTAT5 signaling in OT-1 T cells. A highly significant decrease from 40% $pSTAT5^+$OT-1 T cells down to 15% was observed at 72 h p.i. within the CD4-depleted group (Figure 3.14). This marks a reduction of over 60%. On day 4 p.i. the reduction in pSTAT5 frequency was similar

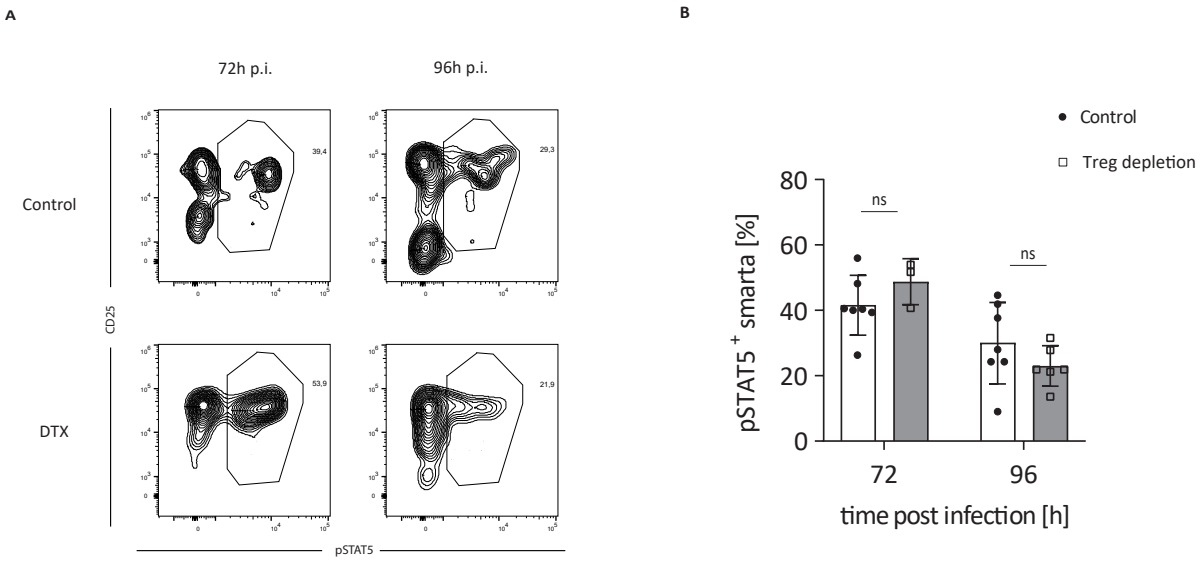

Figure 3.13. Treg do not limit IL-2 seen by CD4 T cells. $2x10^4$-$2x10^5$ smarta T cells were transferred for 96 h and 72 h, respectively. Treg depletion was done for two consecutive days 48 h before analysis. (A) Representative flow cytometry plots pre-gated on smarta cells, showing their expression of CD25 and pSTAT5 72 h and 96 h p.i. DTX indicates depletion of Treg, control group is untreated (B) Plots of pSTAT5 expression comparing Treg depletion vs control. Data is of two independent experiments with n $\geq$ 3 mice. Single significant outliers were removed or sample excluded if too few cells found. Error bars indicated SD, data points represent individual popLN and statistical analysis was done with a two-way ANOVA. ns not significant

from approximately 20% pSTAT5$^+$cells to below 10%. This shows that the absence of CD4 T cells drastically reduces the IL-2 availability of CD8 T cells during the late phase of infection. It indicated that CD8 T cells are largely dependent on CD4-derived IL-2 in the proliferation phase.
This is in line with previously published data showing that CD4 depletion also leads to lower CD8 T cell expansion, arguing for the need for CD4-derived IL-2 (Eickhoff et al., 2015).

Of note, this experimental setup depletes all Treg within the LN and must be interpreted with caution. Changes in IL-2 production mediated by Treg could skew the results and lead to misinterpretation. Since Treg can limit but not enhance IL-2 production of activated T cells directly, this would lead to an underestimation of the reduction in pSTAT5 signal and therefore this setup is sufficient for our question (Bodor et al., 2007; Vaeth et al., 2011).

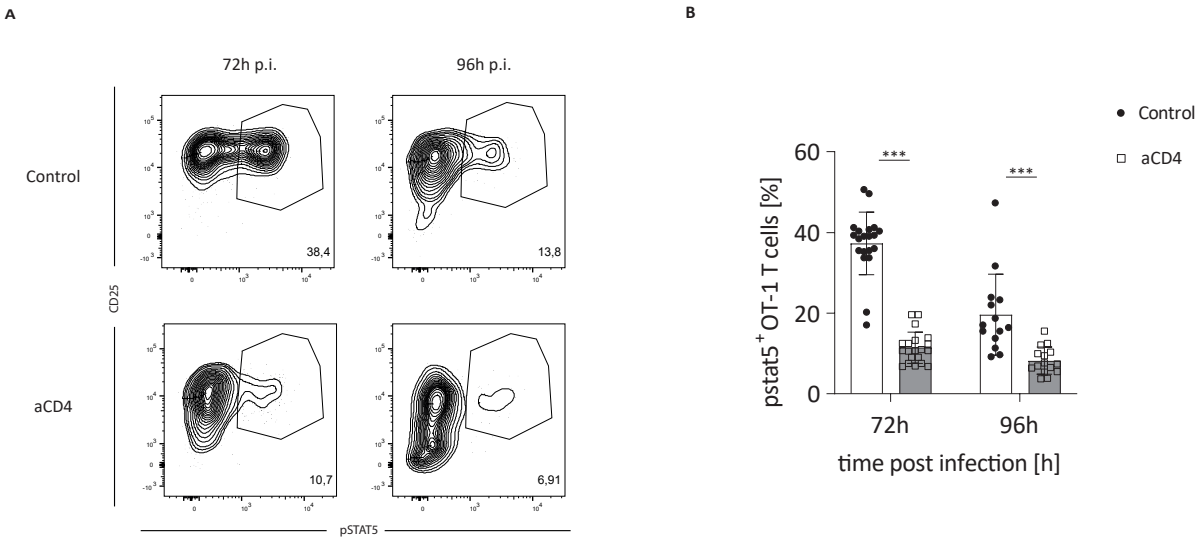

Figure 3.14. CD4 Depletion abrogates pSTAT5 signal in CD8 T cells. $1x10^4$-$1x10^5$ OT-1 T cells were transferred for 96 h and 72 h, respectively. Antibody depletion was performed by a single shot of anti-CD4 24 h before analysis. (A) Representative flow cytometry plots comparing $pSTAT5^+$frequency of the depleted versus untreated group at 72 h and 96 h p.i. The $pSTAT5^+$cell frequency is given by the number next to the gate. Time points are indicated above the panel. (B) Plot of frequency of pSTAT5 among OT-1 T cells within treated vs control group. The data is collected from at least two independent experiments ($n \geq 3$ mice). Error bars indicate SD, data points represent individual popLN and statistical analysis was done with a two-way ANOVA. ***p-value < 0.001

3.7.1 Decay time of STAT5 phosphorylation in Treg and activated T cells after IL-2 deprivation

Gaining an understanding of the overall dynamics of Treg during infection and how IL-2 is consumed by antigen-specific T cells, we were curious to explore cell-intrinsic effects that could explain differences between Treg, OT-1, and smarta T cells in pSTAT5 frequencies. We observed that Treg often had higher levels of pSTAT5 than CD8 T cells with comparable or even higher CD25 expression. Despite the fact that localization could play a role, we wanted to address the time STAT5 phosphorylation persisted after T cells had been deprived of IL-2. The phosphorylation of STAT5 has been reported to be transient and dependent on IL2rβ expression (Smith et al., 2017). However, Treg and CD8 T cells had not been compared in a competitive setting, yet. To exclude cell-intrinsic effects in distinct STAT5 decay times in effector cells compared to Treg we designed the following experiment.

We analyzed the kinetics of STAT5 phosphorylation after IL-2 retrieval in Treg and CD8 T cells. We incubated Treg (naïve CD4 T cells) and CD3/CD28 stimulated CD8 T cells very shortly with IL-2 at different concentrations (10U, 1U, 0.01 U/ml). We then washed the cells and fixed the samples at different time points (every 10 min post-wash). To compare CD8 T cells and Treg within the same culture, we utilized CD8 IL2ko cells and stimulated them overnight with plate-bound CD3/CD28. IL-2ko cells are essential in this experimental setup, as IL-2 production by CD8 T cells within the culture would skew the results. The Treg were added the following day to the culture and the cell suspension spiked with three different concentrations of IL-2.
Then, the mixture of cells was washed, split into different tubes, and individual samples were fixed every ten minutes. In the meantime, unfixed samples were rested in T cell medium at 37 °C. This gave us the chance to analyze the decay time of the STAT5 phosphorylation on both cell types at the same time. Technical variances in staining intensities and exposure to varying IL-2 concentrations were eliminated by this procedure.

CD8 T cells and Treg displayed significantly different pSTAT5 decay kinetics. Treg showed a much higher frequency of pSTAT5 throughout the analyzing time frame of 60 min. Despite both cell types showing the same initial percentage of pSTAT5$^+$cells with 73,1 and 71,0 % pSTAT5$^+$cells initially, Treg retained 56,8% pSTAT5$^+$cells whereas CD8 T cells showed only 29% pSTAT5$^+$CD8 T cells. The representative flow cytometry

plots showed effective phosphorylation of STAT5 reaching 71 % pSTAT5$^+$CD8 T cells in the culture right after the wash (Figure 3.15A, B). The signal declines relatively fast over a period of 60 min. The negative control nicely shows the background levels of the staining and indicates that the signal is almost completely lost after 1h. Additionally, the CD25 signal seems to correlate with the pSTAT5 signal and the stabilization of CD25 by pSTAT5 signals becomes apparent.

Treg reach the same frequency of pSTAT5$^+$Treg within the same culture and therefore the access to IL-2 is comparable (Figure 3.15B). However, the dephosphorylation is much slower in Treg and after 60 min there is still approximately 15% of pSTAT5$^+$Treg detectable.
To determine the halftime of STAT5 phosphorylation we repeated the experiment and plotted the data as can be seen in Figure 3.16 A and B for the different concentrations. To eliminate technical variances in the maximal frequency of pSTAT5$^+$cells at t=0, we normalized the pSTAT5 frequency to 100% at 0 min. The relative expression of pSTAT5 can be seen in Figure 3.16C. Treg significantly have more pSTAT5 signal over the entire time period analyzed. A non-linear fit of sigmoidal curves determined the halftime of pSTAT5 for Treg to be approximately 44 min, whereas it was only 24 min for CD8 T cells.
This indicates that CD8 T cells lose their pSTAT5 signal nearly twice as fast compared to Treg. This led us to conclude that Treg have a more persistent STAT5 phosphorylation signal, which might explain the higher STAT5 frequency of Treg throughout the infection, despite CD8 T cells being competitive in terms of CD25 expression. Not only does this facilitate the maintenance of Treg function and homeostatic proliferation but might lead to a more stable activation of Treg by drastically reducing their need for reoccurring IL-2 consumption. Treg need to encounter IL-2 half as often as CD8 T cells to achieve the same IL-2 downstream signaling frequency in a population-wide comparison. Thus integrated over time Treg have the same pSTAT5 frequency by half the consumption. This also has implications for the interpretation of our data and can explain differences in pSTAT5 frequency comparing OT-1 and regulatory T cells. The signal being less stable in CD8 T cells indicates that CD8 T cells potentially saw more IL-2 over a shorter period of time to achieve the same frequency.

We concluded that Treg need to spend less time with access to IL-2 to get the same downstream IL-2 activation of the pathway. This might be a mechanism to ensure activation and stable maintenance of Treg at all times and possibly explains the competitive

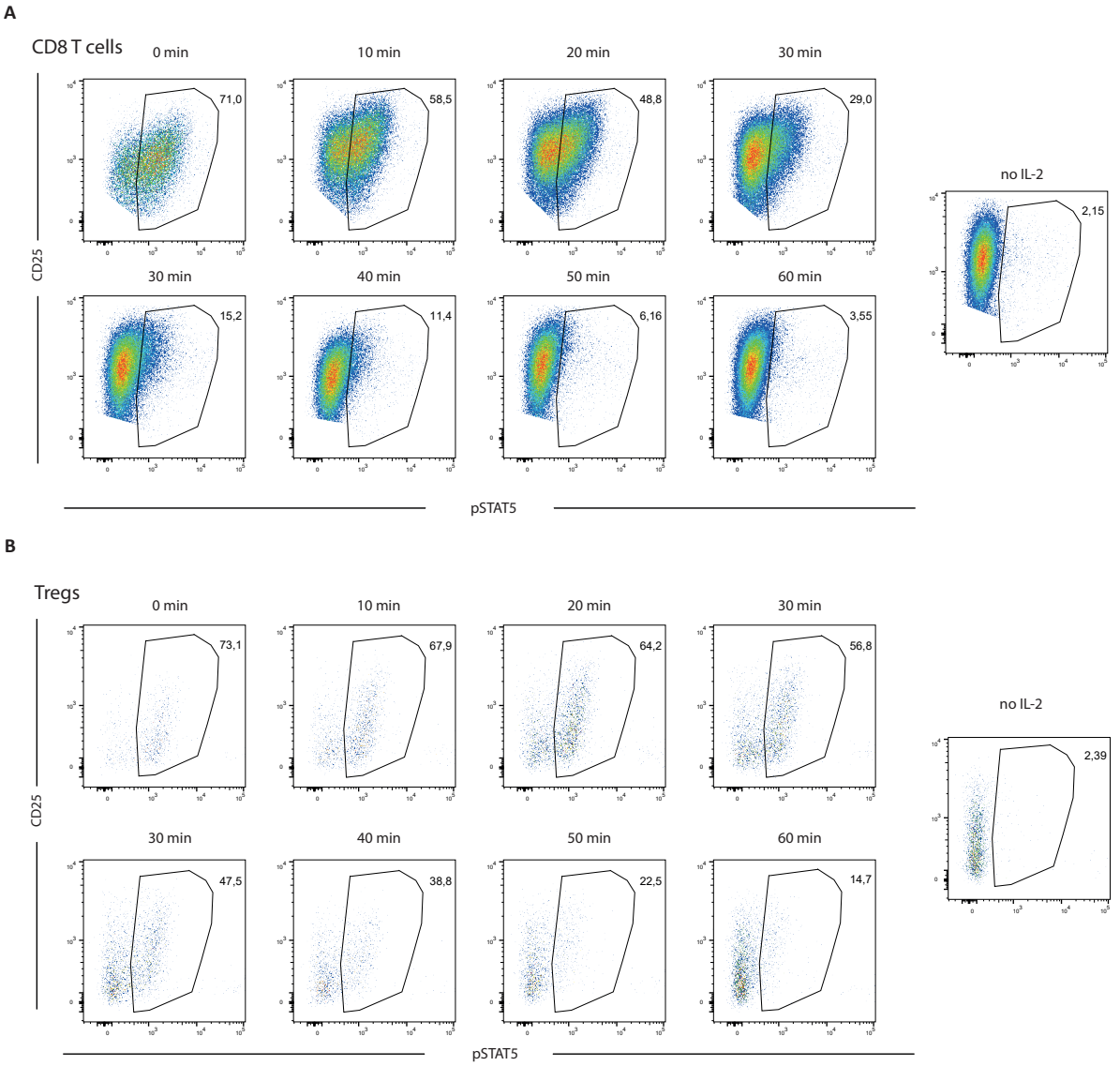

Figure 3.15. Flowcytometry analysis of the dephosphorylation time of STAT5 in Treg and CD8 T cells. (A) IL2ko CD8 T cells were exposed to 10 U/ml hIL-2. The expression of CD25 and pSTAT5 is shown for the indicated time points. A negative control 'no IL-2' is shown to determine the background level of the pSTAT5 staining. The dephosphorylation was documented for at least 60 min. (B) Treg that have been exposed to 10 U/ml hIL-2. The expression of CD25 and pSTAT5 is shown for the indicated time points. A negative control 'no IL-2' is shown to determine the background level of the pSTAT5 staining. The dephosphorylation was documented for at least 60 min. The number next to the gate indicates the frequency of pSTAT5$^+$cells.

pSTAT5 levels seen on Treg despite their lower CD25 gMFI.

3.7.2 Treg control via IL-2 competition

Having shown that Treg have the ability to alter the IL-2 availability for effector T cells, we wanted to conduct an experiment to test whether IL-2 competition has an impact on the size of the CD8 T cell effector population.
Additionally, we were interested in the impact Treg can have on the effector differentiation of CD8 T cells.

CD25ko cells are unable to compete for IL-2 with high-affinity cells. We have shown that CD8 T cells expressed high levels of CD25 already 24 h p.i. and therefore seem to have competitive affinity towards IL-2 (Figure 3.10). By co-transfer of wt and CD25 deficient cells into the same hosts, we can gain an understanding of the impact of the high-affinity receptor expression. If we now additionally remove the suppression exerted by Treg, we can observe the regulatory control Treg had in the non-depleted group.

In order to address the above-mentioned, we conducted a competitive transfer experiment. We transferred OT-1 TCR transgenic T cells at a 1:1 ratio, being either CD25 sufficient or deficient into Foxp3-DTR mice. In one group we depleted Treg on days 1, 2, and 3, whereas the other group remained untreated. This experimental setup enabled us to directly test the regulation of Treg *via* IL-2 competition. Details of the experimental setup can be taken from Figure 3.17A.

We found that at day 8 p.i. the 1:1 ratio of cells initially transferred was skewed towards wt OT-1 T cells (Figure 3.17B). OT-1 wt cells had increased in frequency among all transferred cells. In the control group, a ratio of 80% wt to 20% CD25ko OT-1 was found. This skewed ratio was even more pronounced in the Treg-depleted group where we found 90% OT-1 wt cells and only 10% OT-1 CD25ko cells. To ensure the effect of Treg depletion was present, we looked at the absolute numbers of OT-1 T cells we could retrieve. We found a significantly higher number of OT-1 wt T cells in the Treg-depleted group. This suggested that an increased expansion of CD8 T cells due to lacking Treg suppression, as previously published (Kastenmuller et al., 2011) was present. We saw an increase in the absolute cell counts of OT-1 wt from on average $0{,}43\text{x}10^4$ cells in the control group to $1{,}4\text{x}10^4$ cells in the Treg-depleted group, a 3,5-fold increase (Figure 3.17C). In contrast, the absolute cell counts of OT-1 CD25ko cells were not significantly changed

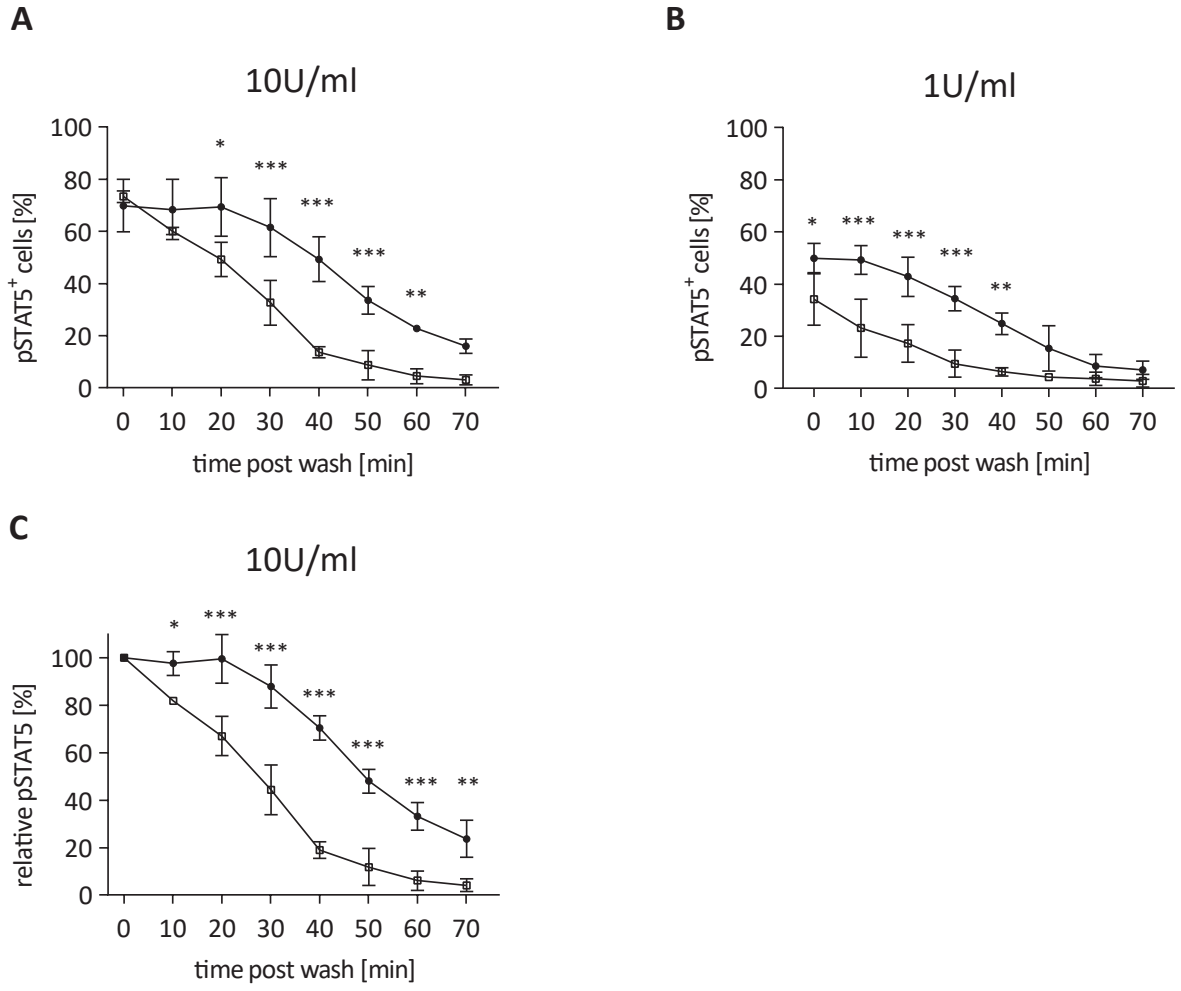

Figure 3.16. Activated CD8 T cells have distinct dephorphorylation time of STAT5 compared to Treg. (A) Absolute frequency of pSTAT5$^+$Treg and CD8 IL2ko T cells compared within one plot. The cells had been exposed to IL-2 shortly and the pSTAT5 frequency was observed overtime after the IL-2 was diluted/washed off. The cells were exposed to 10 U/ml hIL-2 for 20 min. (B) Treg and CD8 IL2ko T cells exposed to 1 U/ml. (C) Normalization of absolute pSTAT5 signal to 100%. Shown is the relative pSTAT5 frequency of Treg and CD8 IL2ko T cells. These cells were exposed to 10 U/ml. The data shown depicts at least two independent experiments. Cells were cultured from at least two different donor mice. Error bars indicate SD, and statistical analysis was done with 2-way ANOVA Sidak's multiple comparison test. *p-value < 0.05, **p-value < 0.01, ***p-value < 0.001

with on average 1x10^3 and 1,5x10^3 OT-1 CD25ko cells found within the control and Treg-depleted group, respectively (Figure 3.17C). Comparing the absolute number of OT-1 wt and CD25ko cells within the control group we found no significant difference. We found on average 0,43x10^4 OT-1 wt cells compared to 0,1x10^4 OT-1 CD25ko cells. This indicated that the CD25ko cells were already limited by their decreased affinity for IL-2. At the same time, CD25 sufficient cells are controlled to the same level while Treg are present.
Additionally, no significantly increased numbers of CD25 deficient cells were found comparing the two groups(Figure 3.17C).

On top of these findings, we also looked at the differentiation of these cells. We found out that the differentiation of both CD25ko and also wt OT-1 T cells is affected by Treg depletion. We analyzed the differentiation of the effector cells by their expression of the commonly used differentiation markers CD127 and KLRG1. The four resulting populations defined by these markers are described as SLEC (KLRG1$^+$ CD127$^-$), DPEC (KLRG1$^+$ CD127$^+$), MPEC (KLRG1$^-$ CD127$^+$), and EEC (KLRG1$^-$ CD127$^-$).
In CD25ko T cells, we found significantly more short-lived effector cells (SLEC) and fewer memory precursor effector cells (MPEC)(Figure 3.17D) comparing the control group with the Treg-depleted group. While we found 10% SLEC in the control group, the frequency significantly increased up to 40% of CD25ko OT-1 T cells being KLRG1 single positive within the Treg-depleted group(Figure 3.17D). Consequently, the frequency of MPEC decreased significantly from approximately 60% in the control group to an average of 30% in the Treg-depleted group among all CD25ko OT-1 T cells (Figure 3.17D).
In contrast, the wt OT-1 T cells showed a significantly higher frequency of double-positive effector cells and a lowered frequency of early effector cells (Figure 3.17E) comparing the control group with the Treg-depleted group. The frequencies increased from approximately 10% to 35% and decreased from 30% to 15%, respectively. Despite the expansion of CD25ko T cells being limited by their knock-out phenotype, the differentiation still changed significantly under Treg depletion.
However, the data shown for the control group was consistent with previously published data, indicating that CD25 deficient cells display a more memory-like phenotype compared to wt cells (Kalia et al., 2010). Furthermore, the Treg depletion induces a shift towards more effector differentiation, as seen by the higher frequency of SLEC in Figure 3.17D, shown previously (Kastenmuller et al., 2011).

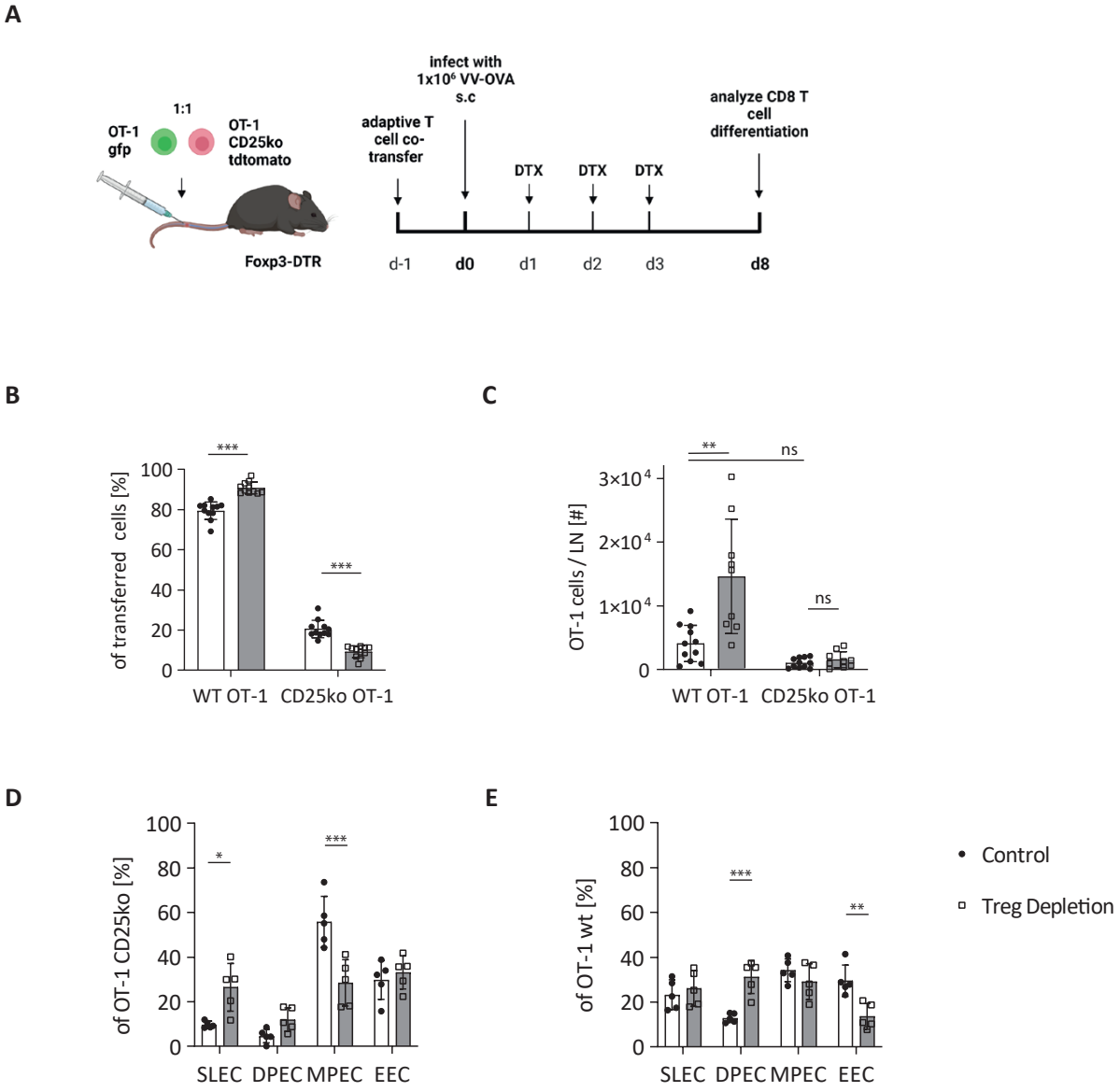

Figure 3.17. Competitive transfer reveals Treg regulate *via* IL-2 restriction. (A) The experimental setup shows the competitive transfer in a 1:1 ratio of OT-1 CD25ko (tdTomato) and OT-1 wt (GFP) CD8 T cells ($5x10^3$ OT-1 T cells each) on day -1 of the experiment. The mice were then infected s.c. with VV-OVA. Treg were depleted in one group from day 1 (three daily injections of 500 µg DTX). popLN from each mouse were pooled and lymphocytes analyzed by flowcytometry on day 8 p.i. (B) Frequency of transferred cells recovered from each animal. (C) Absolute numbers of OT-1 wt and OT-1 CD25ko cell recovered from an individual popLN. (D) Differentiation of CD25ko T cells at day 8 determined by expression of KLRG1 and CD127. (E) Differentiation of OT-1 wt cells at d8 determined by expression of KLRG1 and CD127. Data shown from two independent experiment (B, C) and from one representative (D, E) with n $\geq$ 3 mice per experiment. Error bars indicate SD, and statistical analysis was done with a two-way ANOVA (B,C) and Sidak's multiple comparison (D,E). *p-value $<$ 0.05, **p-value $<$ 0.01, ***p-value $<$ 0.001. SLEC short-live effector cells, DPEC double-positive effector cells, MPEC memory precursor effector cells, EEC early effector cells. Graphical depiction of experimental setup in A was created with BioRender.com

These results confirmed that the IL-2 competition by Treg is a major regulatory mechanism during viral infection. Not only is the population size of CTL regulated by IL-2 availability, but also the differentiation is controlled by Treg. Treg seem to limit IL-2 availability for CD8 T cells in a CD25-dependent manner. The reduced absolute numbers of CD25ko cells within the control group could not be rescued by depleting Treg, an indication that regulation is mediated via this receptor.
To further understand the impact of Treg on the differentiation of CD8 T cells we looked at a prominent chemokine receptor known to be involved in the effector differentiation of CTL. CD8 T cells upregulate CXCR3 rapidly after activation and it helps their positioning in the microenvironment of the LN, but also their emigration into inflamed tissues efficiently (Groom and Luster, 2011; Hu et al., 2011; Kurachi et al., 2011).

3.8 CXCR3, a potential chemokine receptor favoring effector differentiation

As it has been described before, CXCR3 expression has an impact on the effector differentiation of CD8 T cells during viral infection (Kurachi et al., 2011). This might be based on the different localization of the cells within the LN, being able to migrate to different niches, which could indicate that they are exposed to different magnitudes of control exerted by Treg.

To address if CXCR3 expression by CD8 T cells influences the level of regulation received from Treg, we utilized CXCR3ko CD8 T cells to gain insights into this question.
We performed a very similar experiment to the CD25ko experiment, using a competitive transfer of OT-1 CXCR3ko and OT-1 CXCR3 sufficient (wt) cells. This setting gave us the opportunity to compare the cells within the same environment, minimizing technical variances and creating competition between them.
We can compare the expansion and differentiation of CXCR3ko cells and wt cells within the same mouse while under the control of Treg. This sets the baseline for our next experimental group, in which we depleted the Treg compartment after the priming and activation of the OT-1 T cells (24 h p.i.).

We found a ratio of 80:20 CXCR3ko to wt OT-1 T cells in the control group. After depletion of Treg, this ratio shifted in favor of the WT OT-1 T cells (Figure 3.18). In the depleted group, a ratio of 60:40 (CXCR3ko:wt) was found. Not only did OT-1 wt T

cells increase in frequency within the Treg-depleted group but also their differentiation was altered.
In the control group, we found approximately 7,5% and 40% SLEC among CXCR3ko and OT-1 wt T cells, respectively (Figure 3.18B, C). Upon Treg depletion, the frequency of SLEC increased from 7,5% to 20% in the CXCR3ko OT-1 T cells but remained unchanged in the wt OT-1 T cells. Significant changes could be observed in all subsets of effector cells from the CXCR3ko T cells. The frequencies of DPEC, MPEC, and EEC within the control group and the Treg-depleted group changed from 2% to 30%, 75% to 40%, and 20% to 10%, respectively. The OT-1 wt population only showed an increased frequency in DPEC changing from 8,5% DP cells in the control group to 25% in the depleted group. Also, the frequency of EEC among all OT-1 wt T cells changed significantly decreased upon Treg depletion from 20% down to approximately 10%.
These findings are consistent with the notion that $CXCR3^+$ cells are more likely to become short-lived effector T cells. Our findings indicate that Treg supress CXCR3ko cells less strongly compared to CXCR3 sufficient cells.

This hypothesis is supported by the differentiation of both WT and CXCR3ko OT-1 T cells. The knock-out cells develop only up to 8% of short-lived effector cells under normal conditions. In the Treg-deficient group, the frequency of effector cells is increased, whereas the memory populations are decreased. An opposing effect can be seen in the WT cells. Here the frequency of DPEC increased and the early effector population decreased under Treg depletion. It is likely that Treg control effector cells within specific niches that either promote effector or memory differentiation. To gain an understanding of whether these niches are more accessible upon CXCR3 expression we addressed this question next. These results led us to the conclusion that CXCR3 has an additional impact on the expansion and differentiation of CD8 T cells. However, this effect might still be mediated by Treg through IL-2 competition.

3.9 CXCR3 expression as a mediator of IL-2 niche access

We saw that CXCR3 deficient cells are less controlled by Treg compared to their counterpart, CXCR3 expressing cells. We were interested to understand if this effect is mediated by IL-2 access. Does CXCR3 expression increase the cell's ability to achieve IL-2 access

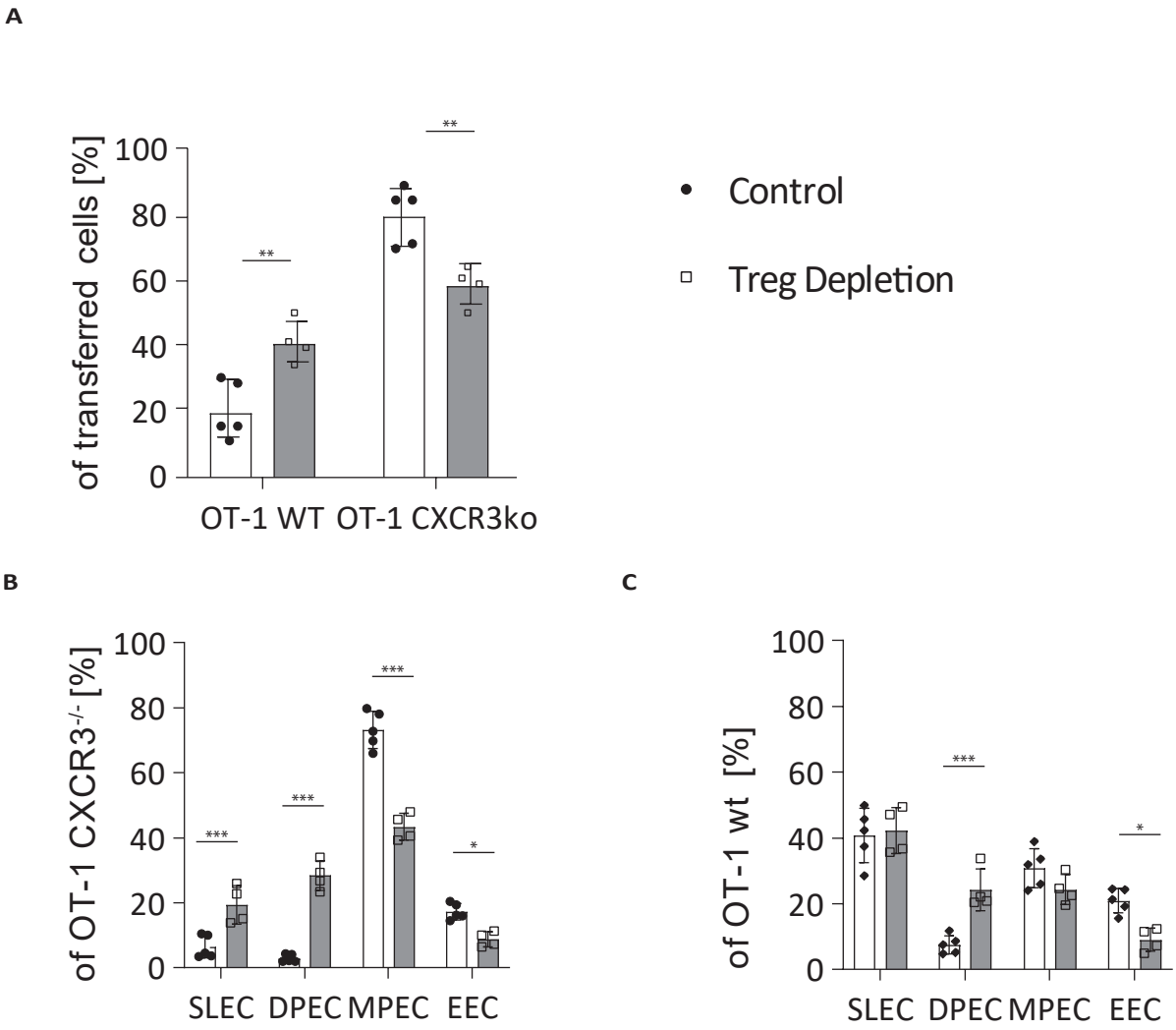

Figure 3.18. Competitive transfer reveals Treg restrict CXCR3$^+$ cells. Foxp3-LUCI-DTR th1.1. mice received a competitive adoptive transfer of a 1:1 ratio of OT-1 CXCR3ko (th1.2) and OT-1 wt (GFP) CD8 T cells (5x10^3 OT-1 T cells each) on day -1. Treg were depleted on day -1 and day 0 by injection of 1 mg of DTX. The mice were infected with VV-OVA (1x10^6 PFU, i.p.) (A) Frequency of recovered donor cells 8 days post-infection from the spleen. (B) Differentiation of CXCR3ko T cells at day 8. (E) Differentiation of OT-1 wt cells at day 8. Data shown represents one experiment with n $\geq$ 3 mice per group. Error bars indicate SD, and statistical analysis was done with a two-way ANOVA (A) and Sidak's multiple comparison test (B, C). *p-value $<$ 0.05, **p-value $<$ 0.01, ***p-value $<$ 0.001

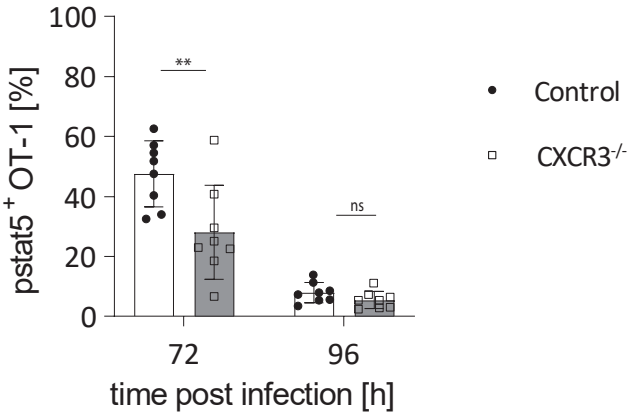

Figure 3.19. CXCR3 deficiency leads to lower pSTAT5 frequency in CD8 T cells. A 1:1 ratio of in total 1x10^4-1x10^5 OT-1 T cells (wt and CXCR3$^{-/-}$) were transferred for 96 h and 72 h, respectively. Mice were infected with VV-OVA (1x10^7 PFU, s.c.) and popLN analyzed separately after 72 h and 96 h post-infection. Data shown from two independent experiment with n $\geq$ 3 mice. Error bars indicate SD, data points represent individual popLN and statistical analysis was done with a two-way ANOVA. **p-value < 0.01, data in cooperation with Anfei Huang

by adequate positioning within the LN? We addressed this question by testing whether CXCR3 deficient cells are less likely to encounter IL-2.

To do so, we conducted a competitive transfer of CXCR3ko and wt cells and compared the pSTAT5 levels on these two populations in the late phase of infection.

Confirming our hypothesis, we found that CXCR3ko cells had a significantly lower frequency of pSTAT5 and therefore were less competitive to access IL-2 (Figure 3.19) at 72 h post-infection. OT-1 wt cells displayed a frequency of up to 50% pSTAT5$^+$cells, whereas only 30% of CXCR3ko cells were pSTAT5$^+$. At 96 h p.i. this difference was not detectable any longer, possibly due to the very drastic expansion of transferred cells indicated by very low pSTAT5 frequency (<10%).

This indicates that CXCR3 expression enables cells to gain facilitated access to IL-2, despite Treg likely controlling the niche. This suggests that CXCR3$^+$ cells reside in an area of the LN, where IL-2 is being produced or have easier or faster access to these niches due to their directed chemotactic migration.

These findings are in accordance with the previous finding, showing that CXCR3ko cells are less susceptible to Treg control (Figure 3.18). This like comes from the fact that Treg control IL-2 niches and CXCR3ko cells have difficulty to competing for access to these niches.

In the future we would like to address the positioning of CXCR3 sufficient and deficient cells within the LN and show that this distinct location can drive differences in IL-2 consumption, conclusively also differentiation, and finally the susceptibility to Treg control.

4 Discussion

4.1 Summary

Treg are a critical cell type that modulates immune responses in the context of autoimmunity and infection. When studying the mechanistic basis of Treg-mediated control of cytotoxic CD8 T cells, we confirmed a critical role for IL-2. Specifically, we found that Treg regulate CD8 T cell expansion and effector differentiation by limiting the access to CD4 T cell-derived IL-2 in lymph nodes. Unlike antigen-specific CD8 T cells that showed migrational arrest upon interaction with dendritic cells for several hours, Treg maintained their migrational activity, as demonstrated by intravital multiphoton microscopy. These results point to a model in which Treg control lymph node niches by limiting local cytokine abundance rather than controlling selected cell types via prolonged interactions. Since our scRNA seq data showed that all Treg subsets have enhanced IL-2 signaling following infection, we conclude that all Treg in LNs are exposed to elevated amounts of IL-2 during infection. In line with our intravital imaging data this suggests that Treg as a population are continuously scanning the whole lymph node and that local Treg cell densities within specific inflammatory niches might determine the level of local suppression. Indeed, we found that CD8 T cells that lacked an inflammatory chemokine receptor (CXCR3) were less strongly suppressed compared to the WT controls. Together our work supports a new concept of Treg-mediated regulation in secondary lymphoid organs based on dynamic regulation of Treg cell densities within inflammatory niches. We believe that our results may provide novel angles to modulate Treg function for immunotherapeutic strategies.

4.2 Spatial dynamics of Treg

A multitude of regulatory mechanisms has been proposed for Treg. We focused on the regulation of adaptive immune responses and wanted to find out, which mechanism is likely to control an antiviral response. One of the long-standing debates in the regulation of Treg is the question of direct versus indirect regulation of target cells. In our case, is an effector T cell directly restricted by e.g. suppressive cytokines, or is the APC

suppressed in its function, which consequently also influences the effector response?
In order to shed light on this question, we addressed the spatial localization of Treg with 2-photon intravital imaging. Most of the published mechanisms described for Treg regulation are based on proximity to the target cell, irrespective of the mode of regulation (direct/indirect)(Shevach, 2009). Despite, many studies showing a plethora of mechanisms, we sought to explore the regulation of Treg *in vivo*, as most of these studies are limited by their *in vitro* setting.

In order to address the regulatory mechanism, we first looked at the spatial dynamics of Treg during viral infection. The regulation of the adaptive immune response requires very fine-tuned regulation of effector cells to restrict tissue damage and allow for effective clearing of the viral infection, at the same time. While the clearing of viral infections and other pathogens has been shown to be improved by Treg depletion in most cases, Treg have been proven to be essential to restrict tissue damage and preserve organ functionality (Arpaia et al., 2015; Loebbermann et al., 2012, 2013). Compromising the immune homeostasis for more efficient clearing of the infection would be beneficial in some scenarios, in which the evasion of the pathogen leads to increased pathogenicity, e.g. malaria or HIV (Hansen and Schofield, 2010; Rushbrook et al., 2005).
In contrast to this, Treg have been shown to be beneficial in controlling pathogenic immune responses towards specific infections, such as Leishmania (Ji et al., 2005), hepatitis C (Rushbrook et al., 2005), HIV (Kinter et al., 2004) and pneumocystis (Hori et al., 2002) among many more.

Treg regulation requires proximity between the different interaction partners of an adaptive immune response. Data from studies in 1998 established that Treg can not exert their inhibitory function without contact with their target cell (Takahashi et al., 1998; Thornton and Shevach, 1998). When cell-cell interactions between Treg and the target cells were prevented by separating the cells with a semi-permeable membrane, Treg suppression was abolished. These results were misinterpreted for a long time creating a dogma that Treg can only regulate in a contact-dependent manner.
However, recent studies show that proximity is essential even in contact-independent mechanisms (Liu et al., 2015; Oyler-Yaniv et al., 2017). The distance the membrane created was enough to abrogate the suppression of Treg irrespective of contact. Hence, proximity is relevant in Treg suppression. Soluble mediators of immune suppression are only effective in high concentrations and proximity to the target. Since diffusion is an incredibly inefficient and slow process, it is difficult to imagine, that Treg can influence

cells over long distances by suppressive cytokines such as IL-10 or IL-35, for example. Additionally, a lot of mediators have a very short half-life, which makes soluble mediators of immune suppression less likely to have an effect on cells over long distances (e.g. adenosine) (Vignali et al., 2008).

One often discussed mechanism of Treg regulation is the deprivation of IL-2 from effector cells. It has been shown before that Treg can influence the IL-2 availability and an *in vitro* study modeled the dynamics and tunability of this system, very elegantly (Liu et al., 2015; Oyler-Yaniv et al., 2017; Wong et al., 2021). A widely accepted theory in this field of research is that Treg use their ubiquitous expression of CD25 to consume IL-2 and act as a scavenger for this cytokine to reduce the IL-2 availability of effector T cells. This is especially relevant in the early phase of infection, as activated T cells rapidly induce CD25 expression and become competitors for the IL-2 later during the course of infection. How this competition dynamically works in terms of the spatial distribution of competitors and if the regulation only takes place in this early time period or also in the later phases of the infection, has not yet been formally addressed. During viral infection, several immune cells interact closely and fulfill the requirement of proximity. Naïve T cells get primed in the LN by an APC and therefore naturally come into close contact.

We hypothesized that the site of priming would be a prominent hotspot for Treg regulation, as it also takes place within the first 24 h prior to effector cells inducing CD25 expression. Interestingly, we did not find long-lasting interactions of Treg with CD8 T cells during the priming phase. Despite cells being in close proximity to each other, the interactions we could observe were short (<5-10 min). Furthermore, Treg did not stay in the vicinity of the CD8 T cell cluster, but rather seemed to move through the area on 'pass-by'. This is also indicated by the duration Treg spend in proximity to a CD8 T cell priming cluster and by the track length shown in Figure 3.1 B.

CD8 T cells move to deeper areas of the LN after priming and readily upregulated their CD25 levels, showing even higher expression than Treg (Figure 3.10). At this point, CD8 T cells receive CD4 help from the XCR1$^+$ cross-presenting DC. We also analyzed the interactions in this phase, but could not detect stable interactions between Treg and effector cells. This points to the fact that Treg regulation of antiviral CD8 T cells does not require prolonged interactions with the APC or the CD8 T cell.

In contrast to our findings, a previous study by Liu et al. has shown co-clustering of Treg and activated T cells, claiming that Treg co-localize with effector T cells in order to

control. Despite the fact that we do see proximity, we believe that no co-arrest takes place during VV infection. The evidence presented is based on static imaging and therefore lacks the temporal resolution to address the stability of these clusters. We did encounter groups of Treg in our imaging analysis as well, however, these clusters were not stable over time. This indicates that Treg do in fact sense IL-2 in the microenvironment of the IL-2 production site, but do not show migrational arrest. This explains pSTAT5$^+$Treg within the vicinity of T cell clusters, which produce IL-2. The dispersion of IL-2 can be assumed to be spherical and due to the short half-life and the fast dephosphorylation of STAT5, the Treg seem to be clustering around effector cells in a static image. Also, a careful assessment of these images shows pSTAT5$^+$Treg outside of stable Treg clusters, indicating that these cells migrated away from the region but maintained pSTAT5. This is only possible if this cell encountered IL-2 again distant to the initial cluster, otherwise more proximal cells would show pSTAT5 signals as well.

The mentioned study looked at the suppression of auto-reactive T cells in steady-state. The suppression of a highly undesired T cell response likely differs drastically from the fine-tuned balance of regulating an adaptive immune response against a pathogen. The number of activated cells differs from a viral infection and the cytokine environment is distinct. This is also indicated by the fact, that transfer of CD4 T cells led to 75% of Treg being positive for pSTAT5, suggesting that a large fraction of this population had access to IL-2. In the study, only a small proportion of cells has access to IL-2. Therefore, we believe the regulation during viral infection might be distinct from the regulation of single auto-reactive T cells. However, the mechanism of Treg sensing IL-2 and competing for it with activated T cells offered a good starting point to address our observations, as it is a contact-independent mechanism, nevertheless relying on proximity.

The lack of long-lasting interactions makes control by direct mechanisms of Treg regulation rather unlikely. Direct suppression of T cells by Lymphocyte-activation gene 3 (LAG-3), an inhibitory co-receptor, has been proposed before and could have been a viable mechanism to suppress T cell responses (Maruhashi et al., 2018). However, tunability during a viral infection is a key argument for a more dynamic regulatory mechanism. Suppressing individual cells in an exponentially expanding population requires equal numbers of Treg and seems unlikely to control viral CD8 T cells.
We also did not find any evidence supporting regulation through LAG-3 or CTLA-4 in our single-cell sequencing data that would argue in favor of these known mechanisms acting *in vivo* during viral infection (Figure 3.3). An additional mechanism described

before is the lysis of effector cells by the release of granzymes, often expressed by Treg. This mechanism has been shown to induce apoptosis in the target cell and eventually leads to control of effector population size, thereby regulating the immune response (Arce-Sillas et al., 2016).
Galectin-1, a β-galactoside-binding protein, has also been shown to restrict activated T cells in their cell-cycle progression and induce apoptosis (Perillo et al., 1995). Despite the fact that these mechanisms might play a role in specific conditions, we think that the mentioned mechanisms do not depict a major regulatory control mechanism for Treg during viral infection, because they rely on contact and lack the dynamic tunability to adjust to changing levels of antigen load and are hindered by their complexity. In contrast, other contact-independent mechanisms or indirect mechanisms, targeting the APC could play a major role during infection. However, the dynamic regulation and adjustability of certain systems, intuitively make sense as the immune response is desired and must not be suppressed.
While mechanisms that utilize the secretion of suppressive cytokines such as IL-35 or IL-10 have been shown to work in certain inflammatory contexts, they seem to be less relevant to regulate a viral infection (Seyer et al., 2010; Wu et al., 2008). However, we did not disregard the possibility for combined regulatory mechanisms or another yet unknown contact-independent mechanism to be relevant in the regulation of antiviral responses. However, we did not find evidence supporting this hypothesis in our single-cell sequencing data(Figure 3.3). We first explored the dynamics of IL-2 availability during viral infection, as there was already evidence for this mechanism *in vivo*.
To address how proximity impacts IL-2 availability among the different cell types, we sought to understand which cells are competitive for IL-2 and what fraction of each population consumes IL-2. If these cells were in close proximity and CD8 T cells produce their own IL-2, how do Treg manage to control CD8 T cells despite their disadvantageous positioning?
To answer this question we tried to determine the source of IL-2 and to get a deeper understanding of the temporal changes in IL-2 availability during the infection.

4.3 Temporal dynamics in IL-2 availability

To understand IL-2 competition as a regulatory mechanism, it is essential to understand the consumption and production of IL-2 by the three major players in the system: CD4,

CD8, and regulatory T cells. We wanted to analyze the contribution of CD4 and CD8 T cells to the IL-2 pool and understand at which phase during the infection the IL-2 availability is given for each consumer cell. Treg cells cannot produce IL-2 and therefore a major part of IL-2 comes from activated CD4 and or CD8 T cells (Humblet-Baron et al., 2016; Liu et al., 2015).

We analyzed the IL-2 availability by detailed kinetics of downstream pSTAT5 signals in different experimental setups. By showing IL-2 signaling, we determined the available IL-2 for each cell type and thereby could also determine their competitiveness, as they compete in a physiological environment during the infection *in vivo*. This enabled us to gain an understanding of the temporal changes during the infection and the changes in IL-2 availability throughout this time. The knowledge about the consumption of IL-2 by each cell type gives us the opportunity to make conclusions about the IL-2 access of activated T cells and lets us determine at which time point during the infection, regulation is happening.

We found that Treg have a high capability to scavenge IL-2 during all phases of the infection (Figure 3.6). Nevertheless, CD8 T cells do gain access to IL-2 early on and can sense approximately the same level of IL-2 in comparison to Treg, up to 40% at 24 h post-infection (Figure 3.11A). This is in line with a competitive situation where Treg and CD8 T cells share the IL-2 equally. However, we have to mention that we only look at the pSTAT5 levels on a population level and as a snapshot in time. This means, the read-out integrates the decay time of the signal and cannot decipher local differences in pSTAT5 expression. Therefore, CD8 T cells within clusters may see more IL-2, while CD8 T cells without access to this area see significantly less.
Equal levels of pSTAT5 argue against strong competition or equal competitiveness, which led us to analyze later time points of infection, when IL-2 limitation increases competition. We believe that competition becomes more prominent during the expansion phase of CD8 T cells, between 36 h and 96 h. The CD8 T cells will start to migrate again after spending a significant amount of time arrested at an APC. After their activation, they must position themselves close to an IL-2 producer. Treg constantly migrate and therefore have the same chance to home to the same niche. We and others have shown that the IL-2 availability during VV infection starts decreasing around days 3-4 p.i. (Kalia et al., 2010) (Figure 3.6). The lower availability caused by decreasing production of IL-2 naturally increases competition. On top of this, more Treg infiltrate the LN and CD8 T cell proliferation leads to drastically increased consumption overall (Oyler-Yaniv et al.,

2017).

Also, we show that CD8 T cells do not majorly contribute to the IL-2 availability by a net positive production of IL-2 (Figure 3.7, Figure 3.8). Importantly, it is challenging to interpret these results, as OT-1 T cells that have been activated can consume, but also produce IL-2. To this point in time, no experimental model can measure the active release of cytokines with high sensitivity *in vivo*. However, conclusions about the overall impact of added OT-1 T cells on IL-2 availability can be made, it either being decreased or increased. Nonetheless, it fails to address if IL-2 production or consumption of CD8 T cells is altered.
Ultimately, CD8 T cells do not sustain their pSTAT5 frequency during infection shown by drastically decreasing levels of pSTAT5 on CD8 T cells at 96 h p.i. (Figure 3.11), which indicates that CD8 T cells are dependent on CD4-derived IL-2. IL-2 becomes more limited in the late periods of infection (Figure 3.11).
We argue that CD8 T cells do locally produce IL-2 to upregulate CD25 (autocrine) and consume paracrine IL-2 on days 3-5 of the infection, with increasing contribution of CD4-derived IL-2. This hypothesis is supported by the fact that a higher fraction of CD4 T cells sees IL-2 at 72 h and 96 h p.i. as they are the local producers of IL-2 and now have direct access to IL-2. At this point, they also have increased CD25 receptor density on their surface and sense more IL-2 compared to Treg (Figure 3.10; Figure 3.11).
Previous studies are in line with this observation showing that CD8 T cells use autocrine signaling early after infection (D'Souza et al., 2002), but do not produce IL-2 later on (Cheng et al., 2002).

Prolonged exposure to IL-2 enhances CD8 T cell effector differentiation (Kalia et al., 2010). We hypothesize that highly activated cells that also express high levels of CD25 very early on, first encounter IL-2 and differentiate into short-lived effector cells, that are rapidly proliferating. As soon as they proliferate, these cells then stop producing IL-2. It is unclear whether they produced IL-2 before or only a certain subset of activated CD8 T cells does so.
This concept has been published for CD4 T cell differentiation into T follicular helper cells (Tfh) (DiToro et al., 2018). Cells producing IL-2 are predominantly differentiating into germinal center Tfh cells, whereas cells that consume high levels of cytokine differentiate and become non-follicular effector cells subsequently. The study argues that the IL-2 producers become resistant to IL-2 signaling and at the same time induce IL-2 signaling in non-producing cells to induce their activation *in trans*. Recently, it was

shown that this concept also applies to CD8 T cells in LCMV infection (Kahan et al., 2022)
The temporal distinct IL-2 production and switch in sensing from autocrine to paracrine signaling make the regulation of this model very elegant.
First, the CD8 T cell response is controlled by the number of CD8 T cells activated by APC priming them. This process is limited by the available priming sites and the amount of antigen present, which already tunes the initial onset of the response. Treg limit bystander activation by competing for IL-2 right away. This ensures that only properly activated CD8 T cells produce IL-2 and express competitive levels of CD25. Switching from the initial autocrine model to a paracrine dependency, the expansion phase of the infection can be adjusted to the load of antigen that is still present in the later phase of the infection and links it to the IL-2 production by CD4 T cells. This enables Treg to control the access to IL-2 niches and reduce the size of the niche constantly, thereby allowing for the control, but not suppression of the response, as strong competitive CD8 T cells will still gain access to IL-2 niches.
However, the number of CTL can be controlled and adjusted to the occurring antigen load driven by the IL-2 production of CD4 T cells. This is especially elegant, because it has been suggested that Treg do not control CD4 T cells strictly *via* IL-2 and therefore do not interfere with the basal supply of IL-2 needed to fight the viral infection (Chinen et al., 2016).
We have shown that Treg depletion does not alter the IL-2 available to CD4 T cells, which argues in the same direction. Treg do not seem to be in direct IL-2 competition with CD4 T cells (Figure 3.13).

4.4 Affinity-based regulation by Treg via CD25 levels

To find out if the regulation solely depends on affinity, we wanted to address the CD25 expression of the effector T cells. Cells with the highest expression of CD25 would likely receive most IL-2 signals. Through this mechanism, Treg could only control *via* IL-2 restriction in the early period of infection when CD8 T cells do not yet express competitive levels of CD25.
We could show that CD25 receptor density does not reflect the access to IL-2 directly. Despite Treg having the highest CD25 levels up to 24 post-infection, CD8 T cells do see IL-2, as well (Figure 3.11).

In contrast, CD4 T cells do not see similar levels of IL-2 (Figure 3.11) indicating that additional factors define the access to IL-2. We hypothesize that the localization of the cells has an impact on their chance to encounter IL-2.
Since CD4 and CD8 T cells spend a disproportionate amount of time arrested at cDC during the first 24h of infection, the distinct IL-2 access could be explained by different localization in different priming clusters and IL-2 production niches. It has been shown before that the localization of CD4 and CD8 T cells is distinct during the priming events in a viral infection (Eickhoff et al., 2015). The temporal changes in IL-2 production are also in line with this (Figure 3.8).
We could show that IL-2 availability for different cell populations correlates with CD25 expression density. The fact that CD8 T cells see autocrine IL-2 during the first 24 h p.i. drastically increases their CD25 expression.
In contrast, CD4 T cells upregulate their CD25 expression much later, while they take over the IL-2 production supplying CD8 T cells in a paracrine manner (Figure 3.10). Despite the data indicating that CD25 expression per se does not correlate with the consumption of IL-2. Affinity seems to be important but not the only defining factor for the competitiveness of IL-2 sensing. Also, we cannot exclude, that cells migrate throughout the LN and might have access to IL-2 at times, expressing CD25 due to recent IL-2 signaling events.
The correlation between CD25 expression levels and IL-2 sensing has been shown before by Kalia et al.. We hypothesize that the localization of the effector cells and their dynamic migration to IL-2 niches define their success. High-affinity cells fulfill the requirement to engage and compete for IL-2 with Treg in those niches. Treg have a very even distribution throughout the LN (Liu et al., 2015) and roam the LN consuming IL-2 (Figure 3.1). This limits the size of the niches and restricts the overall accessibility of IL-2, correlating with available antigen and the number of consumers. This model is supported by data showing that IL-2 production is tied to antigen load in CD4 T cells. The study argues that Treg number and their activation by IL-2 is ensured by low antigen-load as well (Fuhrmann et al., 2016). They also hint toward localization being one of the driving factors for IL-2 access and claim that proximity is important for Treg regulation. To better understand how localization cues impact the IL-2 availability we analyzed this aspect in CXCR3ko mice.

4.5 CXCR3-mediated guidance enhances effector potential

During a viral infection, virus particles are drained to the LN and local infection leads to cDC presenting antigen and priming naïve T cells. As shown before, this happens in spatially distinct clusters in the interfollicular area of the LN (Eickhoff et al., 2015). This is in line with our previous finding, which shows that CD8 T cells see IL-2 early, likely in an autocrine manner and that CD4 T cells do not share this IL-2 access Figure 3.11. However, Treg seem to be able to locate to both niches, as they encounter IL-2, at least on a population level. After priming the activated T cells translocate to deeper areas of the LN within the paracortex, where they receive CD4 T cell help. This interaction is mediated by $XCR1^+$ DC and takes place within the first two days p.i. Cognate T cells spent a large proportion of their time arrested at the aforementioned APC, defining their niche for the early time of infection within the LN. Cells close to a source of IL-2 will encounter it, distant cells will not. We believe that during this phase the IL-2 availability can be reduced by the overall reduction of niche size by Treg. However, it is difficult to imagine that Treg compete actively with cells close to an IL-2 producer.
The inability of Treg to limit the IL-2 availability in the vicinity of IL-2 production, ensures that Treg do not prevent the initial activation of the cells and allows the IL-2 consumption necessary to kick start expression of CD25. As soon as activated CD8 T cells express competitive levels of CD25 (past 24 h), they start migrating again. We believe that this phase determines the active regulation of Treg by reducing the size of IL-2 niches for dynamically moving CTL searching for IL-2. The enforced re-localization of CTL that have successfully received CD4 T cell help within the paracortex enables Treg to compete for CD4-derived IL-2.
The exact localization of CD4 T cells producing IL-2 remains challenging to address. Studies have shown that in steady-state IL-2 producing cells within the LN are mainly CD4 T cells (Yamamoto et al., 2013). The positioning of the cells is very difficult to address, as regular reporter systems are either too insensitive to show endogenous production of IL-2, or it is unclear, whether the cells actually secreting the IL-2 produced. This technical limitation leaves us only speculating about the localization of IL-2 niches. For the same reason, assessing the cell type responsible for the genuine production of IL-2 is challenging to address. We utilized indirect readouts of pSTAT5 to answer the available IL-2 within the LN. Histological staining of IL-2 performed on

sections with auto-reactive CD4 T cells claims localization in the interfollicular area at steady-state,(Liu et al., 2015). If this holds true for antigen-dependent secretion of IL-2 in the late phase of infection, CD8 T cells have to be guided to those IL-2 niches. CXCR3 is a prominent candidate for this, as it has been shown before that CD8 memory T cells preferentially position in those areas based on their CXCR3 expression (Kastenmuller et al., 2013).
On top of this, it has been published that CXCR3 enables cells to locate in more inflammatory regions of the LN (Duckworth et al., 2021; Hu et al., 2011; Kurachi et al., 2011; Sung et al., 2012) and therefore more peripheral areas of the LN with higher antigen and inflammatory cytokine load (Kohlmeier et al., 2011). We wanted to understand if this chemokine receptor also has an impact on IL-2 availability and could show that Treg control CXCR3-expressing cells more tightly than CXCR3ko cells (Figure 3.18). To understand how Treg control is tied to IL-2 availability in this case, we hypothesized that CXCR3 deficient cells see less IL-2 in phases of Treg regulation.
Indeed, during the proliferation of CTL, this was the case and we suggest that regulation is especially efficient in CXCR3-expressing cells as they likely locate in the interfollicular areas, where also IL-2 niches are most likely located (Figure 3.19). Taken together, these findings fit exceptionally well with underlying literature as the differentiation of CXCR3-expressing cells has been reported to be biased towards effector differentiation (Kurachi et al., 2011). This is likely happening in inflammatory cytokine environments, close to the capsule of the LN, where drainage of antigen is occurring.
Having established mechanisms that ensure the competitiveness of Treg and uncovering localization differences in CD8 T cells, we next sought to understand if the IL-2 competition by Treg on its own is a major regulatory mechanism that is sufficient to regulate the response.

4.6 IL-2 competition is a major regulatory mechanism

We analyzed the expansion and differentiation of CD8 T cells *in vivo* under the control of Treg and without. Additionally, we addressed the impact of CD25 expression on CD8 T cells. To make more accurate interpretations of the competitive nature of CD25 expression, we performed competitive transfers, in which CD25-sufficient and CD25ko cells competed against each other within the same environment.
To resolve the contribution of Treg regulation we addressed it by depletion of Treg within

one of two experimental groups. This allowed us to understand the control Treg exert *via* IL-2 competition. Cells deficient in CD25 expression can not be controlled by Treg, if the regulation is mediated *via* IL-2. CD25ko cells do not see competitive levels of IL-2 and are therefore already 'regulated'. These cells should not profit from Treg depletion, whereas CD25-sufficient CD8 T cells should expand significantly more without Treg control.
In fact, we found that CD25ko cells were limited to the same extent with or without Treg (Figure 3.17 B,C). CD25-sufficient cells however increased in frequency and absolute numbers upon Treg depletion (Figure 3.17 B,C). The absolute number of CD25ko cells did not exceed the number of CD25-sufficient cells in the control group. This suggests that the control of CD8 T cells was entirely mediated *via* IL-2 competition.
We also showed that the differentiation is altered in CD25ko cells, which suggests an impact of IL-2 availability for differentiation in the LN. Cells seeing less IL-2 displayed a skewed differentiation towards a more memory-like phenotype (Figure 3.17 D). This result strongly supports the hypothesis that Treg can control CD8 T cells by IL-2 competition, entirely.

Obar and colleagues showed that CD8 T cells deficient in CD25 expression can proliferate to the same extent during the first 4 days post-infection as CD25-sufficient cells (Obar et al., 2010). However, soon after they lose their proliferative capacity due to a lack of IL-2 supply. Compared to CD25-sufficient CD8 T cells, they show significantly less BrdU incorporation on day 8 p.i.
Another finding from this study shows that depletion of CD4 T cells only limits the expansion of CD8 T cells in the late phase of infection, showing a significantly lower frequency of antigen-specific CD8 T cells at day 6 after VV infection. This underlines our findings, showing that CD8 T cells depend on external IL-2 in the late phase of infection. Despite having depleted all CD4 T cells and therefore also all Treg, the availability of IL-2 is still drastically reduced due to the lack of T helper cells. To determine the impact of CD4 T helper cells, a mouse model in which only CD4 T helper cells can be depleted is needed.

4.7 Model of Treg regulation via IL-2 competition

Combining the findings within this study, we propose a model in which Treg control IL-2 availability on a global level in the LN. However, we believe that CD8 T cells can

sustain their initial IL-2 signaling by local sensing of IL-2, produced by CD8 T cells, in order to kick start their CD25 expression and full activation. After receiving CD4 T cell help, CD8 T cells will start proliferating and stop producing IL-2. They now depend on CD4-derived IL-2, and this production is tied to antigen-load within the LN. Treg compete for IL-2 throughout the entire course of the infection. Especially, during the late phases of infection, CD8 need more IL-2 for expansion and Treg limit this access, adjusting the expansion of CD8 T cells to the occurring antigen levels within the LN.
This system is highly dynamic and allows for rapid adaptation. Due to local IL-2 production and the resulting IL-2 signaling in CD8 T cells, the initial activation of CD8 T cells is not restricted. Also, the mode of regulation, limiting the size of IL-2 niches, will ensure that adequately positioned CD8 T cells will receive sufficient amounts of IL-2 by higher affinity towards IL-2. However, Treg always dampen the IL-2 availability and suppress bystander activation and overshooting expansion of CD8 T cells. We believe that CD8 T cells differentiating into effector cells will leave the paracortex towards the interfollicular areas to sense IL-2 produced by activated CD4 T cells. Treg constantly control the size of this niche by consumption on 'pass-by'. A similar model has recently been published, describing the regulation of auto-reactive CD4 T cells (Wong et al., 2021).

Finally, with decreasing IL-2 levels in the LN and the viral infection being cleared, the limited IL-2 resources will lead to enhanced memory differentiation. This ensures, that as soon as the effector population has reached an adequate number, the system is set up in a way, to support much more needed memory differentiation at the appropriate time.

4.8 Limitations of the study

Scientific experiments are simplified approaches to address scientific questions and seek to bring forward new evidence for specific mechanisms and hypotheses. However, experimental setups are regularly hampered by technical limitations and depend on the careful interpretation of the results.
In this study, we addressed the regulatory mechanism of Treg during viral infection. Naturally, we also dealt with certain limitations of the experimental setups, one of them being the transfer of TCR-transgenic T cells as a representative read-out of the endogenous T cell populations. Since only a few endogenous T cell precursors were retrievable

in the early phase of infection, we were limited to analyzing representative T cells that were transferred prior to the experiment.
Due to this, we were able to alter the IL-2 availability within the system and we could make conclusions about the contribution of CD8 and CD4 T cells to the IL-2 pool. However, activated T cells can function as both, IL-2 consumers as well as IL-2 producers. By transferring TCR-transgenic cells into the host, we alter the IL-2 availability within the LN and therefore create an artificial system.
Nevertheless, we believe that the regulatory mechanism of Treg is unchanged within this system and the regulatory activity of Treg might even be more prominent, due to more IL-2 being available. In addition to this, we could show that Treg actively compete for IL-2, which supports our results. Still, we experienced some difficulties, when we transferred to many IL-2 consumer cells. We saw a drastic decrease in pSTAT5 signal on transferred OT-1 T cells in the later phase of infection when these cells underwent strong proliferation. The abolished IL-2 signaling likely was induced by significantly exacerbated IL-2 competition among CD8 T cells itself, decreasing the IL-2 availability. However, we could circumvent these adverse effects by carefully titrating the adequate number of CD8 or CD4 T cells for each time point.

The indirect read-out of IL-2 availability is another limitation that is worth mentioning. We utilized pSTAT5 as a direct read-out for IL-2 signaling and concluded IL-2 availability in correlation to the pSTAT5 signal. While the contribution of other cytokines *via* a shared receptor chain could be excluded, as shown by Liu et al. and assessed by ourselves (data not shown), we can not rule out the possibility of altered IL-2 production or contribution of other cell types. Despite lacking evaluation of these two possibilities, we were most interested in the competition among cells, rather than the overall availability of IL-2. Therefore, analyzing the *de facto* IL-2 signaling of a cell or cell population, was a more conclusive read-out than analyzing the IL-2 abundance within the LN. Nevertheless, interpreting which cell type represents the major source of IL-2 has to be done carefully. To provide further evidence that our considerations are accurate, an ELISA and quantitative PCR of IL-2 transcripts of LN lysates or specific cell populations could help to address possible changes in IL-2 production.
Further, the lack of technical tools to resolve the IL-2 source on a single-cell level makes conclusions about the location of IL-2 production sites difficult. Reporter systems available in our lab are too insensitive to address this question. Also, histological staining of IL-2 was not sufficient and proofed to be too insensitive as well. Re-stimulation of cells *ex vivo* can not address this question, as it is only a tool to show the potential of IL-2

production, but not the *bona fide* IL-2 producers within the LN during infection at specific time points. Alternatively, inhibition of vesicle release in the golgi or endoplasmic reticulum leads to accumulation of the signal with the cell. However, this method can not decipher between the production and release of IL-2. We tested *in vivo* application of those inhibitors, but the approach did not yield reliable results.
Further research is needed to gain a deeper understanding of the IL-2 niche and its spatial characteristics.

While other cell types, such as cDC and innate lymphoid cells have been shown to be able to produce IL-2 in specific contexts or organs, it is very unlikely that they represent a major source of IL-2 in the LN (Granucci et al., 2003; Zhou et al., 2019).
Finally, we do not fully understand the impact of Treg on cDC yet. We performed experiments that address, whether XCR1$^+$ cDC have an impact on the pSTAT5 or CD25 levels of CD8 T cells (data not shown). The indirect regulatory mechanisms of Treg that manipulate the maturation of cDC, expand beyond the scope of this work and ongoing experiments are exploring possible synergistic effects. However, the proximity of XCR1$^+$ cDC and Treg was addressed in 2-photon live imaging experiments, not showing any co-arrest or long-lasting interactions, arguing against a contact-dependent regulation of cDC by Treg (data not shown). Further experiments are needed to address this fully.

4.9 Outlook

The findings presented in this study can be of significant importance for future research projects. Especially in tumor immunology and autoimmune diseases, the clinical relevance is evident. Further research is needed to find ways to bypass Treg control in cases where an expansion of T cells is desired, e.g in tumor treatment and microbial or viral infections. The timing of these interventions can be optimized in a way that Treg functions are reduced during the treatment but enhanced afterward to ensure the restoration of homeostasis. This might be achievable by expanding Treg after the treatment via low-dose IL-2 treatments or expansion of Treg *ex vivo*.
Particularly, the temporal and spatial dynamics of Treg studied in this work could contribute to more sophisticated therapeutic strategies and better avoidance of side effects such as off-target effects and undesired inflammation. Further studies addressing the impact of Treg positioning within the LN or tissue can help to understand the underlying mechanisms for the onset of autoimmunity. Altering the localization of Treg by

expressing specific chemokine receptors on their surface might be a viable therapeutic target to explore and could increase or decrease Treg efficiency.
The data presented supports a concept of Treg control mediated *via* IL-2 competition. CD8 T cells are regulated in their number and differentiation. The dynamic mode of regulation allows for constant fine-tuning and adjusting of the regulatory activity of Treg to the load of inflammatory cytokines and antigen, ultimately representing the severity of the ongoing infection. The regulation is especially prominent during the expansion phase of the anti-viral CD8 T cells. Treg constantly migrate through the LN and compete for IL-2, thereby limiting the size of individual IL-2 niches and consequently also the overall IL-2 availability. Strongly activated T cells that express the adequate chemokine receptors can home to niches that make them less susceptible to IL-2 competition. This is most likely based on proximity to the source for IL-2.

The proposed mechanism of Treg regulation combines three major advantages: It provides mechanisms to tune CD8 T cell responses to the present pathogen load, the unfolding T cell response is not immediately suppressed but tightly controlled in its intensity via CD4-derived IL-2 dependency and is functionally robust due to simple IL-2 scavenging role of Treg.

References

Akira, Uematsu, and Takeuchi. Pathogen recognition and innate immunity. *Cell*, 124 (4):783–801, 2006.

Albert, Sauter, and Bhardwaj. Dendritic cells acquire antigen from apoptotic cells and induce class I-restricted CTLs. *Nature*, 392(6671):86–9, 1998.

Allen, Ansel, Low, Lesley, Tamamura, Fujii, and Cyster. Germinal center dark and light zone organization is mediated by CXCR4 and CXCR5. *Nat Immunol*, 5(9):943–52, 2004.

Allenspach, Lemos, Porrett, Turka, and Laufer. Migratory and lymphoid-resident dendritic cells cooperate to efficiently prime naive CD4 T cells. *Immunity*, 29(5):795–806, 2008.

Amado, Berges, Luther, Mailhe, Garcia, Bandeira, Weaver, Liston, and Freitas. IL-2 coordinates IL-2-producing and regulatory T cell interplay. *J Exp Med*, 210(12):2707–20, 2013.

Aoshi, Zinselmeyer, Konjufca, Lynch, Zhang, Koide, and Miller. Bacterial entry to the splenic white pulp initiates antigen presentation to CD8+ T cells. *Immunity*, 29(3): 476–86, 2008.

Arce-Sillas, Alvarez-Luquin, Tamaya-Dominguez, Gomez-Fuentes, Trejo-Garcia, Melo-Salas, Cardenas, Rodriguez-Ramirez, and Adalid-Peralta. Regulatory T Cells: Molecular Actions on Effector Cells in Immune Regulation. *Journal of Immunology Research*, 2016, 2016.

Arpaia, Green, Moltedo, Arvey, Hemmers, Yuan, Treuting, and Rudensky. A Distinct Function of Regulatory T Cells in Tissue Protection. *Cell*, 162(5):1078–1089, 2015.

Arstila, Casrouge, Baron, Even, Kanellopoulos, and Kourilsky. A direct estimate of the human alphabeta T cell receptor diversity. *Science*, 286(5441):958–61, 1999.

Aruga, Aruga, Cameron, and Chang. Different cytokine profiles released by CD4+ and CD8+ tumor-draining lymph node cells involved in mediating tumor regression. *J Leukoc Biol*, 61(4):507–16, 1997.

Bajenoff, Egen, Koo, Laugier, Brau, Glaichenhaus, and Germain. Stromal cell networks regulate lymphocyte entry, migration, and territoriality in lymph nodes. *Immunity*, 25(6):989–1001, 2006.

Barron, Dooms, Hoyer, Kuswanto, Hofmann, O'Gorman, and Abbas. Cutting edge: mechanisms of IL-2-dependent maintenance of functional regulatory T cells. *J Immunol*, 185(11):6426–30, 2010.

Bodor, Fehervari, Diamond, and Sakaguchi. Frontline: ICER/CREM-mediated transcriptional attenuation of IL-2 and its role in suppression by regulatory T cells. *European Journal of Immunology*, 37(4):884–895, 2007.

Bousso and Robey. Dynamics of CD8+ T cell priming by dendritic cells in intact lymph nodes. *Nat Immunol*, 4(6):579–85, 2003.

Boyman and Sprent. The role of interleukin-2 during homeostasis and activation of the immune system. *Nat Rev Immunol*, 12(3):180–90, 2012.

Breitfeld, Ohl, Kremmer, Ellwart, Sallusto, Lipp, and Forster. Follicular B helper T cells express CXC chemokine receptor 5, localize to B cell follicles, and support immunoglobulin production. *J Exp Med*, 192(11):1545–52, 2000.

Brewitz, Eickhoff, Dahling, Quast, Bedoui, Kroczek, Kurts, Garbi, Barchet, Iannacone, Klauschen, Kolanus, Kaisho, Colonna, Germain, and Kastenmuller. CD8(+) T Cells Orchestrate pDC-XCR1(+) Dendritic Cell Spatial and Functional Cooperativity to Optimize Priming. *Immunity*, 46(2):205–219, 2017.

Brincks, Katewa, Kucaba, Griffith, and Legge. CD8 T cells utilize TRAIL to control influenza virus infection. *J Immunol*, 181(7):4918–25, 2008.

Busse, de la Rosa, Hobiger, Thurley, Flossdorf, Scheffold, and Hofer. Competing feedback loops shape IL-2 signaling between helper and regulatory T lymphocytes in cellular microenvironments. *Proc Natl Acad Sci U S A*, 107(7):3058–63, 2010.

Cao, Cai, Fehniger, Song, Collins, Piwnica-Worms, and Ley. Granzyme B and perforin are important for regulatory T cell-mediated suppression of tumor clearance. *Immunity*, 27(4):635–46, 2007.

Castellino, Huang, Altan-Bonnet, Stoll, Scheinecker, and Germain. Chemokines enhance immunity by guiding naive CD8+ T cells to sites of CD4+ T cell-dendritic cell interaction. *Nature*, 440(7086):890–5, 2006.

Chang and Turley. Stromal infrastructure of the lymph node and coordination of immunity. *Trends Immunol*, 36(1):30–9, 2015.

Charbonnier, Cui, Stephen-Victor, Harb, Lopez, Bleesing, Garcia-Lloret, Chen, Ozen, Carmeliet, Li, Pellegrini, and Chatila. Functional reprogramming of regulatory T cells in the absence of Foxp3. *Nat Immunol*, 20(9):1208–1219, 2019.

Chaudhary and Wesemann. Analyzing Immunoglobulin Repertoires. *Front Immunol*, 9: 462, 2018.

Chen, Jin, Hardegen, Lei, Li, Marinos, McGrady, and Wahl. Conversion of peripheral CD4+CD25- naive T cells to CD4+CD25+ regulatory T cells by TGF-beta induction of transcription factor Foxp3. *J Exp Med*, 198(12):1875–86, 2003.

Chen, Ji, Ngiow, Manne, Cai, Huang, Johnson, Staupe, Bengsch, Xu, Yu, Kurachi, Herati, Vella, Baxter, Wu, Khan, Beltra, Giles, Stelekati, McLane, Lau, Yang, Berger, Vahedi, Ji, and Wherry. TCF-1-Centered Transcriptional Network Drives an Effector versus Exhausted CD8 T Cell-Fate Decision. *Immunity*, 2019.

Cheng, Ohlen, Nelson, and Greenberg. Enhanced signaling through the IL-2 receptor in CD8(+) T cells regulated by antigen recognition results in preferential proliferation and expansion of responding CD8(+) T cells rather than promotion of cell death. *Proceedings of the National Academy of Sciences of the United States of America*, 99 (5):3001–3006, 2002.

Chinen, Kannan, Levine, Fan, Klein, Zheng, Gasteiger, Feng, Fontenot, and Rudensky. An essential role for the IL-2 receptor in Treg cell function. *Nat Immunol*, 17(11): 1322–1333, 2016.

Cohnheim. *Über Entzündung und Eiterung*, volume 40, page 855. Reimer, Berlin, 1867.

Corthay. How do regulatory T cells work? *Scand J Immunol*, 70(4):326–36, 2009.

Cumaraswamy and Gunning. Progress towards direct inhibitors of Stat5 protein. *Horm Mol Biol Clin Investig*, 10(2):281–6, 2012.

Curtsinger, Schmidt, Mondino, Lins, Kedl, Jenkins, and Mescher. Inflammatory cytokines provide a third signal for activation of naive CD4+ and CD8+ T cells. *J Immunol*, 162(6):3256–62, 1999.

Curtsinger, Lins, and Mescher. Signal 3 determines tolerance versus full activation of naive CD8 T cells: dissociating proliferation and development of effector function. *J Exp Med*, 197(9):1141–51, 2003.

Curtsinger, Valenzuela, Agarwal, Lins, and Mescher. Type I IFNs provide a third signal to CD8 T cells to stimulate clonal expansion and differentiation. *J Immunol*, 174(8): 4465–9, 2005.

Cyster and Schwab. Sphingosine-1-phosphate and lymphocyte egress from lymphoid organs. *Annu Rev Immunol*, 30:69–94, 2012.

D'Cruz, Rubinstein, and Goldrath. Surviving the crash: transitioning from effector to memory CD8+ T cell. *Semin Immunol*, 21(2):92–8, 2009.

de la Rosa, Rutz, Dorninger, and Scheffold. Interleukin-2 is essential for CD4(+)CD25(+) regulatory T cell function. *European Journal of Immunology*, 34 (9):2480–2488, 2004.

Deaglio, Dwyer, Gao, Friedman, Usheva, Erat, Chen, Enjyoji, Linden, Oukka, Kuchroo, Strom, and Robson. Adenosine generation catalyzed by CD39 and CD73 expressed on regulatory T cells mediates immune suppression. *J Exp Med*, 204(6):1257–65, 2007.

Delacher, Imbusch, Hotz-Wagenblatt, Mallm, Bauer, Simon, Riegel, Rendeiro, Bittner, Sanderink, Pant, Schmidleithner, Braband, Echtenachter, Fischer, Giunchiglia, Hoffmann, Edinger, Bock, Rehli, Brors, Schmidl, and Feuerer. Precursors for Nonlymphoid-Tissue Treg Cells Reside in Secondary Lymphoid Organs and Are Programmed by the Transcription Factor BATF. *Immunity*, 52(2):295–312 e11, 2020.

DiToro, Winstead, Pham, Witte, Andargachew, Singer, Wilson, Zindl, Luther, Silberger, Weaver, Kolawole, Martinez, Turner, Hatton, Moon, Way, Evavold, and Weaver. Differential IL-2 expression defines developmental fates of follicular versus nonfollicular helper T cells. *Science*, 361(6407), 2018.

Dorner, Dorner, Zhou, Opitz, Mora, Guttler, Hutloff, Mages, Ranke, Schaefer, Jack, Henn, and Kroczek. Selective expression of the chemokine receptor XCR1 on cross-presenting dendritic cells determines cooperation with CD8+ T cells. *Immunity*, 31 (5):823–33, 2009.

D'Souza and Lefrancois. IL-2 is not required for the initiation of CD8 T cell cycling but sustains expansion. *J Immunol*, 171(11):5727–35, 2003.

D'Souza, Schluns, Masopust, and Lefrancois. Essential role for IL-2 in the regulation of antiviral extralymphoid CD8 T cell responses. *J Immunol*, 168(11):5566–72, 2002.

Duckworth, Lafouresse, Wimmer, Broomfield, Dalit, Alexandre, Sheikh, Qin, Alvarado, Mielke, Pellegrini, Mueller, Boudier, Rogers, and Groom. Effector and stem-like memory cell fates are imprinted in distinct lymph node niches directed by CXCR3 ligands. *Nat Immunol*, 22(4):434–448, 2021.

Dudziak, Kamphorst, Heidkamp, Buchholz, Trumpfheller, Yamazaki, Cheong, Liu, Lee, Park, Steinman, and Nussenzweig. Differential antigen processing by dendritic cell subsets in vivo. *Science*, 315(5808):107–11, 2007.

Edwards, Chaussabel, Tomlinson, Schulz, Sher, and Reis e Sousa. Relationships among murine CD11c(high) dendritic cell subsets as revealed by baseline gene expression patterns. *J Immunol*, 171(1):47–60, 2003.

Eickhoff, Brewitz, Gerner, Klauschen, Komander, Hemmi, Garbi, Kaisho, Germain, and Kastenmuller. Robust Anti-viral Immunity Requires Multiple Distinct T Cell-Dendritic Cell Interactions. *Cell*, 162(6):1322–37, 2015.

Fontenot, Rasmussen, Williams, Dooley, Farr, and Rudensky. Regulatory T cell lineage specification by the forkhead transcription factor foxp3. *Immunity*, 22(3):329–41, 2005.

Fremont, Matsumura, Stura, Peterson, and Wilson. Crystal structures of two viral peptides in complex with murine MHC class I H-2Kb. *Science*, 257(5072):919–27, 1992.

Fuhrmann, Lischke, Gross, Scheel, Bauer, Kalim, Radbruch, Herzel, Hutloff, and Baumgrass. Adequate immune response ensured by binary IL-2 and graded CD25 expression in a murine transfer model. *Elife*, 5, 2016.

Garg, Muschaweckh, Moreno, Vasanthakumar, Floess, Lepennetier, Oellinger, Zhan, Regen, Hiltensperger, Peter, Aly, Knier, Palam, Kapur, Kaplan, Waisman, Rad, Schotta, Huehn, Kallies, and Korn. Blimp1 Prevents Methylation of Foxp3 and Loss of Regulatory T Cell Identity at Sites of Inflammation. *Cell Rep*, 26(7):1854–1868 e5, 2019.

Gatto, Wood, Caminschi, Murphy-Durland, Schofield, Christ, Karupiah, and Brink. The chemotactic receptor EBI2 regulates the homeostasis, localization and immunological function of splenic dendritic cells. *Nat Immunol*, 14(5):446–53, 2013.

Gerlach, Moseman, Loughhead, Alvarez, Zwijnenburg, Waanders, Garg, de la Torre, and von Andrian. The Chemokine Receptor CX3CR1 Defines Three Antigen-Experienced CD8 T Cell Subsets with Distinct Roles in Immune Surveillance and Homeostasis. *Immunity*, 45(6):1270–1284, 2016.

Germain. T-cell development and the CD4-CD8 lineage decision. *Nat Rev Immunol*, 2 (5):309–22, 2002.

Gerner, Torabi-Parizi, and Germain. Strategically localized dendritic cells promote rapid T cell responses to lymph-borne particulate antigens. *Immunity*, 42(1):172–85, 2015.

Gonzalez, Lukacs-Kornek, Kuligowski, Pitcher, Degn, Kim, Cloninger, Martinez-Pomares, Gordon, Turley, and Carroll. Capture of influenza by medullary dendritic cells via SIGN-R1 is essential for humoral immunity in draining lymph nodes. *Nat Immunol*, 11(5):427–34, 2010.

Granucci, Feau, Angeli, Trottein, and Ricciardi-Castagnoli. Early IL-2 production by mouse dendritic cells is the result of microbial-induced priming. *Journal of Immunology*, 170(10):5075–5081, 2003.

Greyer, Whitney, Stock, Davey, Tebartz, Bachem, Mintern, Strugnell, Turner, Gebhardt, O'Keeffe, Heath, and Bedoui. T Cell Help Amplifies Innate Signals in CD8(+) DCs for Optimal CD8(+) T Cell Priming. *Cell Rep*, 14(3):586–597, 2016.

Groom and Luster. CXCR3 in T cell function. *Experimental Cell Research*, 317(5): 620–631, 2011.

Guo, Jardetzky, Garrett, Lane, Strominger, and Wiley. Different length peptides bind to HLA-Aw68 similarly at their ends but bulge out in the middle. *Nature*, 360(6402): 364–6, 1992.

Hancock, Lu, Gao, Csizmadia, Faia, King, Smiley, Ling, Gerard, and Gerard. Requirement of the chemokine receptor CXCR3 for acute allograft rejection. *Journal of Experimental Medicine*, 192(10):1515–1519, 2000.

Hansen and Schofield. Natural Regulatory T Cells in Malaria: Host or Parasite Allies? *Plos Pathogens*, 6(4), 2010.

Harding, McArthur, Gross, Raulet, and Allison. CD28-mediated signalling co-stimulates murine T cells and prevents induction of anergy in T-cell clones. *Nature*, 356(6370): 607–9, 1992.

Harwood and Batista. Early events in B cell activation. *Annu Rev Immunol*, 28:185–210, 2010.

Hassin, Garber, Meiraz, Schiffenbauer, and Berke. Cytotoxic T lymphocyte perforin and Fas ligand working in concert even when Fas ligand lytic action is still not detectable. *Immunology*, 133(2):190–6, 2011.

Henri, Vremec, Kamath, Waithman, Williams, Benoist, Burnham, Saeland, Handman, and Shortman. The dendritic cell populations of mouse lymph nodes. *J Immunol*, 167 (2):741–8, 2001.

Hirst, Buzza, Bird, Warren, Cameron, Zhang, Ashton-Rickardt, and Bird. The intracellular granzyme B inhibitor, proteinase inhibitor 9, is up-regulated during accessory cell maturation and effector cell degranulation, and its overexpression enhances CTL potency. *J Immunol*, 170(2):805–15, 2003.

Hogquist, Jameson, Heath, Howard, Bevan, and Carbone. T-Cell Receptor Antagonist Peptides Induce Positive Selection. *Cell*, 76(1):17–27, 1994.

Honke, Shaabani, Cadeddu, Sorg, Zhang, Trilling, Klingel, Sauter, Kandolf, Gailus, van Rooijen, Burkart, Baldus, Grusdat, Lohning, Hengel, Pfeffer, Tanaka, Haussinger, Recher, Lang, and Lang. Enforced viral replication activates adaptive immunity and is essential for the control of a cytopathic virus. *Nat Immunol*, 13(1):51–7, 2011.

Hori, Carvalho, and Demengeot. CD25+CD4+ regulatory T cells suppress CD4+ T cell-mediated pulmonary hyperinflammation driven by Pneumocystis carinii in immunodeficient mice. *Eur J Immunol*, 32(5):1282–91, 2002.

Hu, Kagari, Clingan, and Matloubian. Expression of chemokine receptor CXCR3 on T cells affects the balance between effector and memory CD8 T-cell generation. *Proc Natl Acad Sci U S A*, 108(21):E118–27, 2011.

Humblet-Baron, Franckaert, Dooley, Bornschein, Cauwe, Schonefeldt, Bossuyt, Matthys, Baron, Wouters, and Liston. IL-2 consumption by highly activated CD8 T cells induces regulatory T-cell dysfunction in patients with hemophagocytic lymphohistiocytosis. *Journal of Allergy and Clinical Immunology*, 138(1):200–+, 2016.

Iannacone, Moseman, Tonti, Bosurgi, Junt, Henrickson, Whelan, Guidotti, and von Andrian. Subcapsular sinus macrophages prevent CNS invasion on peripheral infection with a neurotropic virus. *Nature*, 465(7301):1079–83, 2010.

Inaba and Steinman. Resting and sensitized T lymphocytes exhibit distinct stimulatory (antigen-presenting cell) requirements for growth and lymphokine release. *J Exp Med*, 160(6):1717–35, 1984.

Iwasaki and Medzhitov. Toll-like receptor control of the adaptive immune responses. *Nat Immunol*, 5(10):987–95, 2004.

Janeway. Approaching the asymptote? Evolution and revolution in immunology. *Cold Spring Harb Symp Quant Biol*, 54 Pt 1:1–13, 1989.

Ji, Masterson, Sun, and Soong. CD4+CD25+ regulatory T cells restrain pathogenic responses during Leishmania amazonensis infection. *J Immunol*, 174(11):7147–53, 2005.

Joshi, Cui, Chandele, Lee, Urso, Hagman, Gapin, and Kaech. Inflammation directs memory precursor and short-lived effector CD8(+) T cell fates via the graded expression of T-bet transcription factor. *Immunity*, 27(2):281–95, 2007.

Kaech and Cui. Transcriptional control of effector and memory CD8+ T cell differentiation. *Nat Rev Immunol*, 12(11):749–61, 2012.

Kahan, Bakshi, Ingram, Hendrickson, Lefkowitz, Crossman, Harrington, Weaver, and Zajac. Intrinsic IL-2 production by effector CD8 T cells affects IL-2 signaling and promotes fate decisions, stemness, and protection. *Sci Immunol*, 7(68):eabl6322, 2022.

Kalia, Sarkar, Subramaniam, Haining, Smith, and Ahmed. Prolonged interleukin-2Ralpha expression on virus-specific CD8+ T cells favors terminal-effector differentiation in vivo. *Immunity*, 32(1):91–103, 2010.

Kamala. Hock immunization: a humane alternative to mouse footpad injections. *J Immunol Methods*, 328(1-2):204–14, 2007.

Kastenmuller, Gasteiger, Subramanian, Sparwasser, Busch, Belkaid, Drexler, and Germain. Regulatory T cells selectively control CD8+ T cell effector pool size via IL-2 restriction. *J Immunol*, 187(6):3186–97, 2011.

Kastenmuller, Brandes, Wang, Herz, Egen, and Germain. Peripheral prepositioning and local CXCL9 chemokine-mediated guidance orchestrate rapid memory CD8+ T cell responses in the lymph node. *Immunity*, 38(3):502–13, 2013.

Kersh and Allen. Structural basis for T cell recognition of altered peptide ligands: a single T cell receptor can productively recognize a large continuum of related ligands. *J Exp Med*, 184(4):1259–68, 1996.

Kim. FOXP3 and its role in the immune system. *Adv Exp Med Biol*, 665:17–29, 2009.

Kim, Rasmussen, and Rudensky. Regulatory T cells prevent catastrophic autoimmunity throughout the lifespan of mice. *Nat Immunol*, 8(2):191–7, 2007.

Kinter, Hennessey, Bell, Kern, Lin, Daucher, Planta, McGlaughlin, Jackson, Ziegler, and Fauci. CD25(+) CD4(+) regulatory T cells from the peripheral blood of asymptomatic HIV-infected individuals regulate CD4(+) and CD8(+) HIV-specific T cell immune responses in vitro and are associated with favorable clinical markers of disease status. *Journal of Experimental Medicine*, 200(3):331–343, 2004.

Kitano, Yamazaki, Takumi, Ikeno, Hemmi, Takahashi, Shimizu, Fraser, Hoshino, Kaisho, and Okada. Imaging of the cross-presenting dendritic cell subsets in the skin-draining lymph node. *Proc Natl Acad Sci U S A*, 113(4):1044–9, 2016.

Kohlmeier, Reiley, Perona-Wright, Freeman, Yager, Connor, Brincks, Cookenham, Roberts, Burkum, Sell, Winslow, Blackman, Mohrs, and Woodland. Inflammatory chemokine receptors regulate CD8(+) T cell contraction and memory generation following infection. *Journal of Experimental Medicine*, 208(8):1621–1634, 2011.

Kolumam, Thomas, Thompson, Sprent, and Murali-Krishna. Type I interferons act directly on CD8 T cells to allow clonal expansion and memory formation in response to viral infection. *J Exp Med*, 202(5):637–50, 2005.

Komatsu, Okamoto, Sawa, Nakashima, Oh-hora, Kodama, Tanaka, Bluestone, and Takayanagi. Pathogenic conversion of Foxp3+ T cells into TH17 cells in autoimmune arthritis. *Nat Med*, 20(1):62–8, 2014.

Kurachi, Kurachi, Suenaga, Tsukui, Abe, Ueha, Tomura, Sugihara, Takamura, Kakimi, and Matsushima. Chemokine receptor CXCR3 facilitates CD8(+) T cell differentiation into short-lived effector cells leading to memory degeneration. *J Exp Med*, 208(8): 1605–20, 2011.

Kurts, Heath, Carbone, Allison, Miller, and Kosaka. Constitutive class I-restricted exogenous presentation of self antigens in vivo. *J Exp Med*, 184(3):923–30, 1996.

Levine, Arvey, Jin, and Rudensky. Continuous requirement for the TCR in regulatory T cell function. *Nat Immunol*, 15(11):1070–8, 2014.

Liu, Gerner, Van Panhuys, Levine, Rudensky, and Germain. Immune homeostasis enforced by co-localized effector and regulatory T cells. *Nature*, 528(7581):225–30, 2015.

Loebbermann, Thornton, Durant, Sparwasser, Webster, Sprent, Culley, Johansson, and Openshaw. Regulatory T cells expressing granzyme B play a critical role in controlling lung inflammation during acute viral infection. *Mucosal Immunol*, 5(2):161–72, 2012.

Loebbermann, Durant, Thornton, Johansson, and Openshaw. Defective immunoregulation in RSV vaccine-augmented viral lung disease restored by selective chemoattraction of regulatory T cells. *Proceedings of the National Academy of Sciences of the United States of America*, 110(8):2987–2992, 2013.

Luckheeram, Zhou, Verma, and Xia. CD4(+)T cells: differentiation and functions. *Clin Dev Immunol*, 2012:925135, 2012.

Madisen, Zwingman, Sunkin, Oh, Zariwala, Gu, Ng, Palmiter, Hawrylycz, Jones, Lein, and Zeng. A robust and high-throughput Cre reporting and characterization system for the whole mouse brain. *Nature Neuroscience*, 13(1):133–U311, 2010.

Maekawa, Minato, Ishifune, Kurihara, Kitamura, Kojima, Yagita, Sakata-Yanagimoto, Saito, Taniuchi, Chiba, Sone, and Yasutomo. Notch2 integrates signaling by the transcription factors RBP-J and CREB1 to promote T cell cytotoxicity. *Nature Immunology*, 9(10):1140–1147, 2008.

Malek, Yu, Zhu, Matsutani, Adeegbe, and Bayer. IL-2 family of cytokines in T regulatory cell development and homeostasis. *J Clin Immunol*, 28(6):635–9, 2008.

Maruhashi, Okazaki, Sugiura, Takahashi, Maeda, Shimizu, and Okazaki. LAG-3 inhibits the activation of CD4(+) T cells that recognize stable pMHCII through its conformation-dependent recognition of pMHCII. *Nature Immunology*, 19(12):1415–+, 2018.

Mason. A very high level of crossreactivity is an essential feature of the T-cell receptor. *Immunol Today*, 19(9):395–404, 1998.

Matheu, Othy, Greenberg, Dong, Schuijs, Deswarte, Hammad, Lambrecht, Parker, and Cahalan. Imaging regulatory T cell dynamics and CTLA4-mediated suppression of T cell priming. *Nat Commun*, 6:6219, 2015.

McNab, Mayer-Barber, Sher, Wack, and O'Garra. Type I interferons in infectious disease. *Nature Reviews Immunology*, 15(2):87–103, 2015.

McNally, Hill, Sparwasser, Thomas, and Steptoe. CD4+CD25+ regulatory T cells control CD8+ T-cell effector differentiation by modulating IL-2 homeostasis. *Proc Natl Acad Sci U S A*, 108(18):7529–34, 2011.

Medzhitov. Inflammation 2010: new adventures of an old flame. *Cell*, 140(6):771–6, 2010.

Medzhitov and Janeway. Innate immune recognition: mechanisms and pathways. *Immunol Rev*, 173:89–97, 2000.

Mempel, Henrickson, and Von Andrian. T-cell priming by dendritic cells in lymph nodes occurs in three distinct phases. *Nature*, 427(6970):154–9, 2004.

Merad, Sathe, Helft, Miller, and Mortha. The dendritic cell lineage: ontogeny and function of dendritic cells and their subsets in the steady state and the inflamed setting. *Annu Rev Immunol*, 31:563–604, 2013.

Miller, Wei, Parker, and Cahalan. Two-photon imaging of lymphocyte motility and antigen response in intact lymph node. *Science*, 296(5574):1869–73, 2002.

Miragaia, Gomes, Chomka, Jardine, Riedel, Hegazy, Whibley, Tucci, Chen, Lindeman, Emerton, Krausgruber, Shields, Haniffa, Powrie, and Teichmann. Single-Cell Transcriptomics of Regulatory T Cells Reveals Trajectories of Tissue Adaptation. *Immunity*, 50(2):493–504 e7, 2019.

Miyao, Floess, Setoguchi, Luche, Fehling, Waldmann, Huehn, and Hori. Plasticity of Foxp3(+) T cells reflects promiscuous Foxp3 expression in conventional T cells but not reprogramming of regulatory T cells. *Immunity*, 36(2):262–75, 2012.

Mootha, Lindgren, Eriksson, Subramanian, Sihag, Lehar, Puigserver, Carlsson, Ridderstrale, Laurila, Houstis, Daly, Patterson, Mesirov, Golub, Tamayo, Spiegelman, Lander, Hirschhorn, Altshuler, and Groop. PGC-1alpha-responsive genes involved in oxidative phosphorylation are coordinately downregulated in human diabetes. *Nat Genet*, 34(3):267–73, 2003.

Morgan, Ruscetti, and Gallo. Selective in vitro growth of T lymphocytes from normal human bone marrows. *Science*, 193(4257):1007–8, 1976.

Moriggl, Topham, Teglund, Sexl, McKay, Wang, Hoffmeyer, van Deursen, Sangster, Bunting, Grosveld, and Ihle. Stat5 is required for IL-2-induced cell cycle progression of peripheral T cells. *Immunity*, 10(2):249–259, 1999.

Mueller and Germain. Stromal cell contributions to the homeostasis and functionality of the immune system. *Nat Rev Immunol*, 9(9):618–29, 2009.

Murphy, Grajales-Reyes, Wu, Tussiwand, Briseno, Iwata, Kretzer, Durai, and Murphy. Transcriptional Control of Dendritic Cell Development. *Annu Rev Immunol*, 34:93–119, 2016.

Obar, Molloy, Jellison, Stoklasek, Zhang, Usherwood, and Lefrancois. CD4+ T cell regulation of CD25 expression controls development of short-lived effector CD8+ T cells in primary and secondary responses. *Proc Natl Acad Sci U S A*, 107(1):193–8, 2010.

O'Gorman, Dooms, Thorne, Kuswanto, Simonds, Krutzik, Nolan, and Abbas. The initial phase of an immune response functions to activate regulatory T cells. *J Immunol*, 183 (1):332–9, 2009.

Ohl, Mohaupt, Czeloth, Hintzen, Kiafard, Zwirner, Blankenstein, Henning, and Forster. CCR7 governs skin dendritic cell migration under inflammatory and steady-state conditions. *Immunity*, 21(2):279–88, 2004.

Onder, Narang, Scandella, Chai, Iolyeva, Hoorweg, Halin, Richie, Kaye, Westermann, Cupedo, Coles, and Ludewig. IL-7-producing stromal cells are critical for lymph node remodeling. *Blood*, 120(24):4675–83, 2012.

Ovcinnikovs, Ross, Petersone, Edner, Heuts, Ntavli, Kogimtzis, Kennedy, Wang, Bennett, Sansom, and Walker. CTLA-4-mediated transendocytosis of costimulatory molecules primarily targets migratory dendritic cells. *Sci Immunol*, 4(35), 2019.

Oxenius, Bachmann, Zinkernagel, and Hengartner. Virus-specific MHC class II-restricted TCR-transgenic mice: effects on humoral and cellular immune responses after viral infection. *European Journal of Immunology*, 28(1):390–400, 1998.

Oyler-Yaniv, Oyler-Yaniv, Whitlock, Liu, Germain, Huse, Altan-Bonnet, and Krichevsky. A Tunable Diffusion-Consumption Mechanism of Cytokine Propagation Enables Plasticity in Cell-to-Cell Communication in the Immune System. *Immunity*, 46(4):609–620, 2017.

Parish and Kaech. Diversity in CD8(+) T cell differentiation. *Curr Opin Immunol*, 21 (3):291–7, 2009.

Park and Lee. The Role of Skin and Orogenital Microbiota in Protective Immunity and Chronic Immune-Mediated Inflammatory Disease. *Front Immunol*, 8:1955, 2017.

Pearce and Shen. Generation of CD8 T cell memory is regulated by IL-12. *J Immunol*, 179(4):2074–81, 2007.

Perillo, Pace, Seilhamer, and Baum. Apoptosis of T-Cells Mediated by Galectin-1. *Nature*, 378(6558):736–739, 1995.

Pircher, Burki, Lang, Hengartner, and Zinkernagel. Tolerance Induction in Double Specific T-Cell Receptor Transgenic Mice Varies with Antigen. *Nature*, 342(6249): 559–561, 1989.

Popmihajlov, Xu, Morgan, Milligan, and Smith. Conditional IL-2 gene deletion: consequences for T cell proliferation. *Frontiers in Immunology*, 3, 2012.

Prlic, Hernandez-Hoyos, and Bevan. Duration of the initial TCR stimulus controls the magnitude but not functionality of the CD8+ T cell response. *J Exp Med*, 203(9): 2135–43, 2006.

Probst, Lagnel, Kollias, and van den Broek. Inducible transgenic mice reveal resting dendritic cells as potent inducers of CD8+ T cell tolerance. *Immunity*, 18(5):713–20, 2003.

Qi, Kastenmuller, and Germain. Spatiotemporal basis of innate and adaptive immunity in secondary lymphoid tissue. *Annu Rev Cell Dev Biol*, 30:141–67, 2014a.

Qi, Liu, Cheng, Glanville, Zhang, Lee, Olshen, Weyand, Boyd, and Goronzy. Diversity and clonal selection in the human T-cell repertoire. *Proc Natl Acad Sci U S A*, 111 (36):13139–44, 2014b.

Rantakari, Auvinen, Jappinen, Kapraali, Valtonen, Karikoski, Gerke, Iftakhar, Keuschnigg, Umemoto, Tohya, Miyasaka, Elima, Jalkanen, and Salmi. The endothelial protein PLVAP in lymphatics controls the entry of lymphocytes and antigens into lymph nodes. *Nat Immunol*, 16(4):386–96, 2015.

Ratner and Clark. Role of TNF-alpha in CD8+ cytotoxic T lymphocyte-mediated lysis. *J Immunol*, 150(10):4303–14, 1993.

Rock, York, and Goldberg. Post-proteasomal antigen processing for major histocompatibility complex class I presentation. *Nat Immunol*, 5(7):670–7, 2004.

Rubtsov, Niec, Josefowicz, Li, Darce, Mathis, Benoist, and Rudensky. Stability of the regulatory T cell lineage in vivo. *Science*, 329(5999):1667–71, 2010.

Rudensky, Preston-Hurlburt, Hong, Barlow, and Janeway. Sequence analysis of peptides bound to MHC class II molecules. *Nature*, 353(6345):622–7, 1991.

Rushbrook, Ward, Unitt, Vowler, Lucas, Klenerman, and Alexander. Regulatory T cells suppress in vitro proliferation of virus-specific CD8(+) T cells during persistent hepatitis C virus infection. *Journal of Virology*, 79(12):7852–7859, 2005.

Sakaguchi, Yamaguchi, Nomura, and Ono. Regulatory T cells and immune tolerance. *Cell*, 133(5):775–87, 2008.

Sakaguchi, Wing, Onishi, Prieto-Martin, and Yamaguchi. Regulatory T cells: how do they suppress immune responses? *Int Immunol*, 21(10):1105–11, 2009.

Sallusto, Lenig, Forster, Lipp, and Lanzavecchia. Two subsets of memory T lymphocytes with distinct homing potentials and effector functions. *Nature*, 401(6754):708–12, 1999.

Schaefer, Schaefer, Kappler, Marrack, and Kedl. Observation of antigen-dependent CD8(+) T-cell/dendritic cell interactions in vivo. *Cellular Immunology*, 214(2):110–122, 2001.

Schoenberger, Toes, van der Voort, Offringa, and Melief. T-cell help for cytotoxic T lymphocytes is mediated by CD40-CD40L interactions. *Nature*, 393(6684):480–483, 1998.

Seyer, Kirchberger, Majdic, Seipelt, Jindra, Schrauf, and Stockl. Human rhinoviruses induce IL-35-producing Treg via induction of B7-H1 (CD274) and sialoadhesin (CD169) on DC. *European Journal of Immunology*, 40(2):321–329, 2010.

Shedlock and Shen. Requirement for CD4 T cell help in generating functional CD8 T cell memory. *Science*, 300(5617):337–339, 2003.

Shevach. Mechanisms of foxp3+ T regulatory cell-mediated suppression. *Immunity*, 30 (5):636–45, 2009.

Shevach. Application of IL-2 therapy to target T regulatory cell function. *Trends in Immunology*, 33(12):626–632, 2012.

Sim, Martin-Orozco, Jin, Yang, Wu, Washington, Sanders, Lacey, Wang, Vence, Hwu, and Radvanyi. IL-2 therapy promotes suppressive ICOS+ Treg expansion in melanoma patients. *J Clin Invest*, 124(1):99–110, 2014.

Singh, Hjort, Thorvaldson, and Sandler. Concomitant analysis of Helios and Neuropilin-1 as a marker to detect thymic derived regulatory T cells in naive mice. *Sci Rep*, 5: 7767, 2015.

Sixt, Kanazawa, Selg, Samson, Roos, Reinhardt, Pabst, Lutz, and Sorokin. The conduit system transports soluble antigens from the afferent lymph to resident dendritic cells in the T cell area of the lymph node. *Immunity*, 22(1):19–29, 2005.

Smith, Taunton, and Weiss. IL-2R beta abundance differentially tunes IL-2 signaling dynamics in CD4(+) and CD8(+) T cells. *Science Signaling*, 10(510), 2017.

Sporri and Reis e Sousa. Inflammatory mediators are insufficient for full dendritic cell activation and promote expansion of CD4+ T cell populations lacking helper function. *Nat Immunol*, 6(2):163–70, 2005.

Stauber, Debler, Horton, Smith, and Wilson. Crystal structure of the IL-2 signaling complex: paradigm for a heterotrimeric cytokine receptor. *Proc Natl Acad Sci U S A*, 103(8):2788–93, 2006.

Steinman and Witmer. Lymphoid dendritic cells are potent stimulators of the primary mixed leukocyte reaction in mice. *Proc Natl Acad Sci U S A*, 75(10):5132–6, 1978.

Stoll, Delon, Brotz, and Germain. Dynamic imaging of T cell-dendritic cell interactions in lymph nodes. *Science*, 296(5574):1873–6, 2002.

Stuart, Butler, Hoffman, Hafemeister, Papalexi, Mauck, Hao, Stoeckius, Smibert, and Satija. Comprehensive Integration of Single-Cell Data. *Cell*, 177(7):1888–1902 e21, 2019.

Subramanian, Tamayo, Mootha, Mukherjee, Ebert, Gillette, Paulovich, Pomeroy, Golub, Lander, and Mesirov. Gene set enrichment analysis: a knowledge-based approach for interpreting genome-wide expression profiles. *Proc Natl Acad Sci U S A*, 102(43): 15545–50, 2005.

Suffner, Hochweller, Kuhnle, Li, Kroczek, Garbi, and Hammerling. Dendritic Cells Support Homeostatic Expansion of Foxp3(+) Regulatory T Cells in Foxp3.LuciDTR Mice. *Journal of Immunology*, 184(4):1810–1820, 2010.

Sun and Bevan. Defective CD8 T cell memory following acute infection without CD4 T cell help. *Science*, 300(5617):339–342, 2003.

Sung, Zhang, Moseman, Alvarez, Iannacone, Henrickson, de la Torre, Groom, Luster, and von Andrian. Chemokine Guidance of Central Memory T Cells Is Critical for Antiviral Recall Responses in Lymph Nodes. *Cell*, 150(6):1249–1263, 2012.

Surh and Sprent. Homeostasis of naive and memory T cells. *Immunity*, 29(6):848–62, 2008.

Swanson, Hart, Russo, Nayak, Yazew, Pena, Khan, Janse, Pierce, and McGavern. CD8(+) T Cells Induce Fatal Brainstem Pathology during Cerebral Malaria via Luminal Antigen-Specific Engagement of Brain Vasculature. *Plos Pathogens*, 12(12), 2016.

Takahashi, Kuniyasu, Toda, Sakaguchi, Itoh, Iwata, Shimizu, and Sakaguchi. Immunologic self-tolerance maintained by CD25+CD4+ naturally anergic and suppressive T cells: induction of autoimmune disease by breaking their anergic/suppressive state. *Int Immunol*, 10(12):1969–80, 1998.

Teijeira, Russo, and Halin. Taking the lymphatic route: dendritic cell migration to draining lymph nodes. *Semin Immunopathol*, 36(2):261–74, 2014.

Thornton and Shevach. CD4+CD25+ immunoregulatory T cells suppress polyclonal T cell activation in vitro by inhibiting interleukin 2 production. *J Exp Med*, 188(2): 287–96, 1998.

Turley, Fletcher, and Elpek. The stromal and haematopoietic antigen-presenting cells that reside in secondary lymphoid organs. *Nat Rev Immunol*, 10(12):813–25, 2010.

Ulvmar, Werth, Braun, Kelay, Hub, Eller, Chan, Lucas, Novitzky-Basso, Nakamura, Rulicke, Nibbs, Worbs, Forster, and Rot. The atypical chemokine receptor CCRL1 shapes functional CCL21 gradients in lymph nodes. *Nat Immunol*, 15(7):623–30, 2014.

Vaeth, Gogishvili, Bopp, Klein, Berberich-Siebelt, Gattenloehner, Avots, Sparwasser, Grebe, Schmitt, Hunig, Serfling, and Bodor. Regulatory T cells facilitate the nuclear accumulation of inducible cAMP early repressor (ICER) and suppress nuclear factor

of activated T cell c1 (NFATc1). *Proceedings of the National Academy of Sciences of the United States of America*, 108(6):2480–2485, 2011.

Vignali, Collison, and Workman. How regulatory T cells work. *Nat Rev Immunol*, 8(7): 523–32, 2008.

Villarino, Tato, Stumhofer, Yao, Cui, Hennighausen, O'Shea, and Hunter. Helper T cell IL-2 production is limited by negative feedback and STAT-dependent cytokine signals. *Journal of Experimental Medicine*, 204(1):65–71, 2007.

von Andrian and Mempel. Homing and cellular traffic in lymph nodes. *Nat Rev Immunol*, 3(11):867–78, 2003.

Wang, Rickert, and Garcia. Structure of the quaternary complex of interleukin-2 with its alpha, beta, and gammac receptors. *Science*, 310(5751):1159–63, 2005.

Weiss, Bilate, Gobert, Ding, Curotto de Lafaille, Parkhurst, Xiong, Dolpady, Frey, Ruocco, Yang, Floess, Huehn, Oh, Li, Niec, Rudensky, Dustin, Littman, and Lafaille. Neuropilin 1 is expressed on thymus-derived natural regulatory T cells, but not mucosa-generated induced Foxp3+ T reg cells. *J Exp Med*, 209(10):1723–42, S1, 2012.

Willard-Mack. Normal structure, function, and histology of lymph nodes. *Toxicol Pathol*, 34(5):409–24, 2006.

Willerford, Chen, Ferry, Davidson, Ma, and Alt. Interleukin-2 Receptor-Alpha Chain Regulates the Size and Content of the Peripheral Lymphoid Compartment. *Immunity*, 3(4):521–530, 1995.

Wilson, Wilson, Schroder, Pinilla, Blondelle, Houghten, and Garcia. Specificity and degeneracy of T cells. *Mol Immunol*, 40(14-15):1047–55, 2004.

Wong, Park, Gola, Baptista, Miller, Deep, Lou, Boyd, Rudensky, Savage, Altan-Bonnet, Tsang, and Germain. A local regulatory T cell feedback circuit maintains immune homeostasis by pruning self-activated T cells. *Cell*, 184(15):3981–3997 e22, 2021.

Woodruff, Heesters, Herndon, Groom, Thomas, Luster, Turley, and Carroll. Trans-nodal migration of resident dendritic cells into medullary interfollicular regions initiates immunity to influenza vaccine. *J Exp Med*, 211(8):1611–21, 2014.

Worbs, Hammerschmidt, and Forster. Dendritic cell migration in health and disease. *Nat Rev Immunol*, 17(1):30–48, 2017.

Wu, Quintana, and Weiner. Nasal Anti-CD3 Antibody Ameliorates Lupus by Inducing an IL-10-Secreting CD4(+)CD25(-)LAP(+) Regulatory T Cell and Is Associated with Down-Regulation of IL-17(+)CD4(+)ICOS(+)CXCR5(+) Follicular Helper T Cells. *Journal of Immunology*, 181(9):6038–6050, 2008.

Wucherpfennig, Allen, Celada, Cohen, De Boer, Garcia, Goldstein, Greenspan, Hafler, Hodgkin, Huseby, Krakauer, Nemazee, Perelson, Pinilla, Strong, and Sercarz. Polyspecificity of T cell and B cell receptor recognition. *Semin Immunol*, 19(4):216–24, 2007.

Yamamoto, Seki, Iwai, Ko, Martin, Tsuji, Miyagawa, Love, and Iwashima. Ontogeny and localization of the cells produce IL-2 in healthy animals. *Cytokine*, 61(3):831–841, 2013.

Yao, Sun, Lacey, Ji, Moseman, Shih, Heuston, Kirby, Anderson, Cheng, Khan, Handon, Reilley, Fioravanti, Hu, Gossa, Wherry, Gattinoni, McGavern, O'Shea, Schwartzberg, and Wu. Single-cell RNA-seq reveals TOX as a key regulator of CD8(+) T cell persistence in chronic infection. *Nat Immunol*, 20(7):890–901, 2019.

Zheng, Wang, Wang, Gray, and Horwitz. IL-2 is essential for TGF-beta to convert naive CD4+CD25- cells to CD25+Foxp3+ regulatory T cells and for expansion of these cells. *J Immunol*, 178(4):2018–27, 2007.

Zhou, Chu, Teng, Bessman, Goc, Santosa, Putzel, Kabata, Kelsen, Baldassano, Shah, Sockolow, Vivier, Eberl, Smith, and Sonnenberg. Innate lymphoid cells support regulatory T cells in the intestine through interleukin-2. *Nature*, 568(7752):405–+, 2019.

List of Figures

Abbreviations

α alpha

ADP adenosine diphosphate

AICD activation-induced cell death

APC antigen-presenting cell

aPCR quantitive polymerase chain reaction

ATP adenosine triphosphate

BCR b cell receptor

BrdU bromodeoxyuridine

CCL C-C motif ligand

CD cluster of differentiation

cDC conventional dendritic cell

CNS2 conserved non-coding sequence 2

CpG cytosine guanine di-nucleotide

CTL cytotoxic lymphocyte

CTLA-4 cytotoxic t lymphocyte-associate protein 4

cTreg central regulatory T cell

CX3CR C-X-X-X-C motif receptor

CXCL C-X-C motif ligand

CXCR C-X-C motif receptor

DEG differentially expressed genes

DPEC double-positive effector cell

DTR diphtheria toxin receptor

DTX diphtheria toxin

EEC early effector cell

EGFP enhanced green fluorescent protein

ELISA enzyme-linked immunosorbent assay

EOMES eomesodermin

eTreg effector regulatory T cell

FACS fluorescence-activated cell sorter

FasR Fas receptor

FCS fetal calf serum

FDC follicular dendritic cell

Foxp3 forkhead box protein 3

FRC fibroblastic reticular cell

GITR glucocorticoid-induced TNF receptor family gene

gMFI geometric mean fluorescence intensity

GP2 glycoprotein 2

HEV high endothelial venules

HIV human immunodeficiency virus

i.p. intraperiotoneal

i.v. intravenous

IBD inflammatory bowel disease

ICAM-1 intracellular adhesion molecule 1

ID3 inhibitor of DNA binding 3

IFA interfollicular area

IFN-I type-I interferon

IL-2 interleukin-2

IFN-γ interferon gamma

IRES internal ribosome entry site

IVC individually ventilated cage

IZUMO1R also known as folate-receptor 4

JAK janus kinase

ko knock-out

LAG-3 lymphocyte-activation gene 3

LCMV lymphocytic choriomeningitis virus

LFA-1 leukocyte function-associated antigen 1

LN lymph node

MΦ macrophage

MALT mucosa-associated lymphoid tissue

MHC major histocompatibility complex

MMPs matrix metalloproteinases

MPEC memory precursor effector cell

MSM medullary sinus macrophage

NK cell natural killer cell

NMS normal mouse serum

OT-1 MHC class I-restricted, ovalbumin-specific, CD8+ T cells

OVA ovalbumin

p.i. post-infection

PAMP pathogen-associated molecular pattern

PBS phosphate-buffered saline

pDC plasmacytoid dendritic cell

PFU plaque-forming unit

pH potential of hydrogen

PIAS protein inhibitor of activated STAT

PM paracortical macrophage

PNAd peripheral node addressin

popLN popliteal lymph node

PRR pattern recognition receptor

pSTAT5 phosphorylated

pTreg peripheral regulatory T cell

RNA ribonucleic acid

RSV respiratory syncytical virus

RT room temperature

s.c. subcutaneous

S1P sphingosine-1-phosphate

scRNA seq single-cell RNA sequencing

SD standard deviation

SH2 src homology 2

SHP-2 SH2 domain-containing protein tyrosine phosphatase-2

SLEC short-lived effector cell

SLO secondary lymphoid organ

smarta MHC class II-restricted LCMV-GP-specific CD4+ T cells

SSM subcapsular sinus macrophage

STAT5 signal transducer and activator of transcription 5

T-bet T-box expressed in T cells

TCR t cell receptor

TEC terminal effector cell

Tfh t follicular helper cell

TGF-β transforming growth factor beta

Th t helper cell

TLR toll-like receptor

TNF-α tumor necrosis factor alpha

TRAIL TNF-related apoptosis inducing ligand

Treg regulatory T cells

tTreg thymic regulatory T cell

UMAP uniform manifold approximation and projection

VV Vaccinia virus

wt wild-type

XCL X-C motif ligand

XCR X-C motif receptor

Affidavit

I hereby confirm that my thesis entitled 'Regulatory T cells limit antiviral CD8 T cell responses through IL-2 competition' is the result of my own work. I did not receive any help or support from commercial consultants. All sources and / or materials applied are listed and specified in the thesis.

Furthermore, I confirm that this thesis has not yet been submitted as part of another examination process neither in identical nor in similar form.

Würzburg,
Place, Date Signature

Eidesstattliche Erklärung

Hiermit erkläre ich an Eides statt, die Dissertation 'Regulatorische T-Zellen limitieren antivirale CD8 T-Zellantworten durch IL-2 Konkurrenz' eigenständig, d.h. insbesondere selbständig und ohne Hilfe eines kommerziellen Promotionsberaters, angefertigt und keine anderen als die von mir angegebenen Quellen und Hilfsmittel verwendet zu haben.

Ich erkläre außerdem, dass die Dissertation weder in gleicher noch in ähnlicher Form bereits in einem anderen Prüfungsverfahren vorgelegen hat.

Würzburg,
Ort, Datum Unterschrift